R/V *Mirai* Cruise Report

MR15-05

WOCE-revisit in the eastern Indian Ocean

23rd December 2015 – 25th January 2016

Japan Agency for Marine-Earth Science and Technology

(JAMSTEC)

Content

I. Introduction

Indonesian Throughflow is a surface component of the global ocean circulation, which transports fresh Pacific upper water masses into the north Indian Ocean with strong modification from the air-sea interaction and tidal mixing. Paucity of observation data in this part of the world ocean has always been a restriction in understanding global climate change and air-sea coupling — a problem shared amongst emerging international programmes such as Eastern Indian Ocean Upwelling Research Initiative. The main purpose of this cruise is to measure the distribution of water properties (temperature, salinity, dissolved oxygen, carbon, nutrients, etc.) in this important ocean. This is a contribution to International Indian Ocean Expedition 2 and conducted under the Global Ocean Ship-based Hydrographic Investigation Programme (GO-SHIP http://www.go-ship.org).

II. Observation

1. Cruise Information

Katsuro Katsumata (JAMSTEC)

Akihiko Murata (JAMSTEC)

1.1. Basic Information

Title of the cruise	Research cruise on ocean decadal variability -- Indian Ocean GO-SHIP (Global Ocean Ship-based Hydrographic Investigation Program)
Cruise track:	See Fig. 1.1.1
Research area	The northeastern Indian Ocean and the western Pacific Ocean
Cruise code:	MR15-05
Expocode	Leg 1: 49NZ20151223 Leg 2: 49NZ20160113
GHPO section designation:	I10
Ship name:	R/V Mirai
Ports of call:	Leg 1, Jakarta, Indonesia – Bali, Indonesia Leg 2, Bali, Indonesia – Yokohama, Japan
Cruise date:	Leg 1, 23 December 2015 – 11 January 2016 Leg 2, 13 January 2016 – 25 January 2016
Chief scientists:	Leg 1, Katsuro Katsumata (k.katsumata@jamstec.go.jp) Leg 2, Akihiko Murata (murataa@jamstec.go.jp) Ocean Climate Change Research Program Research and Development Centre for Global Change (RIGC) Japan Agency for Marine-Earth Science and Technology (JAMSTEC) 2-15 Natsushima, Yokosuka, Kanagawa, Japan 237-0061 Fax: +81-46-867-9835

Piggyback projects

(1) Aerosol optical characteristics measured by ship-borne Sky radiometer (Toyama University)

(2) Geochemical and microbiological investigation from sea surface to sea bottom at tropical eutrophic ocean (JAMSTEC, University of Tokyo, Tokyo University of Agriculture and Technology, Rakuno Gakuen University, etc.)

(3) Advanced measurements of aerosols in the marine atmosphere: Toward elucidation of interactions with climate and ecosystem (JAMSTEC)

(4) Global distribution of drop size distribution of precipitating particles over pure-oceanic background (JAMSTEC)

(5) Shipboard CO2 observations over the tropical Indo-Pacific Ocean for a simple estimation of the carbon flux between the ocean and the atmosphere from GOSAT data (JAXA)

Principal investigators of the piggyback projects: Kazuma Aoki (University of Toyama)
Takuro Nunoura (JAMSTEC)
Yugo Kanaya (JAMSTEC)
Masaki Katsumata (JAMSTEC)
Kei Shiomi (JAXA)

Number of Stations: Leg 1, 53 stations
Leg 2, none

Floats and drifters deployed: 16 Argo floats (Leg 1), 1 Argo float (Leg 2)

Mooring recovery : none

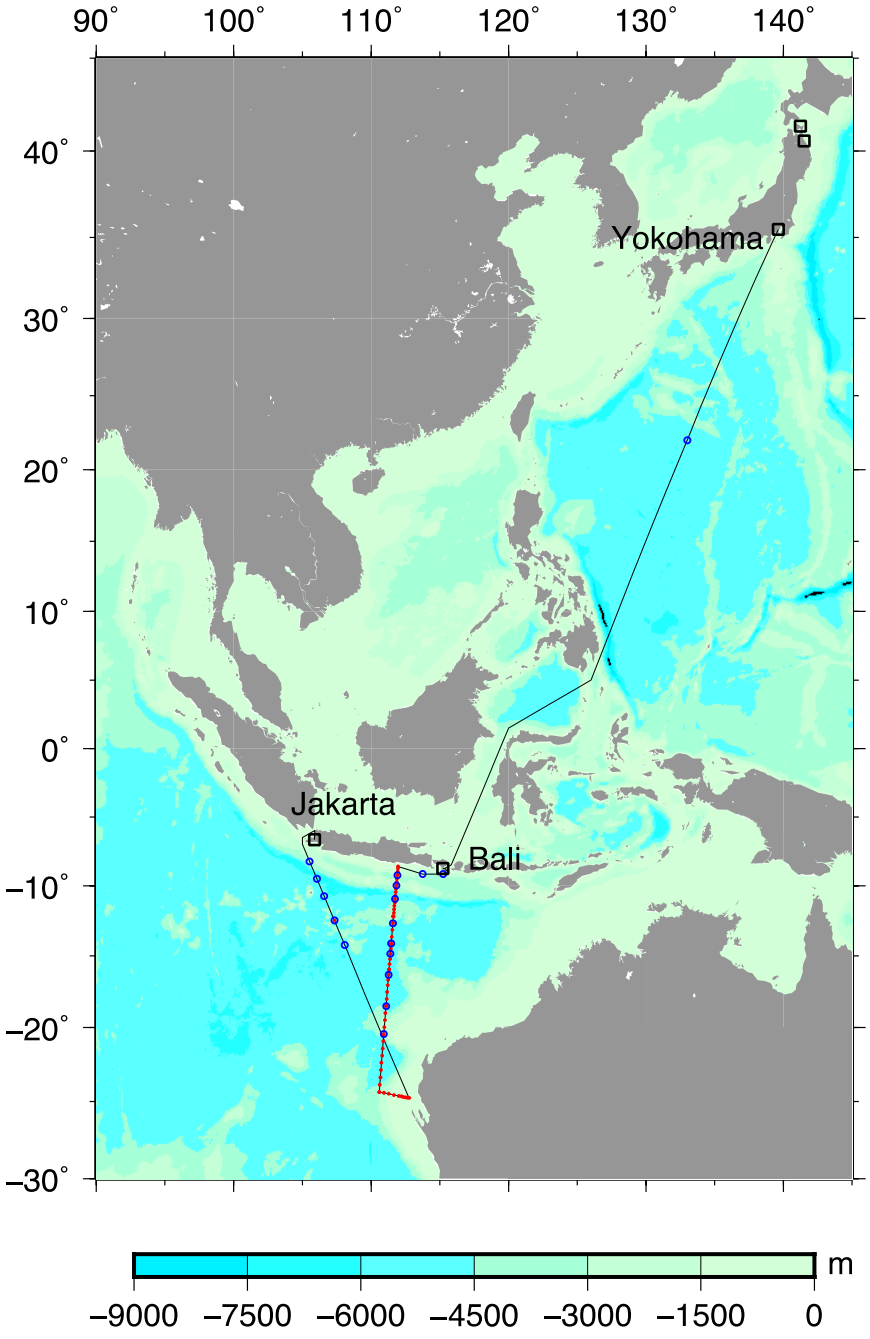

Fig. 1.1.1 MR15-05 cruise. Blue circles show the deployment position of Argo floats. Red dots show CTD/bottle sampling stations.

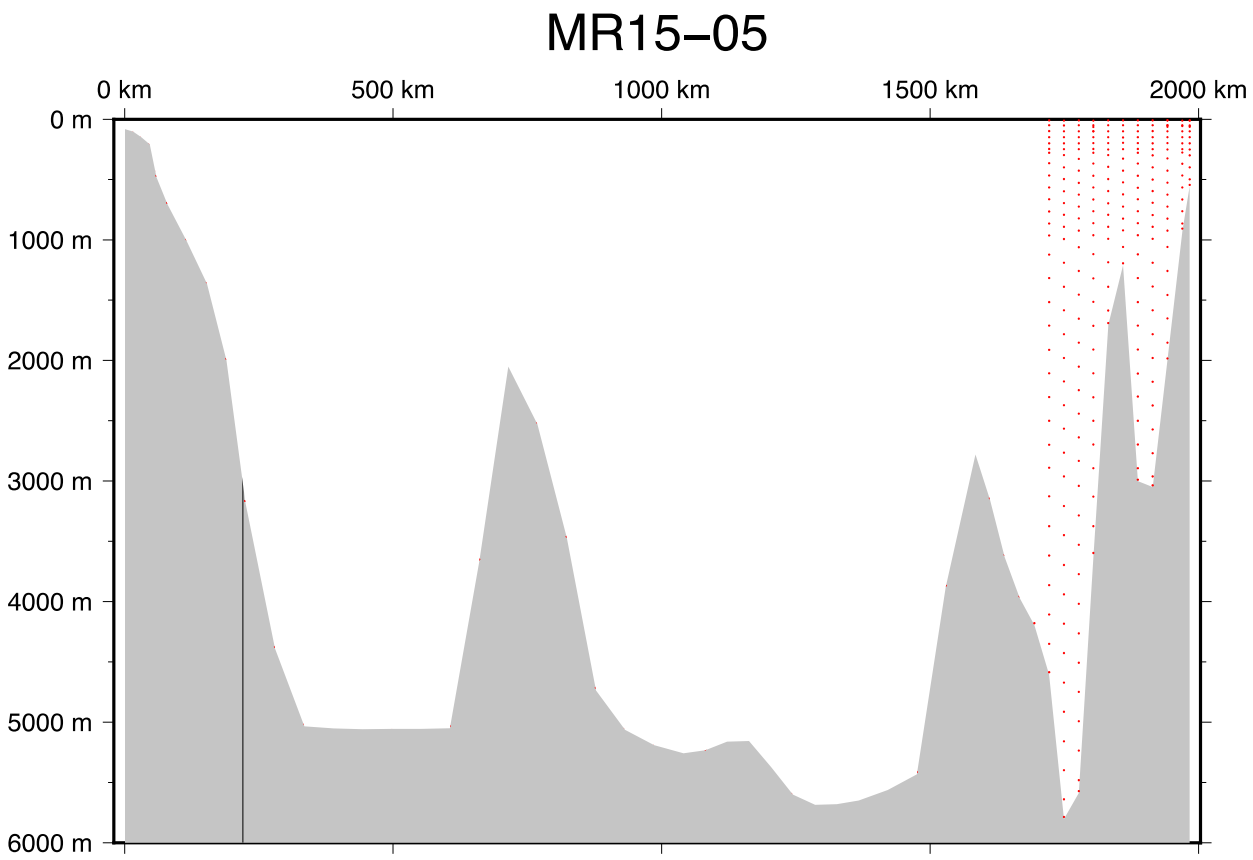

Fig. 1.1.2 Water sampling positions.

1.2. Cruise Participants

List of Participants for leg 1

Katsuro Katsumata	Chief scientist	RCGC/JAMSTEC
Yuichiro Kumamoto	DO/Sampling chief	RCGC/JAMSTEC
Hiroshi Uchida	Thermosalinograph/Salinity	RCGC/JAMSTEC
Ken'ichi Sasaki	CFCs	MIO/JAMSTEC
Kosei Sasaoka	Chlorophyll	RCGC/JAMSTEC
Etsuro Ono	Calcium/total alkalinity	RCGC/JAMSTEC
Kazuhiko Matsumoto	Primary productivity	DEGCR/JAMSTEC
Taichi Yokokawa	Biological sampling	RDCMB/JAMSTEC
Chisato Yoshikawa	Biological sampling	DB/JAMSTEC
Shotoku Kotajima	Biological sampling	TUAC
Kanta Chida	Biological sampling	Rakuno Gakuen University

Harun Idham Akbar	Water sampling	BPPT
Gentio Harusono	Security Officer	Indonesian Navy
Hiroshi Matsumaga	Chief technician/Sampling chief	MWJ
Shinsuke Toyoda	CTD	MWJ
Hiroki Ushiromura	Salinity	MWJ
Syungo Oshitani	CTD	MWJ
Sonoka Wakatsuki	Salinity	MWJ
Keisuke Takeda	CTD	MWJ
Minoru Kamata	Nutrients	MWJ
Tomonori Watai	pH/total alkalinity	MWJ
Makoto Takada	DIC	MWJ
Elena Hayashi	Nutrients	MWJ
Atsushi Ono	DIC	MWJ
Tomomi Sone	Nutrients	MWJ
Katsunori Sagishima	CFCs	MWJ
Hironori Sato	CFCs	MWJ
Misato Kuwahara	DO	MWJ
Masahiro Orui	DO	MWJ
Keitaro Matsumoto	DO	MWJ
Hiroshi Hoshino	CFCs	MWJ
Haruka Tamada	DO	MWJ
Hiroyuki Hayashi	CTD	MWJ
Kanako Yoshida	pH/total alkalinity	MWJ
Kohei Miura	Nutrients	MWJ
Seika Katayama	Water sampling	MWJ
Naoya Yokoi	Water sampling	MWJ
Kohei Kumagai	Water sampling	MWJ
Naoya Kudo	Water sampling	MWJ
Eri Yoshizawa	Water sampling	MWJ
Kei Takamiya	Water sampling	MWJ
Wataru Tokunaga	Chief technician/meterology/geophysics/XCTD	GODI
Yutaro Murakami	Meteorlology/geophysics/XCTD	GODI
Tetsuya Kai	Meteorology/geophysics/XCTD	GODI

List of Participants for leg 2

Akihiko Murata	Chief scientist	RCGC/JAMSTEC
Kousei Sasaoka	Engineer	RCGC/JAMSTEC
Minoru Kamata	Chief marine technician	MWJ
Sinsuke Toyota	Marine technician	MWJ
Tomonori Watai	Marin technician	MWJ
Syungo Oshitani	Marine technician	MWJ
Sonoka Wakatsuki	Marine technician	MWJ
Tomonori Watai	Marine technician	MWJ
Makoto Takada	Marine technician	MWJ
Elena Hayashi	Maine technician	MWJ
Atsushi Ono	Maine technician	MWJ
Katsunori Sagishima	Marine technician	MWJ
Masahiro Oorui	Marine technician	MWJ
Keitaro Matsumoto	Marine technician	MWJ
Koichi Inagaki	Chief technician/meteorology/geophysics	GODI
Yutaro Murakami	Meteorology/geophysics	GODI

BPPT: Badan Pengkajian dan Penerapan Teknologi (Agency for the Assessment and Application of Technology of the Republic of Indonesia)

DB: Department of Biogeochemistry

DEGCR: Department of Environmental Geochemical Cycle Research

GODI: Global Ocean Development Inc.

MWJ: Marine Works Japan

MIO: Mutsu Institute for Oceanography

RCGC: Research and Development Center for Global Change

RDCMB: Research and Development Center for Marine Biosciences

TUAT: Tokyo University of Agriculture and Technology

2. Underway Measurements

2.1 Navigation

(1) Personnel

Katsuro Katsumata	***JAMSTEC: Principal investigator***	***- leg1 -***
Akihiko Murata	***JAMSTEC: Principal investigator***	***- leg2 -***
Wataru Tokunaga	***Global Ocean Development Inc., (GODI)***	***- leg1 -***
Tetsuya Kai	***GODI***	***- leg1 -***
Koichi Inagaki	***GODI***	***- leg2 -***
Yutaro Murakami	***GODI***	***- leg1, leg2 -***
Ryo Kimura	***MIRAI crew***	***- leg1 -***
Masanori Murakami	***MIRAI crew***	***- leg2 -***

(2) System description

Ship's position and velocity were provided by Navigation System on R/V MIRAI. This system integrates GNSS position, Doppler sonar log speed, Gyro compass heading and other basic data for navigation. This system also distributed ship's standard time synchronized to GPS time server via Network Time Protocol. These data were logged on the network server as "SOJ" data every 5 seconds. Sensors for navigation data are listed below;

i) GNSS system:
R/V MIRAI has four GNSS systems, all GNSS positions were offset to radar-mast position, datum point. Anytime changeable manually switched as to GNSS receiving state.
   a) StarPack-D (version 1), Differential GNSS system.
      Antenna: Located on compass deck, starboard.
   b) StarPack-D (version 1), Differential GNSS system.
      Antenna: Located on compass deck, portside.
   c) Standalone GPS system.
      Receiver: Trimble SPS751
      Antenna: Located on navigation deck, starboard.
   d) Standalone GPS system.
      Receiver: Trimble SPS751
      Antenna: Located on navigation deck, portside.

ii) Doppler sonar log:
FURUNO DS-30, which use three acoustic beam for current measurement under the hull.

iii) Gyro compass:
TOKYO KEIKI TG-6000, sperry type mechanical gyrocompass.

iv) GPS time server:
SEIKO TS-2540 Time Server, synchronizing to GPS satellites every 1 second.

(3) Cruise period **(Times in UTC)**

Leg1: 03:10, 23 Dec. 2015 to 00:50, 11 Jan. 2016
Leg2: 01:00, 13 Jan. 2016 to 23:50, 24 Jan. 2016

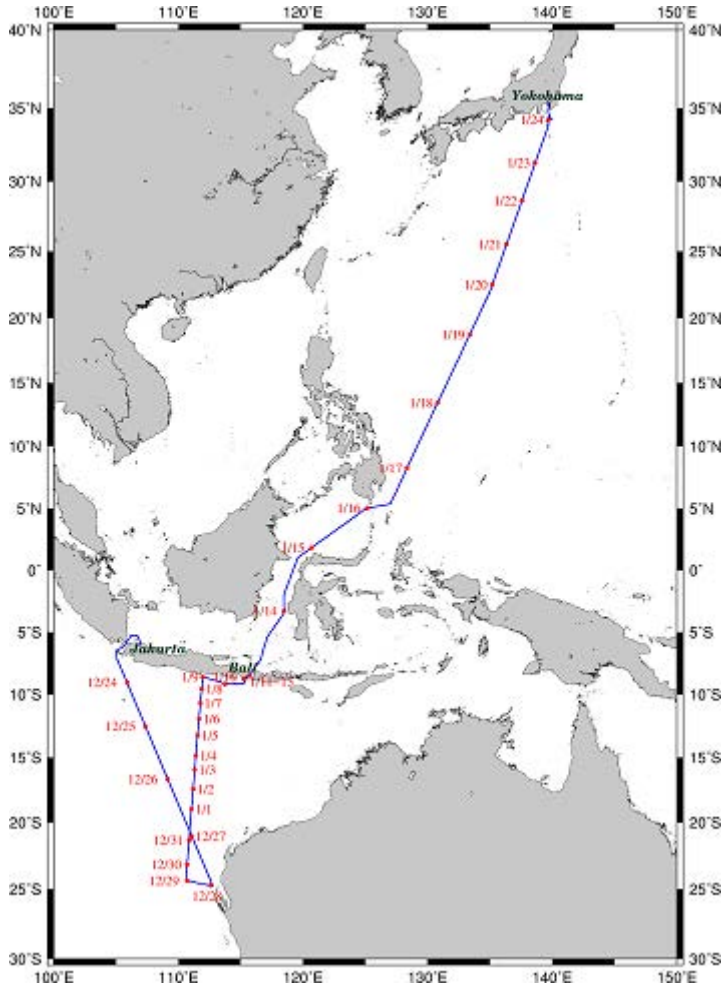

Fig.2.1-1 Cruise track of MR15-05Leg1, Leg2

2.2 Swath Bathymetry

(1) Personnel

Katsuro Katsumata	***JAMSTEC: Principal investigator***	***- leg1 -***
Akihiko Murata	***JAMSTEC: Principal investigator***	***- leg2 -***
Wataru Tokunaga	***Global Ocean Development Inc., (GODI)***	***- leg1 -***
Tetsuya Kai	***GODI***	***- leg1 -***
Koichi Inagaki	***GODI***	***- leg2 -***
Yutaro Murakami	***GODI***	***- leg1, leg2 -***
Ryo Kimura	***MIRAI crew***	***- leg1 -***
Masanori Murakami	***MIRAI crew***	***- leg2 -***

(2) Introduction

R/V MIRAI is equipped with a Multi narrow Beam Echo Sounding system (MBES), SEABEAM 3012 (L3 Communications, ELAC Nautik). The objective of MBES is collecting continuous bathymetric data along ship's track to make a contribution to geological and geophysical investigations and global datasets.

(3) Data Acquisition

The "SEABEAM 3012" on R/V MIRAI was used for bathymetry mapping during this cruise.

To get accurate sound velocity of water column for ray-path correction of acoustic multibeam, we used Surface Sound Velocimeter (SSV) data to get the sea surface sound velocity (at 6.62m), and the deeper depth sound velocity profiles were calculated by temperature and salinity profiles from CTD and XCTD data by the equation in Del Grosso (1974) during this cruise.

Table 2.2-1 shows system configuration and performance of SEABEAM 3012.

Table 2.2-1 SEABEAM 3012 system configuration and performance

Frequency:	12 kHz
Transmit beam width:	2.0 degree
Transmit power:	4 kW
Transmit pulse length:	2 to 20 msec.
Receive beam width:	1.6 degree
Depth range:	50 to 11,000 m
Number of beams:	301 beams
Beam spacing:	Equi-angle
Swath width:	60 to 150 degrees
Depth accuracy:	< 1 % of water depth (average across the swath)

(4) Data processing

i) Sound velocity correction

Each bathymetry data were corrected with sound velocity profiles calculated from the nearest CTD or XCTD data in the distance. The equation of Del Grosso (1974) was used for calculating sound velocity. The data correction were carried out using the HIPS software version 8.1.8 (CARIS, Canada)

ii) Editing and Gridding

Editing for the bathymetry data were carried out using the HIPS. Firstly, the bathymetry data during ship's turning was basically deleted, and spike noise of each swath data was removed. Then the bathymetry data were checked by "BASE surface (resolution: 50 m averaged grid)".

Finally, all accepted data were exported as XYZ ASCII data (longitude [degree], latitude [degree], depth [m]), and converted to 150 m grid data using "nearneighbor" utility of GMT (Generic Mapping Tool) software.

Table 2.2-2 Parameters for gridding on "nearneighbor" in GMT

Gridding mesh size:	150 m
Search radius size:	150 m
Minimum number of neighbors for grid:	1

(5) Data Archives

Bathymetric data obtained during this cruise will be submitted to the Data Management Group (DMG) of JAMSTEC, and will be archived there.

(6) Remarks (Times in UTC)

i) The following periods, the observation were carried out.

Leg1: 19:35, 23 Dec. 2015 to 09:40, 24 Dec. 2015
11:20, 24 Dec. 2015 to 22:05, 10 Jan. 2016
Leg2: 14:35, 17 Jan. 2016 to 06:26, 23 Jan. 2016

2.3 Surface Meteorological Observations

(1) Personnel

Katsuro Katsumata	***JAMSTEC: Principal investigator***	***- leg1 -***
Akihiko Murata	***JAMSTEC: Principal investigator***	***- leg2 -***
Wataru Tokunaga	***Global Ocean Development Inc., (GODI)***	***- leg1 -***
Tetsuya Kai	***GODI***	***- leg1 -***
Koichi Inagaki	***GODI***	***- leg2 -***
Yutaro Murakami	***GODI***	***- leg1, leg2 -***
Ryo Kimura	***MIRAI crew***	***- leg1 -***
Masanori Murakami	***MIRAI crew***	***- leg2 -***

(2) Objectives

Surface meteorological parameters are observed as a basic dataset of the meteorology. These parameters provide the temporal variation of the meteorological condition surrounding the ship.

(3) Methods

Surface meteorological parameters were observed during this cruise, except for the Republic of Indonesia territorial waters and Republic of Philippine EEZ. In this cruise, we used two systems for the observation.

i) MIRAI Surface Meteorological observation (SMet) system

Instruments of SMet system are listed in Table 2.3-1 and measured parameters are listed in Table 2.3-2. Data were collected and processed by KOAC-7800 weather data processor made by Koshin-Denki, Japan. The data set consists of 6-second averaged data.

ii) Shipboard Oceanographic and Atmospheric Radiation (SOAR) measurement system

SOAR system designed by BNL (Brookhaven National Laboratory, USA) consists of major five parts.

a) Portable Radiation Package (PRP) designed by BNL – short and long wave downward radiation.
b) Analog meteorological data sampling with CR1000 logger manufactured by Campbell Inc. Canada – wind, pressure, and rainfall (by a capacitive rain gauge) measurement.
c) Digital meteorological data sampling from individual sensors - air temperature, relative humidity and rainfall (by ORG (optical rain gauge)) measurement.
d) Photosynthetically Available Radiation (PAR) and UV (Ultraviolet Irradiance) sensor manufactured by Biospherical Instruments Inc. (USA) - PAR measurement.
e) Scientific Computer System (SCS) developed by NOAA (National Oceanic and Atmospheric Administration, USA) – centralized data acquisition and logging of all data sets.

SCS recorded PRP, CR1000 data, air temperature and relative humidity data, ORG data. SCS composed Event data (JamMet) from these data and ship's navigation data every 6 seconds. Instruments and their locations are listed in Table 2.3-3 and measured parameters are listed in Table 2.3-4.

For the quality control as post processing, we checked the following sensors, before and after the cruise.

i. Young rain gauge (SMet and SOAR)
Inspect of the linearity of output value from the rain gauge sensor to change input value by adding fixed quantity of test water.
ii. Barometer (SMet and SOAR)
Comparison with the portable barometer value, PTB220, VAISALA
iii. Thermometer (air temperature and relative humidity) (SMet and SOAR)
Comparison with the portable thermometer value, HM70, VAISALA

(4) Preliminary results

Fig. 2.3-1 shows the time series of the following parameters;
Wind (SOAR)
Air temperature (SMet)
Relative humidity (SMet)
Precipitation (SOAR, rain gauge)
Short/long wave radiation (SMet and SOAR)
SMet: 18:51, 23 Dec. 2015 to 00:49, 28 Dec. 2015
SOAR: 00:50, 28 Dec. 2015 to end of cruise
Pressure (SMet)
Sea surface temperature (SMet)
Significant wave height (SMet)

(5) Data archives

These meteorological data will be submitted to the Data Management Group (DMG) of JAMSTEC just after the cruise.

(6) Remarks (Times in UTC)

i) The following periods, the observation were carried out.
Leg1: 18:51, 23 Dec. 2015 to 22:40, 10 Jan. 2016
Leg2: 13:35, 17 Jan. 2016 to 00:00, 25 Jan. 2016

ii) The following periods, sea surface temperature of SMet data were available.
Leg1: 18:51, 23 Dec. 2015 to 22:03, 10 Jan. 2016
Leg2: 13:35, 17 Jan. 2016 to 06:30, 23 Jan. 2016

iii) The following periods, PRP data were invalid due to system trouble.
18:51, 23 Dec. 2015 to 00:49, 28 Dec. 2015
16:42, 21 Jan. 2016 to 20:54, 21 Jan. 2016

iv) The following periods, PRP data acquisition were suspended due to maintenance.
07:27, 24 Jan. 2016 to 07:30, 24 Jan. 2016

v) The following time, increasing of SMet capacitive rain gauge data were invalid due to transmitting for MF/HF or VHF radio.
06:37, 06 Jan. 2016
23:57, 20 Jan. 2016
01:01, 21 Jan. 2016
20:31, 24 Jan. 2016
22:07, 24 Jan. 2016

Table 2.3-1 Instruments and installation locations of MIRAI Surface Meteorological observation system

Sensors	Type	Manufacturer	Location (altitude from surface)
Anemometer	KE-500	Koshin Denki, Japan	Foremast (24 m)
Tair/RH	HMP155	Vaisala, Finland	
with 43408 Gill aspirated radiation shield		R.M. Young, USA	Compass deck (21 m) starboard and portside
Thermometer: SST	RFN2-0	Koshin Denki, Japan	4th deck (-1m, inlet -5m)
Barometer	Model-370	Setra System, USA	Captain deck (13 m) weather observation room
Capacitive rain gauge	50202	R. M. Young, USA	Compass deck (19 m)
Optical rain gauge	ORG-815DS	Osi, USA	Compass deck (19 m)
Radiometer (short wave)	MS-802	Eko Seiki, Japan	Radar mast (28 m)
Radiometer (long wave)	MS-202	Eko Seiki, Japan	Radar mast (28 m)
Wave height meter	WM-2	Tsurumi-seiki, Japan	Bow (10 m) Stern (8m)

Table 2.3-2 Parameters of MIRAI Surface Meteorological observation system

Parameter	Units	Remarks
1 Latitude	degree	
2 Longitude	degree	
3 Ship's speed	knot	MIRAI log DS-30, Furuno
4 Ship's heading	degree	MIRAI gyro, TG-6000, TOKYO-KEIKI
5 Relative wind speed	m/s	6sec./10min. averaged
6 Relative wind direction	degree	6sec./10min. averaged
7 True wind speed	m/s	6sec./10min. averaged
8 True wind direction	degree	6sec./10min. averaged
9 Barometric pressure	hPa	adjusted to sea surface level 6sec. averaged
10 Air temperature (starboard side)	degC	6sec. averaged
11 Air temperature (port side)	degC	6sec. averaged
12 Dewpoint temperature (starboard side)	degC	6sec. averaged
13 Dewpoint temperature (port side)	degC	6sec. averaged
14 Relative humidity (starboard side)	%	6sec. averaged
15 Relative humidity (port side)	%	6sec. averaged
16 Sea surface temperature	degC	6sec. averaged
17 Rain rate (optical rain gauge)	mm/hr	hourly accumulation
18 Rain rate (capacitive rain gauge)	mm/hr	hourly accumulation
19 Down welling shortwave radiation	W/m^2	6sec. averaged
20 Down welling infra-red radiation	W/m^2	6sec. averaged
21 Significant wave height (bow)	m	hourly
22 Significant wave height (aft)	m	hourly
23 Significant wave period (bow)	second	hourly
24 Significant wave period (aft)	second	hourly

Table 2.3-3 Instruments and installation locations of SOAR system

Sensors (Meteorological)	Type	Manufacturer	Location (altitude from surface)
Anemometer	05106	R.M. Young, USA	Foremast (25 m)
Barometer	PTB210	Vaisala, Finland	
with 61002 Gill pressure port		R.M. Young, USA	Foremast (23 m)
Capacitive rain gauge	50202	R.M. Young, USA	Foremast (24 m)
Tair/RH	HMP155	Vaisala, Finland	
with 43408 Gill aspirated radiation shield		R.M. Young, USA	Foremast (23 m)
Optical rain gauge	ORG-815DR	Osi, USA	Foremast (24 m)

Sensors (PRP)	Type	Manufacturer	Location (altitude from surface)
Radiometer (short wave)	PSP	Epply Labs, USA	Foremast (25 m)
Radiometer (long wave)	PIR	Epply Labs, USA	Foremast (25 m)
Fast rotating shadowband radiometer		Yankee, USA	Foremast (25 m)

Sensor (PAR)	Type	Manufacturer	Location (altitude from surface)
PAR sensor	PUV-510	Biospherical Instru ments Inc., USA	Navigation deck (18m)

Table 2.3-4 Parameters of SOAR system (JamMet)

Parameter	Units	Remarks
1 Latitude	degree	
2 Longitude	degree	
3 SOG	knot	
4 COG	degree	
5 Relative wind speed	m/s	
6 Relative wind direction	degree	
7 Barometric pressure	hPa	
8 Air temperature	degC	
9 Relative humidity	%	
10 Rain rate (optical rain gauge)	mm/hr	
11 Precipitation (capacitive rain gauge)	mm	reset at 50 mm
12 Down welling shortwave radiation	W/m^2	
13 Down welling infra-red radiation	W/m^2	
14 Defuse irradiance	W/m^2	
15 PAR	$microE/cm^2/sec$	
16 UV305nm	$microW/ cm^2/nm$	
17 UV320nm	$microW/ cm^2/nm$	
18 UV340nm	$microW/ cm^2/nm$	
19 UV380nm	$microW/ cm^2/nm$	

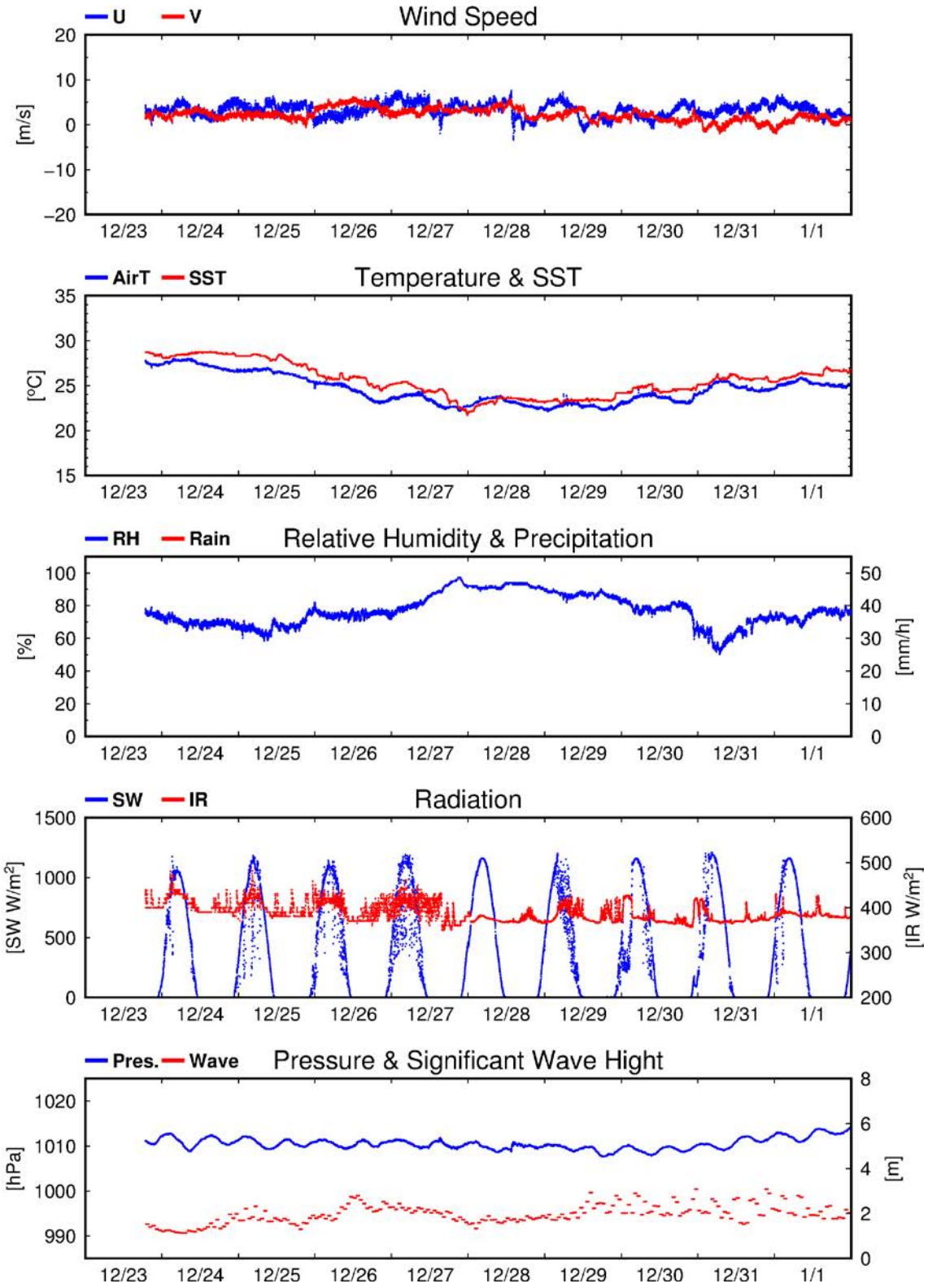

Fig. 2.3-1 Time series of surface meteorological parameters during this cruise (Leg1).

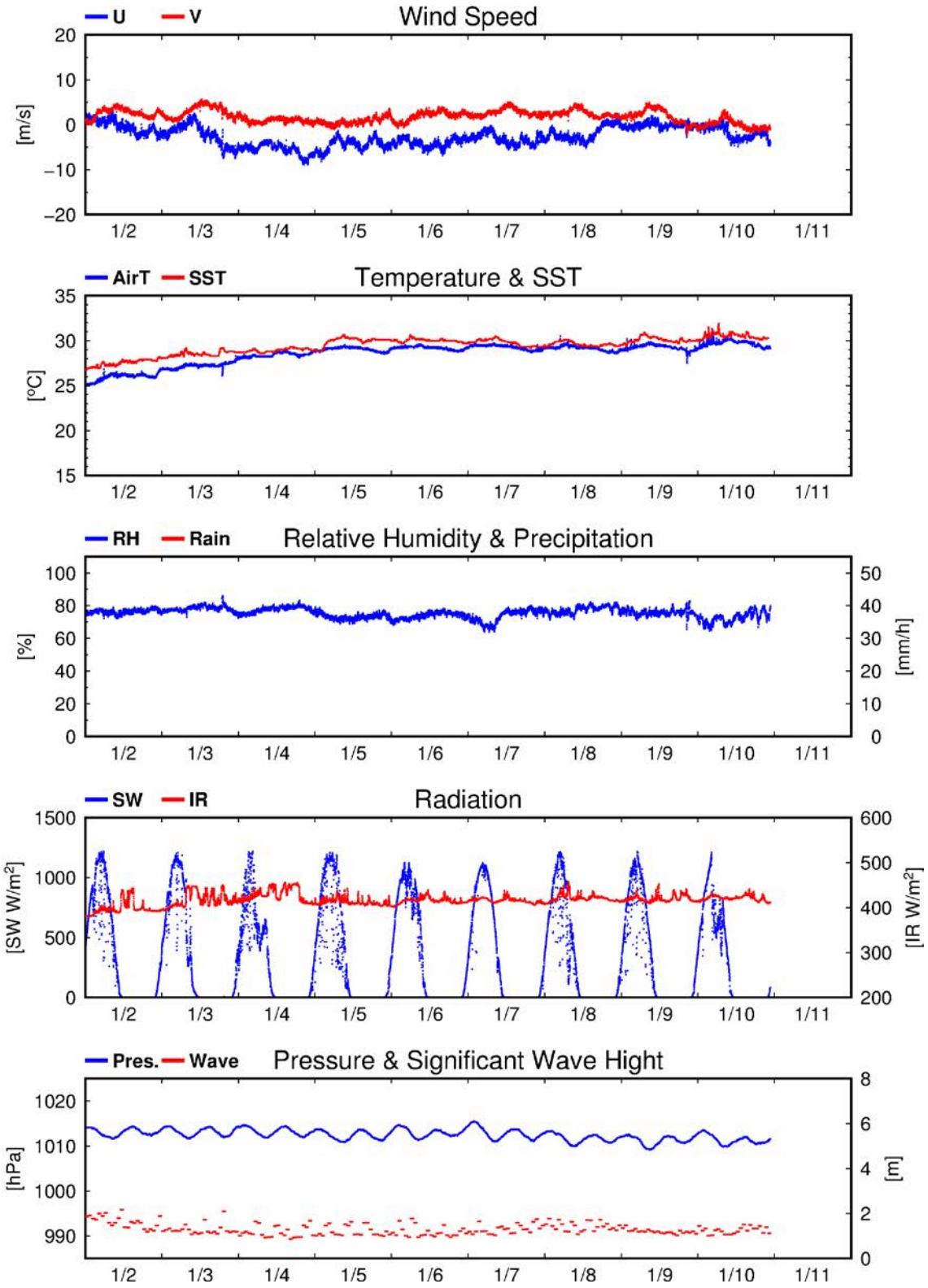

Fig. 2.3-1 Continued (Leg1).

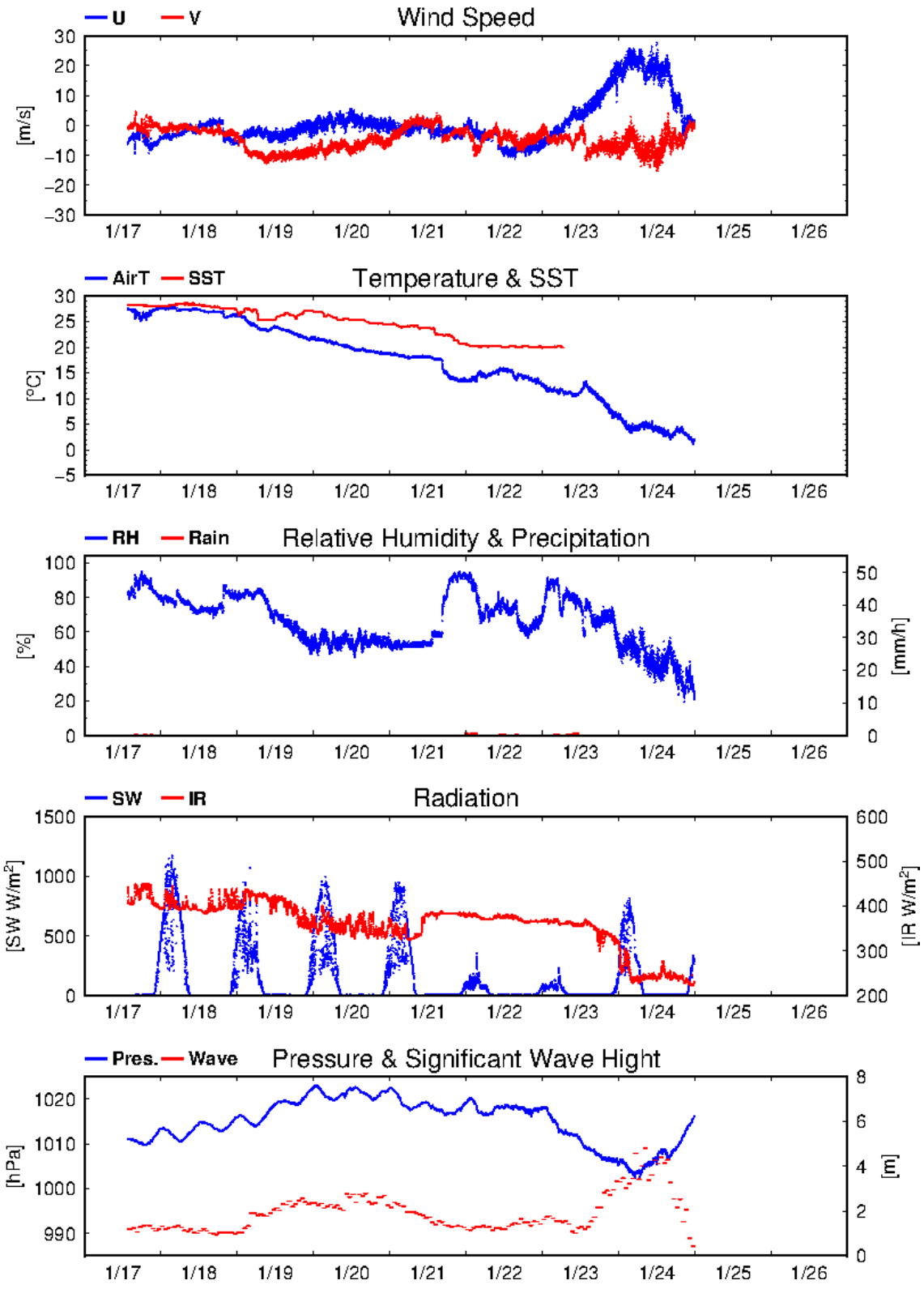

Fig. 2.3-1 Continued (Leg2).

2.4 Thermo-Salinograph and Related Measurements

February 22, 2016

(1) Personnel

Hiroshi Uchida (JAMSTEC)

Kosei Sasaoka (JAMSTEC)

Masahiro Orui (MWJ)

Misato Kuwahara (MWJ)

Keitaro Matsumoto (MWJ)

Haruka Tamada (MWJ)

(2) Objectives

The objective is to collect sea surface salinity, temperature, dissolved oxygen, fluorescence, turbidity, and nitrate data continuously along the cruise track.

(3) Materials and methods

The Continuous Sea Surface Water Monitoring System (Marine Works Japan Co, Ltd.) has seven sensors and automatically measures salinity, temperature, dissolved oxygen, fluorescence, and turbidity in sea surface water every one minute. This system is located in the sea surface monitoring laboratory and bottom of the ship and connected to shipboard LAN system. Measured data along with time and location of the ship were displayed on a monitor and stored in a desktop computer. The sea surface water was continuously pumped up to the laboratory from about 5 m water depth and flowed into the system through a vinyl-chloride pipe. One thermometer is located just before the sea water pump at bottom of the ship. The flow rate of the surface seawater was controlled to be about 1.2 L/min. Periods of measurement, maintenance and problems are listed in Table 2.4.1.

A chemical-free nitrate sensor was also used with the Continuous Sea Surface Water Monitoring System. The nitrate sensor was attached using a flow cell next to the thermo-salinograph.

Software and sensors used in this system are listed below.

i. Software

Seamoni-kun Ver.1.50

ii. Sensors

Temperature and conductivity sensor

Model:	SBE 45, Sea-Bird Electronics, Inc.
Serial number:	4552788-0264
Pre-cruise calibration:	30 August 2014, Sea-Bird Electronics, Inc.

Bottom of ship thermometer

Model:	SBE 38, Sea-Bird Electronics, Inc.
Serial number:	3852788-0457
Pre-cruise calibration:	31 October 2014, Sea-Bird Electronics, Inc.

Dissolved oxygen sensor

Model: RINKO-II, JFE Adantech Co. Ltd.

Serial number: 0013

Pre-cruise calibration: 10 May 2015, JAMSTEC

Model: OPTODE 3835, Aanderaa Data Instruments, AS.

Serial number: 1519

Pre-cruise calibration: 13 May 2015, JAMSTEC

Fluorometer and turbidity sensor

Model: C3, Turner Designs, Inc.

Serial number: 2300384

Nitrate sensor

Model: Deep SUNA, Satlantic, LP.

Serial number: 0385

Table 2.4.1. Events of the Continuous Sea Surface Water Monitoring System operation.

System Date [UTC]	System Time [UTC]	Event
2015/12/23	19:00	Logging for leg 1 start
2015/12/24	05:23–06:07	Flow rate for a line of RINKO and Optode would be small, though both data seem to be normal.
2015/12/29	10:11	Logging stop for C3/filter cleaning
2015/12/29	11:23	Logging restart
2016/01/05	11:27	Logging stop for C3/filter cleaning
2016/01/05	13:05	Logging restart
2016/01/05	13:05–13:25	Optode was unstable.
2016/01/11	22:00	Logging for leg 1 end
2016/01/17	13:35	Logging for leg 2 start
2016/01/23	06:23	Logging for leg 2 end

(4) Pre-cruise calibration

Pre-cruise sensor calibrations for the SBE 45 and SBE 38 were performed at Sea-Bird Electronics, Inc.

Pre-cruise sensor calibrations for the oxygen sensors were performed at JAMSTEC. The oxygen sensors were immersed in fresh water in a 1-L semi-closed glass vessel, which was immersed in a temperature-controlled water bath. Temperature of the water bath was set to 1, 10, 20 and 29ºC. Temperature of the fresh water in the vessel was measured

by a thermistor thermometer (expanded uncertainty of smaller than 0.01ºC, ARO-PR, JFE Advantech, Co., Ltd.). At each temperature, the fresh water in the vessel was bubbled with standard gases (4, 10, 17 and 25% oxygen consisted of the oxygen-nitrogen mixture, whose relative expanded uncertainty is 0.5%) for more than 30 minutes to insure saturation. Absolute pressure of the vessel headspace was measured by a reference quartz crystal barometer (expanded uncertainty of 0.01% of reading) and ranged from about 1040 to 1070 hPa. The data were averaged over 5 minutes at each calibration point (a matrix of 24 points). As a reference, oxygen concentration of the fresh water in the calibration vessel was calculated from the oxygen concentration of the gases, temperature and absolute pressure at the water depth (about 8 cm) of the sensor's sensing foil as follows:

$$O_2\ (\mu mol/L) = \{1000 \times c(T) \times (A_p - pH_2O)\} / \{0.20946 \times 22.3916 \times (1013.25 - pH_2O)\}$$

where c(T) is the oxygen solubility, A_p is absolute pressure [in hPa], and pH_2O is the water vapor pressure [in hPa].

The RINKO was calibrated by the modified Stern-Volmer equation slightly modified from a method by Uchida et al. (2010):

$$O_2\ (\mu mol/L) = [(V_0 / V)^E - 1] / K_{sv}$$

where V is raw phase difference, V_0 is raw phase difference in the absence of oxygen, K_{sv} is Stern-Volmer constant. The coefficient E corrects nonlinearity of the Stern-Volmer equation. The V_0 and the K_{sv} are assumed to be functions of temperature as follows.

$$K_{sv} = C_0 + C_1 \times T + C_2 \times T^2$$

$$V_0 = 1 + C_3 \times T$$

$$V = C_4 + C_5 \times V_b$$

where T is CTD temperature (°C) and V_b is raw output. The oxygen concentration is calculated using accurate temperature data from the SBE 45 instead of temperature data from the RINKO. The calibration coefficients were as follows:

C_0 = 5.048509438066593e-03

C_1 = 2.212851808960770e-04

C_2 = 3.735982971782336e-06

C_3 = -7.847113805097885e-04

C_4 = 3.011495646664952e-02

C_5 = 0.1926948014214438

E = 1.5

(5) Data processing and post-cruise calibration

Data from the Continuous Sea Surface Water Monitoring System were obtained at 1 minute intervals. Data from the nitrate sensor were obtained at 2 minute intervals and linearly interpolated at 1 minute intervals.

These data were processed as follows. Spikes in the temperature and salinity data were removed using a median filter with a window of 3 scans (3 minutes) when difference between the original data and the median filtered data was larger than 0.1ºC for temperature and 0.5 for salinity. Data gaps were linearly interpolated when the gap was ≤ 13 minutes. Fluoromete and turbidity data were low-pass filtered using a median filter with a window of 3 scans (3 minutes)

to remove spikes. Raw data from the RINKO oxygen sensor, fluorometer, turbidity and nitrate data were low-pass filtered using a Hamming filter with a window of 15 scans (15 minutes).

A slope correction was applied to the nitrate sensor before post-cruise calibration. RMNS (Reference Material for Nutrients in Seawater, Kanso Technos Co., Ltd., Osaka, Japan) lot BU and CA were measured by the nitrate sensor during the cruise (Fig. 2.4.1 and Table 2.4.2) and a slope (a_1) for the correction was estimated to be 0.897966 on average from the following equation:

$$NRA\ [\mu mol/kg] = a_0 + a_1\ NRA_{org}$$

where NRA is corrected nitrate concentration, NRA_{org} is raw data, and a_0 is the offset at the time of RMNS measurement.

Salinity (S [PSU]), dissolved oxygen (O [μmol/kg]), fluorescence (Fl [RFU]), and nitrate (NRA [μmol/kg]) data were corrected using the water sampled data. Details of the measurement methods are described in Sections 3.2, 3.4, 3.5, and 3.10 for salinity, dissolved oxygen, nitrate and chlorophyll-a, respectively. Corrected salinity (S_{cor}), dissolved oxygen (O_{cor}), estimated chlorophyll *a* (Chl-a), and nitrate (NRA_{cor}) were calculated from following equations

$$S_{cor}\ [PSU] = c_0 + c_1\ S + c_2\ t$$

$$O_{cor}\ [\mu mol/kg] = c_0 + c_1\ O + c_2\ T + c_3\ t$$

$$Chl\text{-}a\ [\mu g/L] = c_0 + c_1\ Fl$$

$$NRA_{cor}\ [\mu mol/kg] = a_1\ NRA_{org} + c_0 + c_1\ t$$

where S is practical salinity, t is days from a reference time (2015/12/23 19:00 [UTC]), T is temperature in ºC. The best fit sets of calibration coefficients (c_0~c_3) were determined by a least square technique to minimize the deviation from the water sampled data. The calibration coefficients were listed in Table 2.4.2. Comparisons between the Continuous Sea Surface Water Monitoring System data and water sampled data are shown in Figs. 2.4.2, and 2.4.3.

For fluorometer data, water sampled data obtained at night [PAR (Photosynthetically Available Radiation) < 50 μE/(m^2 sec)] were used for the calibration, since sensitivity of the fluorometer to chlorophyll *a* is different at nighttime and daytime (Section 2.4 in Uchida et al., 2015). Sensitivity of the fluorometer to chlorophyll *a* may also have regional differences. Therefore, slope (c_1) of the calibration coefficients will be changed between legs 1 and 2.

Post-cruise calibration of the nitrate sensor will be carried out after quality control of the water sampled nitrate data is finished.

(6) References

Uchida, H., G. C. Johnson, and K. E. McTaggart (2010): CTD oxygen sensor calibration procedures, The GO-SHIP Repeat Hydrography Manual: A collection of expert reports and guidelines, IOCCP Rep., No. 14, ICPO Pub. Ser. No. 134.

Uchida, H., K. Katsumata, and T. Doi (2015): WHP P14S, S04I Revisit Data Book, JASTEC, Yokosuka, 187 pp.

Table 2.4.2. Nitrate concentration measured by the nitrate sensor for RMNS lot BU (3.888±0.063 [k=2] μmol/kg) and lot CA (19.66±0.15 [k = 2] μmol/kg). Offset (a_0) of the correction equation (see text for detail) at the time of measurement was also shown.

Date	RMNS lot BU	RMNS lot CA	a_0
2016/01/05 11:40-11:47	–17.71±0.58	–0.20±0.88	19.815
2016/01/05 12:02-12:09	8.70±0.16	26.46±0.17	–4.012
2016/01/10 00:06-00:11	–11.08±0.38	6.11±0.29	14.005
2016/01/17 05:51-05:58	9.65±0.18	27.84±0.20	–5.058
2016/01/23 06:54-07:01	–17.82±0.64	–0.61±0.45	20.049

Table 2.4.3. Calibration coefficients for the salinity, dissolved oxygen, chlorophyll *a*, and nitrate.

	c_0	c_1	c_2	c_3
Salinity				
	9.031385e-02	0.9976929	1.379279e-04	
Dissolved oxygen				
	9.417670	0.9360383	0.0	-8.925093e-03
Chlorophyll a				
Nitrate				

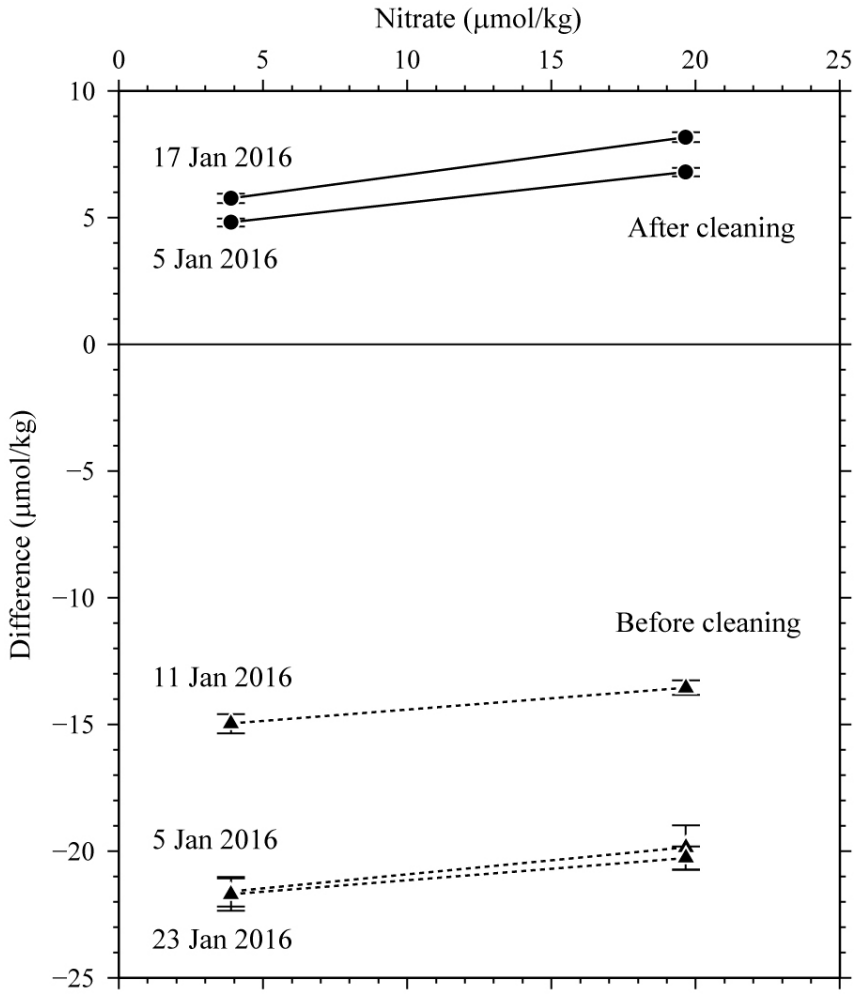

Figure 2.4.1. Results of RMNS measurements by the nitrate sensor. Differences between measured value and certified

value are shown. Error bar shows the standard deviation of the measurements.

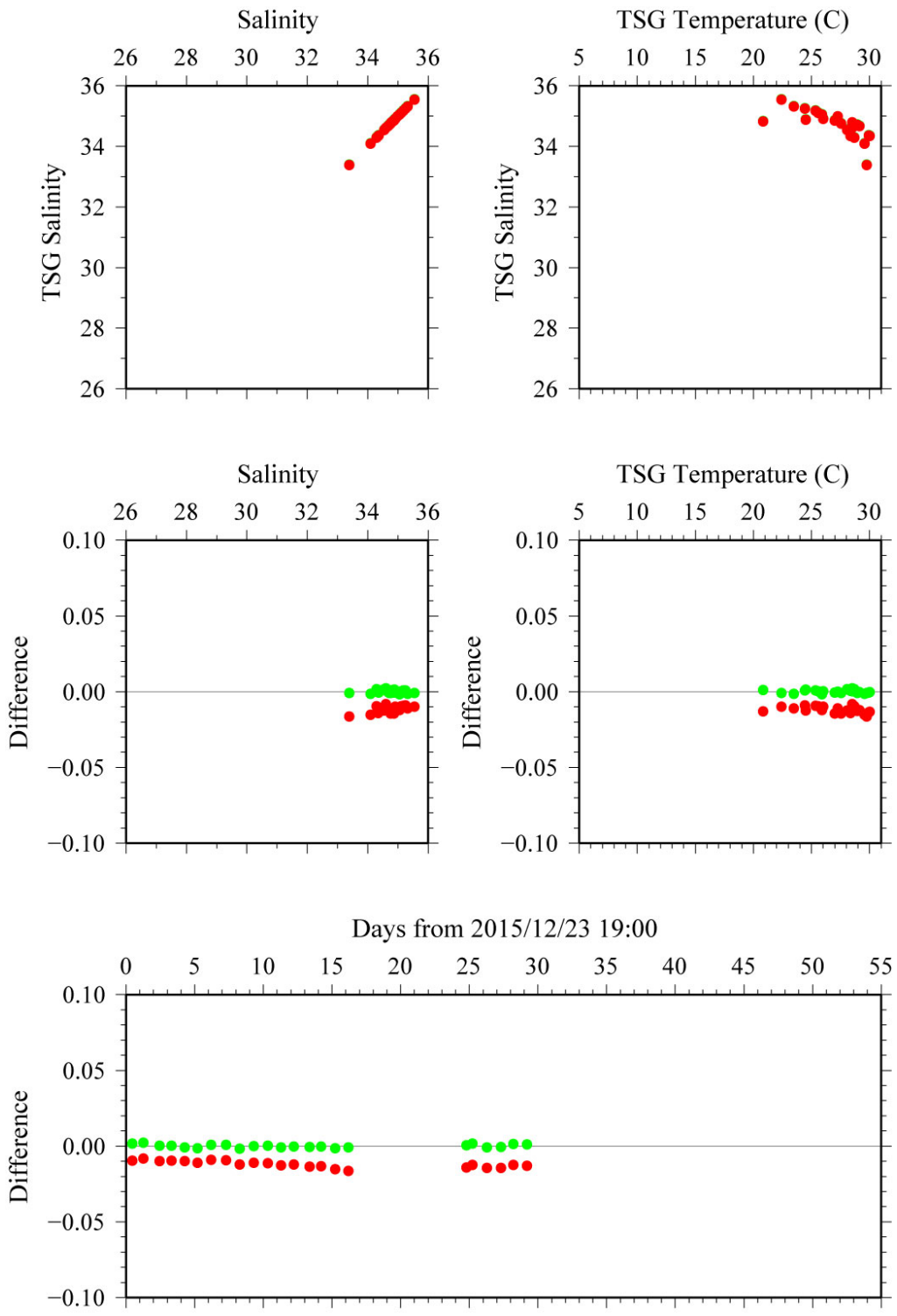

Figure 2.4.2. Comparison between TSG salinity (red: before correction, green: after correction) and sampled salinity.

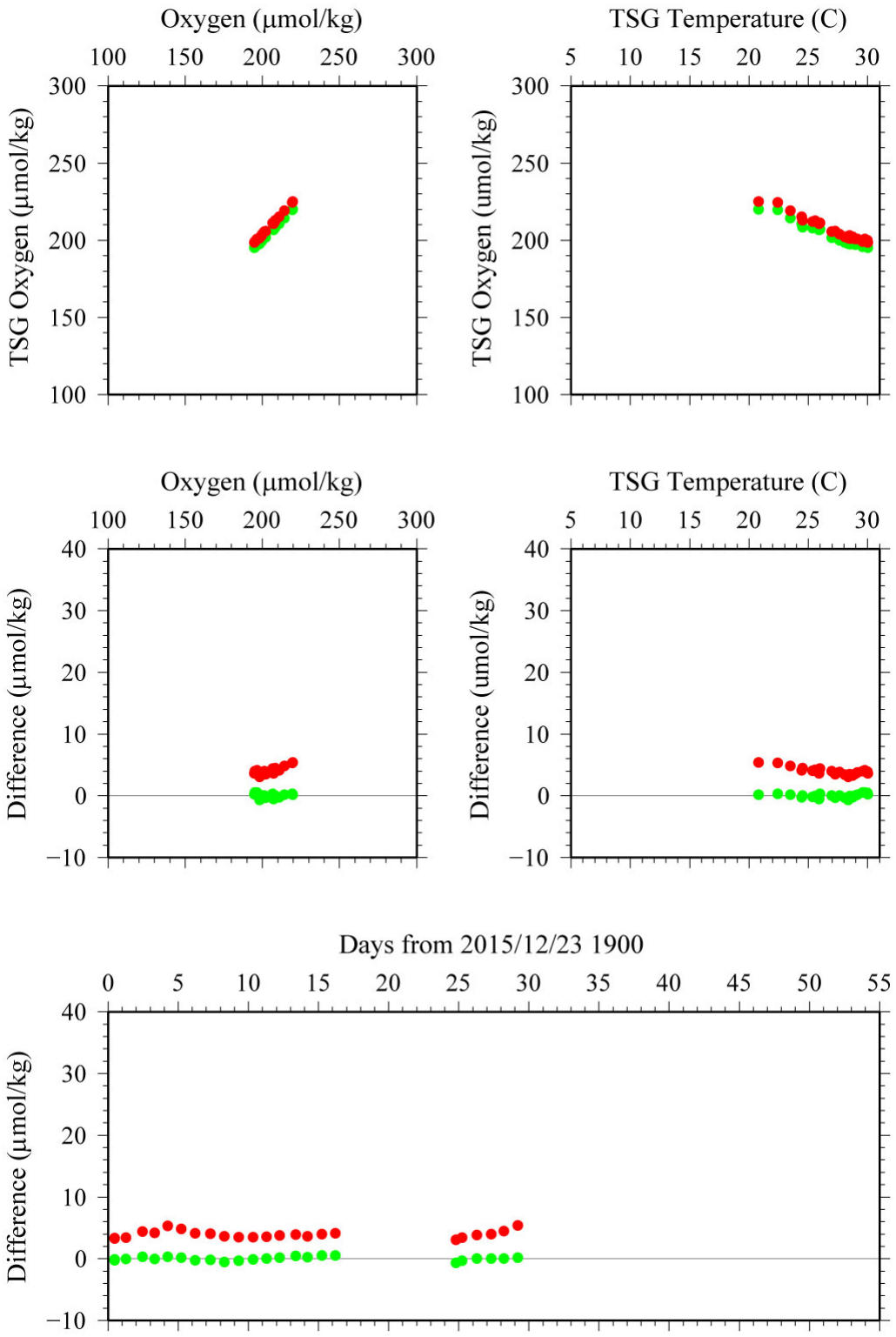

Figure 2.4.3. Comparison between TSG oxygen (red: before correction, green: after correction) and sampled oxygen.

2.5. Surface pCO_2

(1) Personnel

Akihiko Murata (JAMSTEC)

Atsushi Ono (NIO)

Makoto Takada (MWJ)

Tomonori Watai (MWJ)

(2) Objective

Concentrations of CO_2 in the atmosphere are now increasing at a rate of about 2.0 ppmv y^{-1} owing to human activities such as burning of fossil fuels, deforestation, and cement production. It is an urgent task to estimate as accurately as possible the absorption capacity of the oceans against the increased atmospheric CO_2, and to clarify the mechanism of the CO_2 absorption, because the magnitude of the anticipated global warming depends on the levels of CO_2 in the atmosphere, and because the ocean currently absorbs 1/3 of the 6 Gt of carbon emitted into the atmosphere each year by human activities.

In this cruise, we were aimed at quantifying how much anthropogenic CO_2 absorbed in the surface ocean in the eastern part of the Indian Ocean and in the western North Pacific. For the purpose, we measured pCO_2 (partial pressure of CO_2) in the atmosphere and surface seawater along the observation line.

(3) Apparatus

Concentrations of CO_2 in the atmosphere and the sea surface were measured continuously during the cruise using an automated system with a non-dispersive infrared (NDIR) analyzer (Li-COR LI-7000). The automated system (Nippon ANS) was operated by about one and a half hour cycle. In one cycle, standard gasses, marine air and an air in a headspace of an equilibrator were analyzed subsequently. The nominal concentrations of the standard gas were 270, 330, 359 and 419 ppmv. The standard gases will be calibrated after the cruise.

The marine air taken from the bow was introduced into the NDIR by passing through a mass flow controller, which controlled the air flow rate at about 0.6 – 0.8 L/min, a cooling unit, a perma-pure dryer (GL Sciences Inc.) and a desiccant holder containing $Mg(ClO_4)_2$.

A fixed volume of the marine air taken from the bow was equilibrated with a stream of seawater that flowed at a rate of 4.0 – 5.0 L/min in the equilibrator. The air in the equilibrator was circulated with a pump at 0.7-0.8L/min in a closed loop passing through two cooling units, a perma-pure dryer (GL Science Inc.) and a desiccant holder containing $Mg(ClO_4)_2$.

(4) Results

Concentrations of CO_2 (xCO_2) of marine air and surface seawater are shown in Fig. 2.5.1, together with SST.

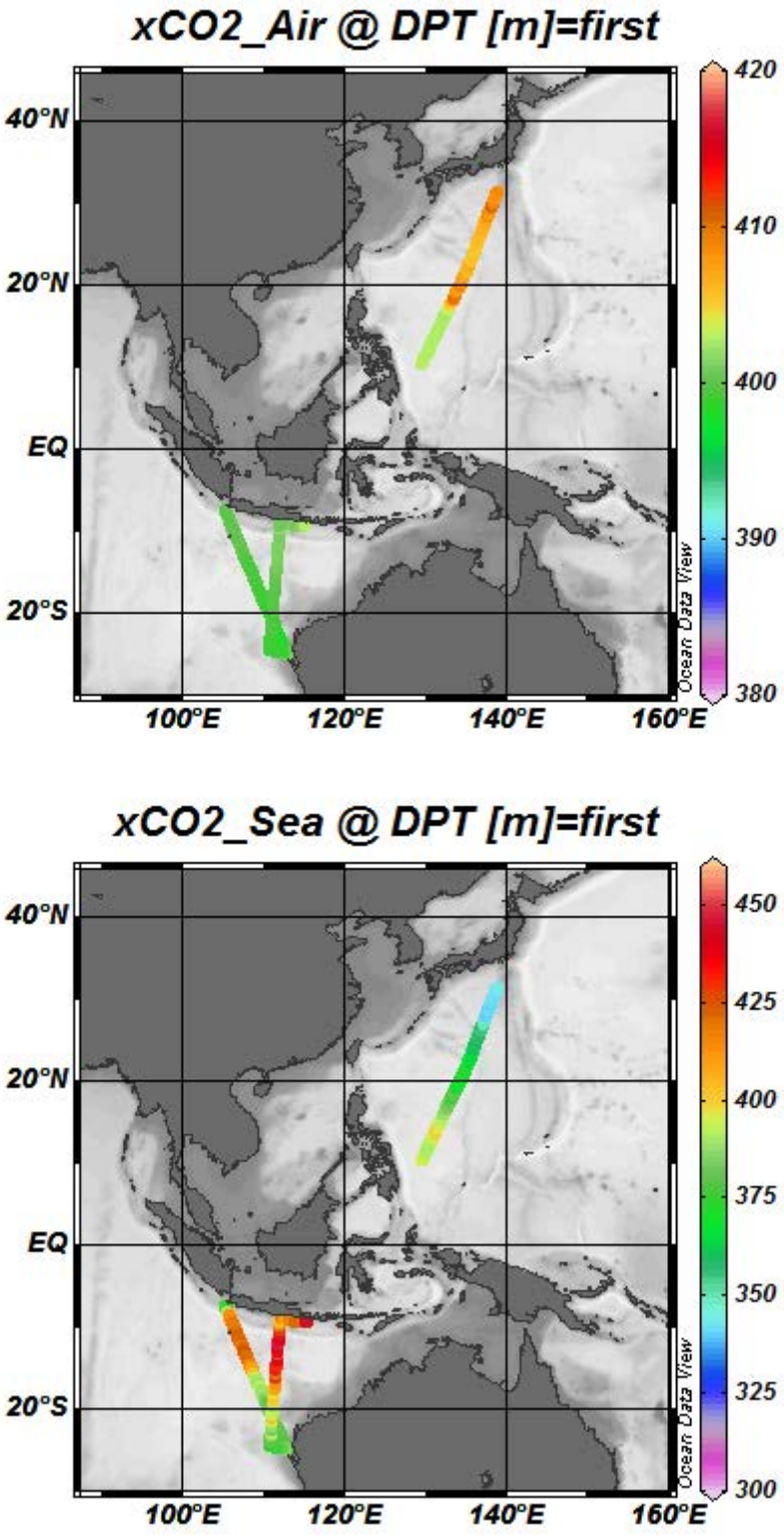

Fig. 2.5.1. Preliminary results of concentrations of CO_2 (xCO_2) in atmosphere (upper panel) and surface seawater (lower panel) observed during MR15-05.

2.6 Ceilometer observation

(1) Personnel

Katsuro Katsumata	***JAMSTEC: Principal investigator***	***- leg1 -***
Akihiko Murata	***JAMSTEC: Principal investigator***	***- leg2 -***
Wataru Tokunaga	***Global Ocean Development Inc., (GODI)***	***- leg1 -***
Tetsuya Kai	***GODI***	***- leg1 -***
Koichi Inagaki	***GODI***	***- leg2 -***
Yutaro Murakami	***GODI***	***- leg1, leg2 -***
Ryo Kimura	***MIRAI crew***	***- leg1 -***
Masanori Murakami	***MIRAI crew***	***- leg2 -***

(2) Objectives

The information of cloud base height and the liquid water amount around cloud base is important to understand the process on formation of the cloud. As one of the methods to measure them, the ceilometer observation was carried out.

(3) Parameters

1. Cloud base height [m].
2. Backscatter profile, sensitivity and range normalized at 10 m resolution.
3. Estimated cloud amount [oktas] and height [m]; Sky Condition Algorithm.

(4) Methods

We measured cloud base height and backscatter profile using ceilometer (CL51, VAISALA, Finland). Major parameters for the measurement configuration are shown in Table 2.6-1;

Table 2.6-1 Major parameters

Laser source:	Indium Gallium Arsenide (InGaAs) Diode
Transmitting center wavelength:	910±10 nm at 25 degC
Transmitting average power:	19.5 mW
Repetition rate:	6.5 kHz
Detector:	Silicon avalanche photodiode (APD) Responsibility at 905 nm: 65 A/W
Cloud detection range:	0 ~ 13 km
Measurement range:	0 ~ 15 km
Resolution:	10 meter in full range
Sampling rate:	36 sec
Sky Condition:	Cloudiness in octas (0 ~ 9) (0: Sky Clear, 1: Few, 3: Scattered, 5-7: Broken, 8: Overcast, and 9: Vertical Visibility)

On the archive dataset, cloud base height and backscatter profile are recorded with the resolution of 10 m (33 ft).

(5) Preliminary results

Fig.2.6-1 shows the time series of 1st, 2nd and 3rd lowest cloud base height during the cruise.

(6) Data archives

The raw data obtained during this cruise will be submitted to the Data Management Group (DMG) of JAMSTEC.

(7) Remarks (Times in UTC)

i) The following periods, the observation were carried out.
Leg1: 18:51, 23 Dec. 2015 to 22:40, 10 Jan. 2016
Leg2: 13:35, 17 Jan. 2016 to 23:50, 24 Jan. 2016

ii) The following time, the window was cleaned.
01:27, 27 Dec. 2015
01:10, 03 Jan. 2016
01:30, 21 Jan. 2016

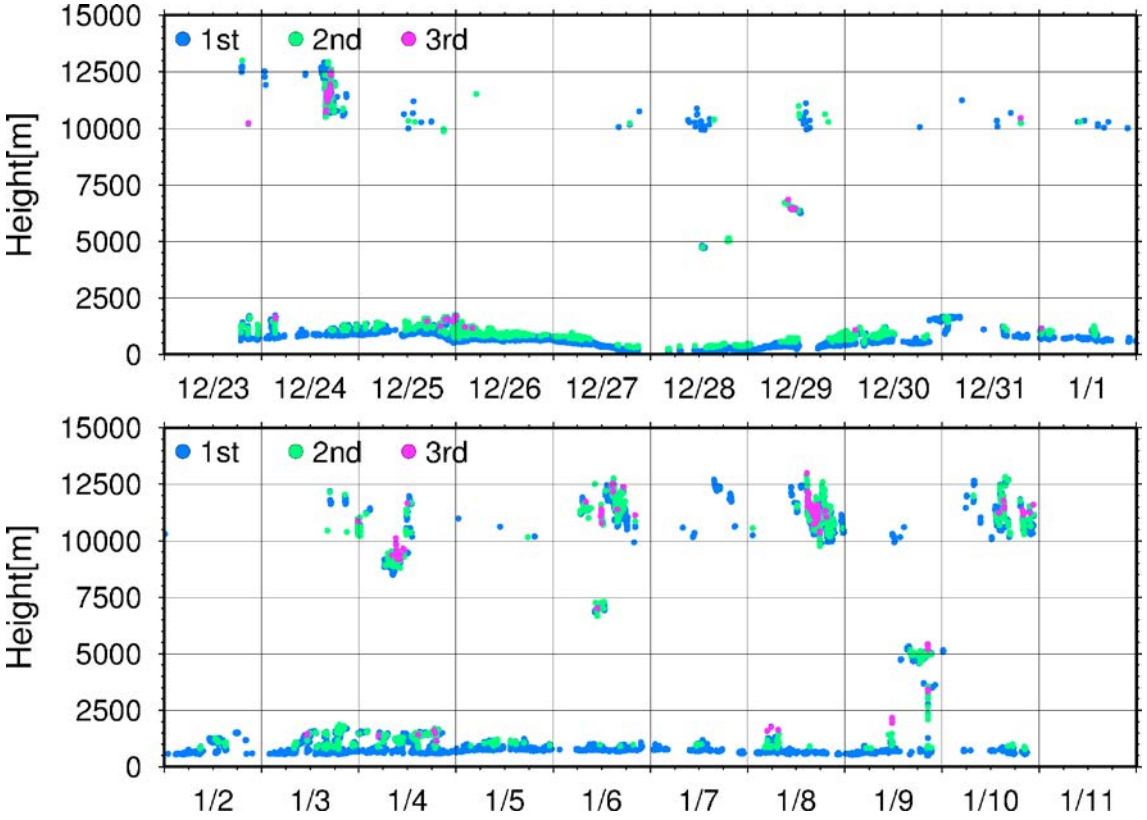

Fig. 2.6-1 1st, 2nd and 3rd lowest cloud base height during this cruise (Leg1).

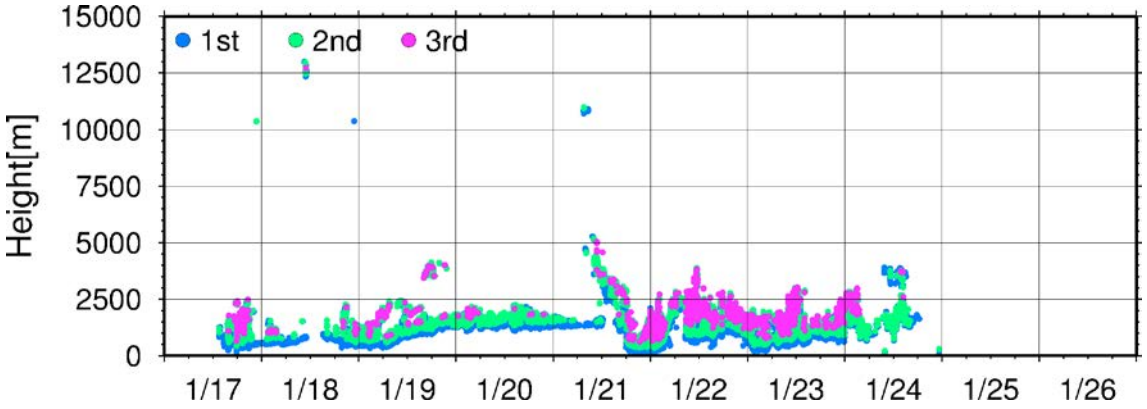

Fig. 2.6-1 Continued (Leg2).

2.7 Surface CO_2 fluxes

Kei Shiomi (JAXA)
Shuji KAWAKAMI (JAXA)
Masakatsu NAKAJIMA (JAXA)
Yoshiyuki NAKANO (JAMSTEC)

(1) Objective

Greenhouse gases Observing SATellite (GOSAT) was launched on 23 January 2009 in order to observe the global distributions of atmospheric greenhouse gas concentrations: column-averaged dry-air mole fractions of carbon dioxide (CO_2) and methane (CH_4). A network of ground-based high-resolution Fourier transform spectrometers provides essential validation data for GOSAT. Vertical CO_2 profiles obtained during ascents and descents of commercial airliners equipped with the in-situ CO_2 measuring instrument are also used for the GOSAT validation. Because such validation data are obtained mainly over land, there are very few data available for the validation of the over-sea GOSAT products. The objectives of our research are to acquire the validation data over the Indian Ocean and the tropical Pacific Ocean using an automated compact instrument, to compare the acquired data with the over-sea GOSAT products, and to develop a simple estimation of the carbon flux between the ocean and the atmosphere from GOSAT data.

(2) Description of instruments deployed

The column-averaged dry-air mole fractions of CO_2 and CH_4 can be estimated from absorption by atmospheric CO_2 and CH_4 that is observed in a solar spectrum. An optical spectrum analyzer (OSA, Yokogawa M&I co., AQ6370) was used for measuring the solar absorption spectra in the near-infrared spectral region. A solar tracker (PREDE co., ltd.) and a small telescope (Figure 1) collected the sunlight into the optical fiber that was connected to the OSA. The solar tracker searches the sun every one minute until the sunlight with a defined intensity. The measurements of the solar spectra were performed during solar zenith angles less than 80°.

Figure 1. Solar tracker and telescope. The sunlight collected into optical fiber was introduced into the OSA that was installed in an observation room in the MIRAI.

(3) Analysis method

The CO_2 absorption spectrum at the 1.6 μm band measured with the OSA is shown in Figure 2. The absorption spectrum can be simulated based on radiative transfer theory using assumed atmospheric profiles of pressure, temperature, and trace gas concentrations. The column abundance of CO_2 (CH_4) was retrieved by adjusting the assumed CO_2 (CH_4) profile to minimize the differences between the measured and simulated spectra.

Figure 3 shows an example of spectral fit performed for the spectral region with the CO_2 absorption lines. The column-averaged dry-air mole fraction of CO_2 (CH_4) was obtained by taking the ratio of the CO_2 (CH_4) column to the dry-air column.

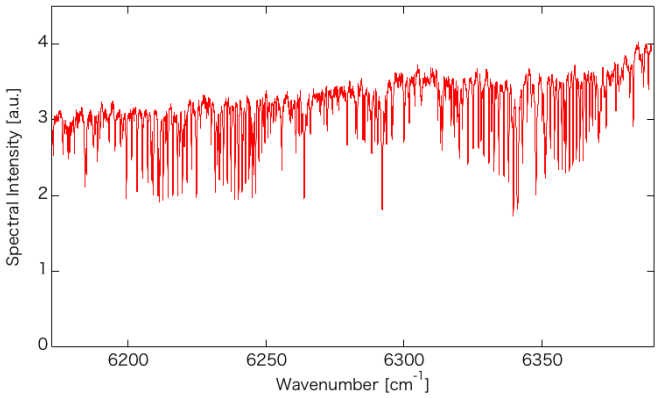

Figure 2. 1.6 μm CO_2 absorption spectrum measured with the OSA.

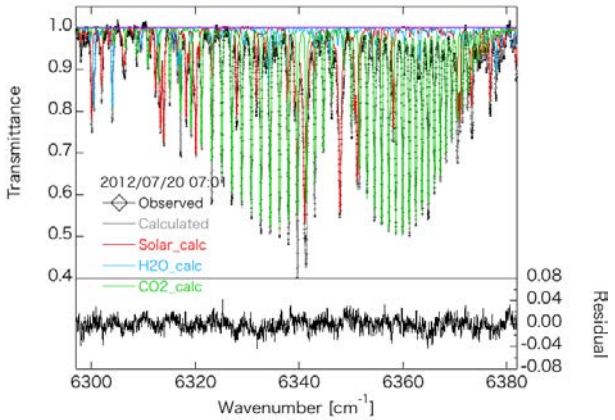

Figure 3. Spectral fit performed for the 6297–6382 cm^{-1} region using an OSA spectrum. Open diamonds denote the measured spectrum, and the solid line denotes the spectrum calculated from the retrieval result. The residual between the measured and calculated spectra is also shown.

(4) Preliminary results

The observations were made from December 24, 2015 to January 24, 2016 continuously in daytime (Table 1 and Figure 2).

CO_2 observations		
Date	Start Time(JST)	End Time(JST)
2015/12/24	09:14	19:34
2015/12/25	08:14	19:36
2015/12/26	08:14	19:44
2015/12/27	08:09	18:43
2015/12/28	07:44	19:31
2015/12/29	07:39	19:37
2015/12/30	07:55	19:49
2015/12/31	07:47	19:29
2016/01/01	07:50	19:45
2016/01/02	07:53	19:38
2016/01/03	07:56	18:11
2016/01/04	07:58	16:37
2016/01/05	08:00	19:03
2016/01/06	08:05	18:54
2016/01/07	08:04	19:15
2016/01/08	08:06	19:06
2016/01/09	08:08	19:10
2016/01/18	07:32	17:15
2016/01/19	07:38	13:16
2016/01/20	07:38	16:38
2016/01/21	07:38	16:38
2016/01/24	09:15	16:10

Table 1. Period of CO_2 observations

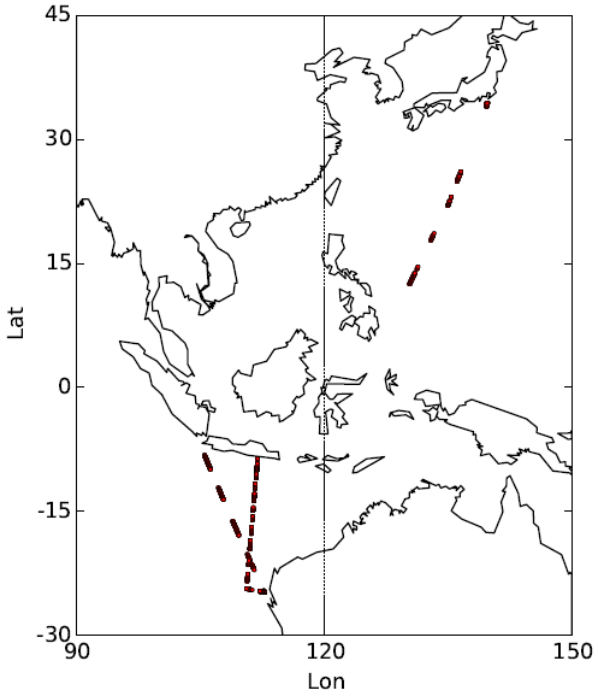

Figure 2. Locations of CO_2 observations

(5) Data archive

The column-averaged dry-air mole fractions of CO_2 and CH_4 retrieved from the OSA spectra will be submitted to JAMSTEC Data Management Group (DMG).

2.8. Radars and Disdrometers

(1) Personnel

Masaki Katsumata (JAMSTEC)

Yuki Kaneko (JAXA)

Kazuhide Yamamoto (JAXA) (not on board)

(2) Objectives

Accurate measurement of the precipitating particle on its amount, phase and their spatiotemporal distributions is crucial to understand the climate system, thru evaluating the latent heating of the atmosphere, radiative heating of the atmosphere and ocean, fresh water flux into the ocean, etc. To better measure and understand the global precipitation, we deployed various instruments to measure the various characteristics of the precipitation on R/V Mirai which deployed globally. The objective of this observation is (a) to reveal various characteristics of the rainfall, depends on the type, temporal stage, etc. of the precipitating clouds, (b) to retrieve the coefficient to convert radar reflectivity to the rainfall amount, and (c) to validate the algorithms and the product of the satellite-borne precipitation radars; TRMM/PR and GPM/DPR.

(3) Apparatus

(3-1) Disdrometers

Four different types of disdrometers are utilized to obtain better reasonable and accurate value on the moving vessel. Three of the disdrometers and one optical rain gauge are installed in one place, the starboard side on the roof of the anti-rolling system of R/V Mirai, as in Fig. 2.8-1. One of the disdrometers named “micro rain radar” is installed at the starboard side of the anti-rolling systems (see Fig. 2.8-2).

The details of the sensors are described below. All the sensors archive data every one minute.

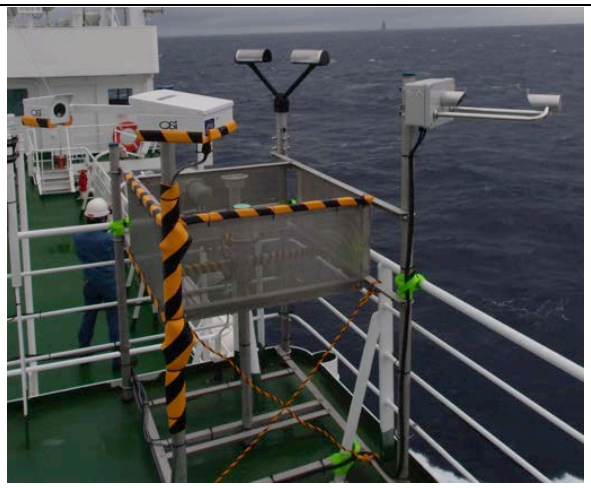

Fig. 2.8-1: The three disdrometers (Parsivel, LPM and Joss-Waldvogel disdrometer) and an optical rain gauge, installed on the roof of the anti-rolling tank.

(3-1-1) Joss-Waldvogel type disdrometer

The “Joss-Waldvogel-type” disdrometer system (RD-80, Disdromet Inc.) (hereafter JW) equipped a microphone on the top of the sensor unit. When a raindrop hit the microphone, the magnitude of induced sound is

converted to the size of raindrops. The logging program “DISDRODATA” determines the size as one of the 20 categories as in Table 2.8-1, and accumulates the number of raindrops at each category. The rainfall amount could be also retrieved from the obtained drop size distribution. The number of raindrops in each category, and converted rainfall amount, are recorded every one minute.

(3-1-2) Laser Precipitation Monitor (LPM) optical disdrometer

The “Laser Precipitation Monitor (LPM)” (Adolf Thies GmbH & Co) is an optical disdrometer. The instrument consists of the transmitter unit which emit the infrared laser, and the receiver unit which detects the intensity of the laser come thru the certain path length in the air. When a precipitating particle fall thru the laser, the received intensity of the laser is reduced. The receiver unit detect the magnitude and the duration of the reduction and then convert them onto particle size and fall speed. The sampling volume, i.e. the size of the laser beam “sheet”, is 20 mm (W) x 228 mm (D) x 0.75 mm (H).

The number of particles are categorized by the detected size and fall speed and counted every minutes. The categories are shown in Table 2.8-2.

(3-1-3) “Parsivel” optical disdrometer

The “Parsivel” (OTT Hydromet GmbH) is another optical disdrometer. The principle is same as the LPM. The sampling volume, i.e. the size of the laser beam “sheet”, is 30 mm (W) x 180 mm (D). The categories are shown in Table 2.8-3.

(3-1-4) Optical rain gauge

The optical rain gauge, which detect scintillation of the laser by falling raindrops, is installed beside the above three disdrometers to measure the exact rainfall. The ORG-815DR (Optical Scientific Inc.) is utilized with the controlling and recording software (manufactured by Sankosha Co.).

Table 2.8-1: Category number and corresponding size of the raindrop for JW disdrometer.

Category	Corresponding size range [mm]		
1	0.313	-	0.405
2	0.405	-	0.505
3	0.505	-	0.696
4	0.696	-	0.715
5	0.715	-	0.827
6	0.827	-	0.999
7	0.999	-	1.232
8	1.232	-	1.429
9	1.429	-	1.582
10	1.582	-	1.748
11	1.748	-	2.077
12	2.077	-	2.441
13	2.441	-	2.727
14	2.727	-	3.011
15	3.011	-	3.385
16	3.385	-	3.704
17	3.704	-	4.127
18	4.127	-	4.573
19	4.573	-	5.145
20	5.145	or larger	

Table 2.8-2: Categories of the size and the fall speed for LPM.

Particle Size		
Class	Diameter [mm]	Class width [mm]
1	≥ 0.125	0.125
2	≥ 0.250	0.125
3	≥ 0.375	0.125
4	≥ 0.500	0.250
5	≥ 0.750	0.250
6	≥ 1.000	0.250
7	≥ 1.250	0.250
8	≥ 1.500	0.250
9	≥ 1.750	0.250
10	≥ 2.000	0.500
11	≥ 2.500	0.500
12	≥ 3.000	0.500
13	≥ 3.500	0.500
14	≥ 4.000	0.500
15	≥ 4.500	0.500
16	≥ 5.000	0.500
17	≥ 5.500	0.500
18	≥ 6.000	0.500
19	≥ 6.500	0.500
20	≥ 7.000	0.500
21	≥ 7.500	0.500
22	≥ 8.000	unlimited

Fall Speed		
Class	Speed [m/s]	Class width [m/s]
1	≥ 0.000	0.200
2	≥ 0.200	0.200
3	≥ 0.400	0.200
4	≥ 0.600	0.200
5	≥ 0.800	0.200
6	≥ 1.000	0.400
7	≥ 1.400	0.400
8	≥ 1.800	0.400
9	≥ 2.200	0.400
10	≥ 2.600	0.400
11	≥ 3.000	0.800
12	≥ 3.400	0.800
13	≥ 4.200	0.800
14	≥ 5.000	0.800
15	≥ 5.800	0.800
16	≥ 6.600	0.800
17	≥ 7.400	0.800
18	≥ 8.200	0.800
19	≥ 9.000	1.000
20	≥ 10.000	10.000

Table 2.8-3: Categories of the size and the fall speed for Parsivel.

Particle Size		
Class	Average Diameter [mm]	Class spread [mm]
1	0.062	0.125
2	0.187	0.125
3	0.312	0.125
4	0.437	0.125
5	0.562	0.125
6	0.687	0.125
7	0.812	0.125
8	0.937	0.125
9	1.062	0.125
10	1.187	0.125
11	1.375	0.250
12	1.625	0.250
13	1.875	0.250
14	2.125	0.250
15	2.375	0.250
16	2.750	0.500
17	3.250	0.500
18	3.750	0.500
19	4.250	0.500
20	4.750	0.500
21	5.500	1.000
22	6.500	1.000
23	7.500	1.000
24	8.500	1.000
25	9.500	1.000
26	11.000	2.000
27	13.000	2.000
28	15.000	2.000
29	17.000	2.000
30	19.000	2.000
31	21.500	3.000
32	24.500	3.000

Fall Speed		
Class	Average Speed [m/s]	Class Spread [m/s]
1	0.050	0.100
2	0.150	0.100
3	0.250	0.100
4	0.350	0.100
5	0.450	0.100
6	0.550	0.100
7	0.650	0.100
8	0.750	0.100
9	0.850	0.100
10	0.950	0.100
11	1.100	0.200
12	1.300	0.200
13	1.500	0.200
14	1.700	0.200
15	1.900	0.200
16	2.200	0.400
17	2.600	0.400
18	3.000	0.400
19	3.400	0.400
20	3.800	0.400
21	4.400	0.800
22	5.200	0.800
23	6.000	0.800
24	6.800	0.800
25	7.600	0.800
26	8.800	1.600
27	10.400	1.600
28	12.000	1.600
29	13.600	1.600
30	15.200	1.600
31	17.600	3.200
32	20.800	3.200

(3-2) Micro rain radar

The MRR-2 (METEK GmbH) was utilized. The specifications are in Table 2.8-4. The antenna unit was installed at the starboard side of the anti-rolling systems (see Fig. 2.8-2), and wired to the junction box and laptop PC inside the vessel.

The data was averaged and stored every one minute. The vertical profile of each parameter was obtained every 200 meters in range distance (i.e. height) up to 6200 meters, i.e. well beyond the melting layer. The drop size distribution is recorded, as well as radar reflectivity, path-integrated attenuation, rain rate, liquid water content and fall velocity.

Fig. 2.8-2: The micro rain radar, installed on the starboard side of the anti-rolling tank.

Table 2.8-4: Specifications of the MRR-2.

Transmitter power	50 mW
Operating mode	FM-CW
Frequency	24.230 GHz (modulation 1.5 to 15 MHz)
3dB beam width	1.5 degrees
Spurious emission	< -80 dBm / MHz
Antenna Diameter	600 mm
Gain	40.1 dBi

(3-3) Ka-band radar

The Ka-band radar (Manufactured by Mitsubishi Electric Co.) was utilized. The specifications are in Table 2.8-5. The antenna unit was installed at the stern (starboard side) of the vessel (see Fig. 2.8-x), and wired to the signal processing unit inside the vessel (so-called “dry labo”). Antenna direction is fixed to zenith relative to the ship.

Table 2.8-5: Specifications of the Ka-band radar

Frequency	35.25 GHz (Ka-band)

Modulation Principle	FMCW
Minimum Detect Zm	-20 dBZ at 10 km
Minimum Range Resolution	12.5 m
Minimum Time Resolution	10 sec
Niquist Velocity	±10.6 m/s
Observable range	From 500 m to 30 km (Depends on the observation mode)
Antenna beam width	0.6 deg
Antenna sidelobe	< 25 dBZ
Radar Variables	Radar reflectivity and Doppler spectrum

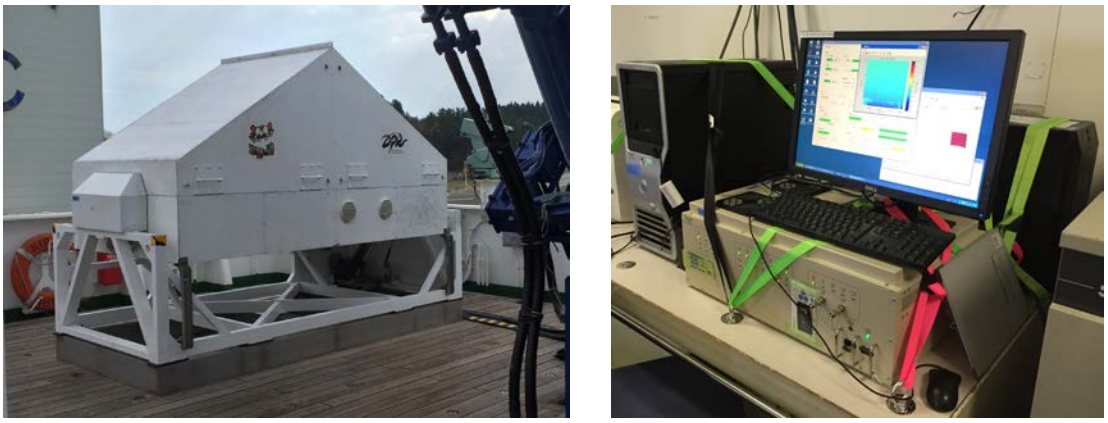

Fig. 2.8-3: The Ka-band radar system. (left) Antenna part, at the right-side of the stern of the upper deck. (right) Signal processer part, in the “dry labo.”

(3-3) C-band radar

The C-band polarimetric weather radar in R/V Mirai was utilized. The basic specifications are in Table 2.4-4. The antenna is controlled to point the commanded ground-relative direction, by controlling the azimuth and elevation to cancel the ship attitude (roll, pitch and yaw) detected by the laser gyro. The Doppler velocity is also corrected by subtracting the ship movement in beam direction.

For the maintenance, internal signals of the radar are checked and calibrated at the beginning and the end of the cruise. Meanwhile, the following parameters are checked daily; (1) frequency, (2) mean output power, (3) pulse width, and (4) PRF (pulse repetition frequency).

During the cruise, parameters in Table 2.x-x were obtained. Scan strategies are shown in Table 2.x-x. The radar is operated to repeat the cycle every 6 minutes basically, while every 30 minutes to obtain surveillance PPI. A dual PRF mode is used for a volume scan. For vertical pointing scan and surveillance PPI scans, a single PRF mode is used.

Table 5.3-1 Scan settings of the C-band radar in the cruise.

	Surveillance PPI Scan	Volume Scan	Vertical Point Scan

Repeated Cycle (min.)	30	6					6
Times in One Cycle	1	1					3
Pulse Width (long / short, in microsec)	200 / 2	64 / 1		32 / 1		32 / 1	32 / 1
Scan Speed (deg/sec)	36	18		24		36	36
PRF(s) (Hz)	400	dual PRF (ray alternative)					2000
		667	833	938	1250	1333	2000
Pulses / Ray	8	26	33	27	34	37	55	64
Ray Spacing (deg.)	0.7	0.7		0.7		1.0	1.0
Azimuth (deg)	Full Circle						
Bin Spacing (m)	150						
Max. Range (km)	300	150		100		60	60
Elevation Angle(s) (deg.)	0.5	0.5		1.0, 1.8, 2.6, 3.4, 4.2, 5.1, 6.2, 7.6, 9.7, 12.2, 15.2		18.7, 23.0, 27.9, 33.5, 40.0	90

(4) Results

The data were obtained continuously thru the cruise from Dec.23, 2015 to Jan.23, 2016, except the period when Mirai was in the area where the observation is not permitted. The further analyses will be done after the cruise.

(5) Data Archive

All data obtained during this cruise will be submitted to the JAMSTEC Data Management Group (DMG).

2.9. Aerosol optical characteristics measured by Ship-borne Sky radiometer

(1) Personnel

Kazuma Aoki (University of Toyama) - Principal Investigator (not on board)
Tadahiro Hayasaka (Tohoku University) - Co-Investigator (not onboard)
(Sky radiometer operation was supported by Global Ocean Development Inc.)

(2) Objectives

Objective of this observation is to study distribution and optical characteristics of marine aerosols by using a ship-borne sky radiometer (POM-01 MKII: PREDE Co. Ltd., Japan). Furthermore, collections of the data for calibration and validation to the remote sensing data were performed simultaneously.

(3) Methods and Instruments

The sky radiometer measures the direct solar irradiance and the solar aureole radiance distribution with seven interference filters (0.34, 0.4, 0.5, 0.675, 0.87, 0.94, and 1.02 μm). Analysis of these data was performed by SKYRAD.pack version 4.2 developed by Nakajima *et al*. 1996.

@ Measured parameters

- Aerosol optical thickness at five wavelengths (400, 500, 675, 870 and 1020 nm)
- Ångström exponent
- Single scattering albedo at five wavelengths
- Size distribution of volume (0.01 μm – 20 μm)

GPS provides the position with longitude and latitude and heading direction of the vessel, and azimuth and elevation angle of the sun. Horizon sensor provides rolling and pitching angles.

(4) Preliminary results

Only data collection were performed onboard. At the time of writing, the data obtained in this cruise are under post-cruise processing at University of Toyama.

(5) Data archives

Aerosol optical data are to be archived at University of Toyama (K.Aoki, SKYNET/SKY: http://skyrad.sci.u-toyama.ac.jp/) after the quality check and will be submitted to JAMSTEC.

2.10. Aerosol and gases

(1) Personnel

Yugo Kanaya (JAMSTEC) not on board

Kazuhiko Matsumoto (JAMSTEC) on board (Leg 1)

Fumikazu Taketani (JAMSTEC) not on board

Takuma Miyakawa (JAMSTEC) not on board

Hisahiro Takashima (JAMSTEC) not on board

Yuichi Komazaki (JAMSTEC) not on board

Hitoshi Matsui (JAMSTEC) not on board

Operation was supported by Global Ocean Development Inc.

(2) Objectives

The major objective is to investigate processes of biogeochemical cycles between the atmosphere and the ocean. Particularly, we characterize the atmospheric aerosol particles by fluorescence techniques (autofluorescence and stained fluorescence) to observe biologically-produced particles. To study the possibility that those particles are ejected from the ocean surface as sea spray, relationship with the density/types of plankton in seawater is studied. Also, we investigate roles of atmospheric aerosols and gases, including black carbon and ozone, in the marine atmosphere in relation to climate change.

(3) Methods and Instruments

i. Parameters continuously observed species and parameters

- Number density of autofluorescent atmospheric aerosol particles
- Mass concentrations of black carbon (BC) particles
- Surface ozone (O_3), and carbon monoxide (CO) mixing ratios
- Aerosol optical depth (AOD) and aerosol extinction coefficient (AEC)

Online observations fluorescent particles and black carbon (BC) particles were made by the instruments based on flash-lamp-induced fluorescence (WIBS-4A, Droplet Measurement Technologies) and laser-induced incandescence (SP2, Droplet Measurement Technologies). Ambient air was continuously sampled from the flying bridge and drawn through a ~3-m-long conductive tube and introduced to the instruments after dried. In WIBS-4A, two pulsed xenon lamps emitting UV light (280 nm and 370 nm) were used for excitation and fluorescence emitted from a single particle within 310–400 nm and 420–650 nm wavelength windows was recorded.

Multi-Axis Differential Optical Absorption Spectroscopy (MAX-DOAS), a passive remote sensing technique measuring spectra of scattered visible and ultraviolet (UV) solar radiation, was used for atmospheric aerosol and gas profile measurements. Our MAX-DOAS instrument consists of two main parts: an outdoor telescope unit and an indoor spectrometer (Acton SP-2358 with Princeton Instruments PIXIS-400B), connected to each other by a 14-m bundle

optical fiber cable. The line of sight was in the directions of the portside of the vessel and the multiple elevation angles, 1.5, 3, 5, 10, 20, 30, 90 degrees, were scanned repeatedly (every ~15-min) using a movable prism. For the selected spectra recorded with elevation angles with good accuracy, DOAS spectral fitting was performed to quantify the slant column density (SCD) of NO_2 (and other gases) and O4 (O_2-O_2, collision complex of oxygen) for each elevation angle. Then, the O_4 SCDs were converted to the aerosol optical depth (AOD) and the vertical profile of aerosol extinction coefficient (AEC) using an optimal estimation inversion method with a radiative transfer model. Using derived aerosol information, retrievals of the tropospheric vertical column/profile of NO_2 and other gases were made.

For ozone and CO measurements, ambient air was continuously sampled on the compass deck and drawn through ~20-m-long Teflon tubes connected to a gas filter correlation CO analyzer (Model 48C, Thermo Fisher Scientific) and a UV photometric ozone analyzer (Model 49C, Thermo Fisher Scientific), located in the Research Information Center. The data will be used for characterizing air mass origins.

ii. Sampling and offline analysis

During Leg 1, atmospheric aerosol particles and surface seawater samples were manually collected for the offline measurements of stained fluorescence from particles. The collected timing and locations are listed in Table 2.10.1. The stained fluorescence observations were made with Bioplorer KB-VKH01 (Koyo Sangyo Co.,Ltd). Double staining with DAPI and PI was utilized, for the detection of total and dead biological particles upon fluorescence signal from individual particles induced by the UV and green light excitation. The atmospheric aerosol particles were directly collected onto membrane filters to be used in the Bioplorer. The seawater samples were filtrated by the membrane filter and then the filter was set in the Bioplorer for the stained fluorescence measurements. For reference, autofluorescence was also analyzed by the Bioplorer before staining.

During Leg 1 and 2, ambient aerosol particles were collected along cruise track using a high-volume air sampler (HV-525PM, SIBATA) located on the flying bridge operated at a flow rate of 500 L min^{-1}. To avoid collecting particles emitted from the funnel of the own vessel, the sampling period was controlled automatically by using a "wind-direction selection system". Coarse and fine particles separated at the diameter of 2.5 μm were collected. The filter samples obtained during the cruise are subject to chemical analysis of aerosol composition, including water-soluble ions and trace metals.

(4) Preliminary results

N/A (Data analysis is to be conducted.)

(5) Data archives

These data obtained in this cruise will be submitted to the Data Management Group of JAMSTEC, and will be opened to the public via "Data Research System for Whole Cruise Information in JAMSTEC (DARWIN)" in JAMSTEC web site.

http://www.godac.jamstec.go.jp/darwin/e

Table 2.10.1. Timing and locations of atmospheric aerosol and seawater samples for stained fluorescence analysis

No.	Sample ID	Type	Collection timing (UTC)	Latitude (deg-min)	Longitude (deg-min)	Depth (m)
1	MR15-05_001a	aerosol	Dec 26, 2015 6:50 UTC	17-11.7 S	109-22.09 E	
2	MR15-05_002a	aerosol	Dec 29, 2015 7:10 UTC	24-22.56 S	110-35.73 E	
3	MR15-05_003s	seawater	Dec 29, 2015 4:30 UTC	24-22.59 S	110-35.41 E	0
4	MR15-05_004a	aerosol	Dec 30, 2015 9:20 UTC	22-51.57 S	110-43.98 E	
5	MR15-05_005s	seawater	Dec 29, 2015 23:31 UTC	23-23.8 S	110-40.52 E	0
6	MR15-05_006a	aerosol	Dec 31, 2015 7:20 UTC	20-57.96 S	110-53.24 E	
7	MR15-05_007a	aerosol	Jan 3, 2016 8:05 UTC	15-36.15 S	111-20.07 E	
8	MR15-05_008a	aerosol	Jan 5, 2016 5:15 UTC	13-10.18 S	111-32.49 E	
9	MR15-05_009a	aerosol	Jan 7, 2016 4:40 UTC	10-42.94 S	111-45.81 E	
10	MR15-05_010a	aerosol	Jan 7, 2016 23:40 UTC	10-2.79 S	111-49.87 E	
11	MR15-05_011s	seawater	Jan 8, 2016 5:03 UTC	9-28.97 S	111-52.94 E	0
12	MR15-05_012a	aerosol	Jan 9, 2016 2:00 UTC	8-38.38 S	111-57.36 E	
13	MR15-05_013a	aerosol	Jan 10, 2016 7:15 UTC	9-11.8 S	113-44.21 E	

2.11 Sea Surface Gravity

(1) Personnel

Katsuro Katsumata	***JAMSTEC: Principal investigator***	***- leg1 -***
Akihiko Murata	***JAMSTEC: Principal investigator***	***- leg2 -***
Wataru Tokunaga	***Global Ocean Development Inc., (GODI)***	***- leg1 -***
Tetsuya Kai	***GODI***	***- leg1 -***
Koichi Inagaki	***GODI***	***- leg2 -***
Yutaro Murakami	***GODI***	***- leg1, leg2 -***
Ryo Kimura	***MIRAI crew***	***- leg1 -***
Masanori Murakami	***MIRAI crew***	***- leg2 -***

(2) Introduction

The local gravity is an important parameter in geophysics and geodesy. We collected gravity data at the sea surface.

(3) Parameters

Relative Gravity [CU: Counter Unit]
[mGal] = (coef1: 0.9946) * [CU]

(4) Data Acquisition

We measured relative gravity using LaCoste and Romberg air-sea gravity meter S-116 (Micro-G LaCoste, LLC) during this cruise.

To convert the relative gravity to absolute gravity, we measured gravity, using portable gravity meter (CG-5, Scintrex), at Sekinehama and Yokohama as the reference points.

(5) Preliminary Results

Absolute gravity table is shown in Table 2.11-1.

Table 2.11-1. Absolute gravity table of the MR15-05 cruise

No.	Date mm/dd	UTC	Port	Absolute Gravity [mGal]	Sea Level [cm]	Ship Draft [cm]	Gravity at Sensor * [mGal]	S-116 Gravity [mGal]
#1	11/05	01:07	Sekinehama	980,371.87	251	607	980,372.81	12662.42
#2	01/25	06:38	Yokohama	979,741.75	196	625	979,742.56	12035.96

*: Gravity at Sensor = Absolute Gravity + Sea Level*0.3086/100 + (Draft-530)/100*0.2222

(6) Data Archive

Surface gravity data obtained during this cruise will be submitted to the Data Management Group (DMG) in JAMSTEC, and will be archived there.

(7) Remarks (Times in UTC)

i) The following periods, the observation was carried out.
Leg1: 18:51, 23 Dec. 2015 to 22:40, 10 Jan. 2016
Leg2: 13:47, 17 Jan 2016 to 00:00, 25 Jan. 2016

ii) The following periods, depth data were available

Leg1: 19:35, 23 Dec. 2015 to 22:05, 10 Jan. 2016
Leg2: 13:47, 17 Jan 2016 to 06:26, 23 Jan. 2016

2.12 Sea Surface Magnetic Field

(1) Personnel

Katsuro Katsumata	***JAMSTEC: Principal investigator***	***- leg1 -***
Akihiko Murata	***JAMSTEC: Principal investigator***	***- leg2 -***
Wataru Tokunaga	***Global Ocean Development Inc., (GODI)***	***- leg1 -***
Tetsuya Kai	***GODI***	***- leg1 -***
Koichi Inagaki	***GODI***	***- leg2 -***
Yutaro Murakami	***GODI***	***- leg1, leg2 -***
Ryo Kimura	***MIRAI crew***	***- leg1 -***
Masanori Murakami	***MIRAI crew***	***- leg2 -***

(2) Introduction

Measurement of magnetic force on the sea is required for the geophysical investigations of marine magnetic anomaly caused by magnetization in upper crustal structure. We measured geomagnetic field using a three-component magnetometer during this cruise.

(3) Principle of ship-board geomagnetic vector measurement

The relation between a magnetic-field vector observed on-board, **H**ob, (in the ship's fixed coordinate system) and the geomagnetic field vector, **F**, (in the Earth's fixed coordinate system) is expressed as:

$$\mathbf{H}ob = \mathbf{A}\ \mathbf{R}\ \mathbf{P}\ \mathbf{Y}\ \mathbf{F} + \mathbf{H}p \qquad (a)$$

where $\mathbf{R}$, $\mathbf{P}$ and $\mathbf{Y}$ are the matrices of rotation due to roll, pitch and heading of a ship, respectively. $\mathbf{A}$ is a 3 x 3 matrix which represents magnetic susceptibility of the ship, and **H**p is a magnetic field vector produced by a permanent magnetic moment of the ship's body. Rearrangement of Eq. (a) makes

$$\mathbf{R}\ \mathbf{H}ob + \mathbf{H}bp = \mathbf{R}\ \mathbf{P}\ \mathbf{Y}\ \mathbf{F} \qquad (b)$$

where $\mathbf{R} = \mathbf{A}^{-1}$, and $\mathbf{H}bp = -\mathbf{R}\ \mathbf{H}p$. The magnetic field, **F**, can be obtained by measuring $\mathbf{R}$, $\mathbf{P}$, $\mathbf{Y}$ and **H**ob, if $\mathbf{R}$ and **H**bp are known. Twelve constants in $\mathbf{R}$ and **H**bp can be determined by measuring variation of **H**ob with $\mathbf{R}$, $\mathbf{P}$ and $\mathbf{Y}$ at a place where the geomagnetic field, **F**, is known.

(4) Instruments on R/V MIRAI

A shipboard three-component magnetometer system (Tierra Tecnica SFG1214) is equipped on-board R/V MIRAI. Three-axes flux-gate sensors with ring-cored coils are fixed on the fore mast. Outputs from the sensors are digitized by a 20-bit A/D converter (1 nT/LSB), and sampled at 8 times per second. Ship's heading, pitch, and roll are measured by the Inertial Navigation System (INS) for controlling attitude of a Doppler radar. Ship's position and speed data are taken from LAN every second.

(5) Data Archive

Sea surface magnetic data obtained during this cruise will be submitted to the Data Management Group (DMG) in JAMSTEC, and will be archived there.

(6) Remarks (Times in UTC)

i) The following periods, the observation were carried out.
Leg1: 18:51, 23 Dec. 2015 to 22:40, 10 Jan. 2016
Leg2: 13:47, 17 Jan 2016 to 23:50, 24 Jan. 2016

ii) The following periods, we made a “figure-eight” turn (a pair of clockwise and anti-clockwise rotation) for calibration of the ship’s magnetic effect.
Leg1: 03:28 - 03:54, 28 Dec. 2015 around 24-44S, 122-36E
09:42 - 10:05, 01 Jan. 2016 around 18-32S, 110-05E
14:30 - 14:56, 04 Jan. 2016 around 14-08S, 111-28E
22:08 - 22:29, 09 Jan. 2016 around 09-10S, 113-45E

Leg2: 01:15 - 01:41, 18 Jan. 2016 around 13-07N, 130-39E
01:29 - 01:53, 23 Jan. 2016 around 31-10N, 138-35E

iii) The following periods, depth data was available
Leg1: 19:35, 23 Dec. 2015 to 22:05, 10 Jan. 2016
Leg2: 13:47, 17 Jan 2016 to 06:26, 23 Jan. 2016

2.13. Satellite image acquisition

(1) Personnel

Katsuro Katsumata	***JAMSTEC: Principal investigator***	***- leg1 -***
Akihiko Murata	***JAMSTEC: Principal investigator***	***- leg2 -***
Wataru Tokunaga	***Global Ocean Development Inc., (GODI)***	***- leg1 -***
Tetsuya Kai	***GODI***	***- leg1 -***
Koichi Inagaki	***GODI***	***- leg2 -***
Yutaro Murakami	***GODI***	***- leg1, leg2 -***
Ryo Kimura	***MIRAI crew***	***- leg1 -***
Masanori Murakami	***MIRAI crew***	***- leg2 -***

(2) Objectives

The objectives are to collect cloud data in a high spatial resolution mode from the Advance Very High Resolution Radiometer (AVHRR) on the NOAA and MetOp polar orbiting satellites, and to verify the data from Doppler radar on board.

(3) Methods

We received the down link High Resolution Picture Transmission (HRPT) signal from satellites, which passed over the area around the R/V MIRAI. We processed the HRPT signal with the in-flight calibration and computed the brightness temperature. A cloud image map around the R/V MIRAI was made from the data for each pass of satellites.

We received and processed polar orbiting satellites data throughout this cruise.

(4) Data archives

The raw data obtained during this cruise will be submitted to the Data Management Group (DMG) in JAMSTEC.

3. Station Observation

3.1 $CTDO_2$ Measurements

February 17, 2016

(1) Personnel

Hiroshi Uchida (JAMSTEC)

Shinsuke Toyoda (MWJ)

Hiroyuki Hayashi (MWJ)

Shungo Oshitani (MWJ)

Keisuke Takeda (MWJ)

Michinari Sunamura (The University of Tokyo) (CDOM measurement)

(2) Winch arrangements

The CTD package was deployed by using 4.5 Ton Traction Winch System (Dynacon, Inc., Bryan, Texas, USA), which was renewed on the R/V Mirai in April 2014 (e.g. Fukasawa et al., 2004). Primary system components include a complete CTD Traction Winch System with up to 9000 m of 9.53 mm armored cable (Rochester Wire & Cable, LLC, Culpeper, Virginia, USA).

To minimize attitude motion of the CTD package (rotation, pitching and rolling) and twist of the armored cable, a slip ring swivel was introduced between the armored cable and the CTD package.

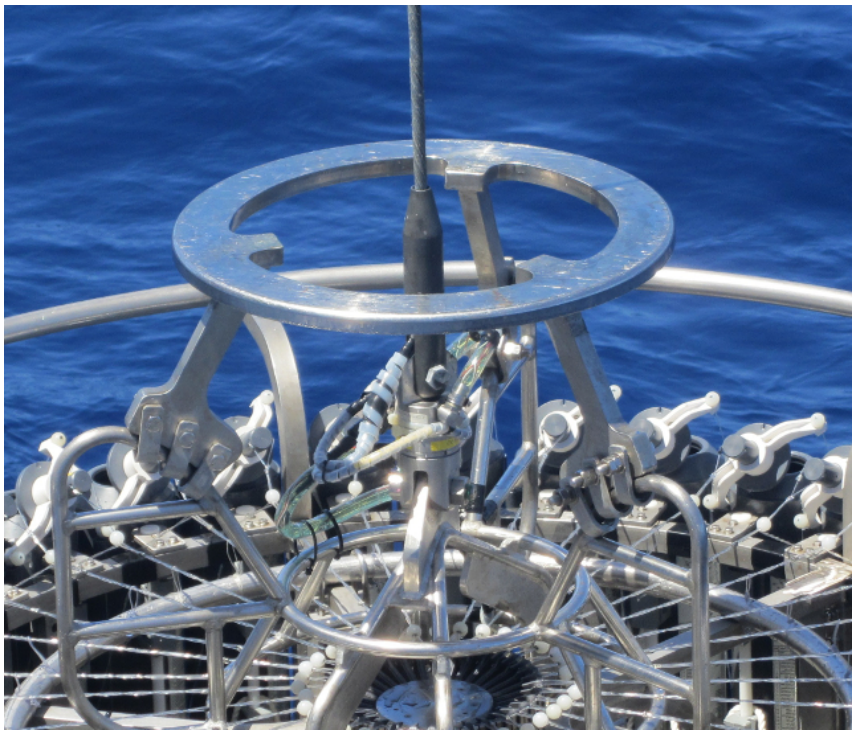

Fig. 3.1.1 A photo of the slip ring swivel attached between the armored cable and the CTD.

(3) Overview of the equipment

The CTD system was SBE 911plus system (Sea-Bird Electronics, Inc., Bellevue, Washington, USA). The SBE 911plus system controls 36-position SBE 32 Carousel Water Sampler. The Carousel accepts 12-litre Niskin-X water sample bottles (General Oceanics, Inc., Miami, Florida, USA). The SBE 9plus was mounted horizontally in a 36-position carousel frame. SBE's temperature (SBE 3) and conductivity (SBE 4) sensor modules were used with the SBE 9plus underwater unit. The pressure sensor is mounted in the main housing of the underwater unit and is ported to outside through the oil-filled plastic capillary tube. A modular unit of underwater housing pump (SBE 5T) flushes water through sensor tubing at a constant rate independent of the CTD's motion, and pumping rate (3000 rpm) remain nearly constant over the entire input voltage range of 12-18 volts DC. Flow speed of pumped water in standard TC duct is about 2.4 m/s. Two sets of temperature and conductivity modules were used. An SBE's dissolved oxygen sensor (SBE 43) was placed between the primary conductivity sensor and the pump module. Auxiliary sensors, a Deep Ocean Standards Thermometer (SBE 35), an altimeter (PSA-916T; Teledyne Benthos, Inc., North Falmous, Massachusetts, USA), an oxygen optodes (RINKO-III; JFE Advantech Co., Ltd, Kobe Hyogo, Japan), a fluorometers (Seapoint sensors, Inc., Kingston, New Hampshire, USA), a transmissometer (C-Star Transmissometer; WET Labs, Inc., Philomath, Oregon, USA), a Photosynthetically Active Radiation (PAR) sensor (Satlantic, LP, Halifax, Nova Scotia, Canada), and a colored dissolved organic matter (ECO FL CDOM, WET Labs, Inc., Philomath, Oregon, USA) were also used with the SBE 9plus underwater unit. To minimize rotation of the CTD package, a heavy stainless frame (total weight of the CTD package without sea water in the bottles is about 1000 kg) was used with an aluminum plate (54 × 90 cm).

Summary of the system used in this cruise

36-position Carousel system

Deck unit:

SBE 11plus, S/N 11P54451-0872

Under water unit:

SBE 9plus, S/N 09P38273_74766 (pressure sensor S/N: 0786)

Temperature sensor:

SBE 3plus, S/N 03P4815 (primary)

SBE 3, S/N 031525 (secondary)

Conductivity sensor:

SBE 4, S/N 042435 (primary)

SBE 4, S/N 042854 (secondary)

Oxygen sensor:

SBE 43, S/N 430330

JFE Advantech RINKO-III, S/N 0024 (foil batch no. 144002A)

Pump:

SBE 5T, S/N 054595 (primary)

SBE 5T, S/N 054598 (secondary)

Altimeter:

PSA-916T, S/N 1157

Deep Ocean Standards Thermometer:

SBE 35, S/N 0022

Fluorometer:

Seapoint Sensors, Inc., S/N 3497 (measurement range: 0-10 μg/L)

Transmissometer:

C-Star, S/N CST-1363DR

PAR:

Satlantic LP, S/N 0049

CDOM:

ECO FL CDOM, S/N FLCDRTD-2014 (measurement range: 0-500 ppb)

Carousel Water Sampler:

SBE 32, S/N 0924

Water sample bottle:

12-litre Niskin-X model 1010X (no TEFLON coating)

(4) Pre-cruise calibration

i. Pressure

The Paroscientific series 4000 Digiquartz high pressure transducer (Model 415K: Paroscientific, Inc., Redmond, Washington, USA) uses a quartz crystal resonator whose frequency of oscillation varies with pressure induced stress with 0.01 per million of resolution over the absolute pressure range of 0 to 15000 psia (0 to 10332 dbar). Also, a quartz crystal temperature signal is used to compensate for a wide range of temperature changes at the time of an observation. The pressure sensor has a nominal accuracy of 0.015 % FS (1.5 dbar), typical stability of 0.0015 % FS/month (0.15 dbar/month), and resolution of 0.001 % FS (0.1 dbar). Since the pressure sensor measures the absolute value, it inherently includes atmospheric pressure (about 14.7 psi). SEASOFT subtracts 14.7 psi from computed pressure automatically.

Pre-cruise sensor calibrations for linearization were performed at SBE, Inc. The time drift of the pressure sensor is adjusted by periodic recertification corrections against a dead-weight piston gauge (Model 480DA, S/N 23906; Piston unit, S/N 079K; Weight set, S/N 3070; Bundenberg Gauge Co. Ltd., Irlam, Manchester, UK). The corrections are performed at JAMSTEC, Yokosuka, Kanagawa, Japan by Marine Works Japan Ltd. (MWJ), Yokohama, Kanagawa, Japan, usually once in a year in order to monitor sensor time drift and linearity.

S/N 0786, 13 July 2015

slope = 0.99980434

offset = –0.13013

ii. Temperature (SBE 3)

The temperature sensing element is a glass-coated thermistor bead in a stainless steel tube, providing a pressure-free measurement at depths up to 10500 (6800) m by titanium (aluminum) housing. The SBE 3 thermometer has a nominal accuracy of 1 mK, typical stability of 0.2 mK/month, and resolution of 0.2 mK at 24 samples per second. The premium temperature sensor, SBE 3plus, is a more rigorously tested and calibrated version of standard temperature sensor (SBE 3).

Pre-cruise sensor calibrations were performed at SBE, Inc.

S/N 03P4815, 16 April 2015

S/N 031525, 28 July 2015

Pressure sensitivities of SBE 3s were corrected according to a method by Uchida et al. (2007), for the following sensors.

S/N 03P4815, –3.4597e–7 [°C/dbar]

iii. Conductivity (SBE 4)

The flow-through conductivity sensing element is a glass tube (cell) with three platinum electrodes to provide in-situ measurements at depths up to 10500 (6800) m by titanium (aluminum) housing. The SBE 4 has a nominal accuracy of 0.0003 S/m, typical stability of 0.0003 S/m/month, and resolution of 0.00004 S/m at 24 samples per second. The conductivity cells have been replaced to newer style cells for deep ocean measurements.

Pre-cruise sensor calibrations were performed at SBE, Inc.

S/N 042435, 1 May 2015

S/N 042854, 1 May 2014

The value of conductivity at salinity of 35, temperature of 15 °C (IPTS-68) and pressure of 0 dbar is 4.2914 S/m.

iv. Oxygen (SBE 43)

The SBE 43 oxygen sensor uses a Clark polarographic element to provide in-situ measurements at depths up to 7000 m. The range for dissolved oxygen is 120 % of surface saturation in all natural waters, nominal accuracy is 2 % of saturation, and typical stability is 2 % per 1000 hours.

Pre-cruise sensor calibration was performed at SBE, Inc.

S/N 430330, 10 May 2015

v. Deep Ocean Standards Thermometer

Deep Ocean Standards Thermometer (SBE 35) is an accurate, ocean-range temperature sensor that can be standardized against Triple Point of Water and Gallium Melt Point cells and is also capable of measuring temperature in the ocean to depths of 6800 m. The SBE 35 was used to calibrate the SBE 3 temperature sensors in situ (Uchida et al., 2007).

Pre-cruise sensor linearization was performed at SBE, Inc.

S/N 0022, 4 March 2009

Then the SBE 35 is certified by measurements in thermodynamic fixed-point cells of the TPW (0.01 °C) and GaMP (29.7646 °C). The slow time drift of the SBE 35 is adjusted by periodic recertification corrections. Pre-cruise sensor calibration was performed at SBE, Inc. Since 2014, fixed-point cells traceable to NIST temperature standards is directly used in the manufacturer's calibration of the SBE 35 (Uchida et al., 2015).

S/N 0022, 4 February 2015 (slope and offset correction)

Slope = 1.000007

Offset = 0.000246

The time required per sample = 1.1 × NCYCLES + 2.7 seconds. The 1.1 seconds is total time per an acquisition cycle. NCYCLES is the number of acquisition cycles per sample and was set to 4. The 2.7 seconds is required for converting the measured values to temperature and storing average in EEPROM.

vi. Altimeter

Benthos PSA-916T Sonar Altimeter (Teledyne Benthos, Inc.) determines the distance of the target from the unit by generating a narrow beam acoustic pulse and measuring the travel time for the pulse to bounce back from the target surface. It is rated for operation in water depths up to 10000 m. The PSA-916T uses the nominal speed of sound of 1500 m/s.

vii. Oxygen optode (RINKO)

RINKO (JFE Alec Co., Ltd.) is based on the ability of selected substances to act as dynamic fluorescence quenchers. RINKO model III is designed to use with a CTD system which accept an auxiliary analog sensor, and is designed to operate down to 7000 m.

Data from the RINKO can be corrected for the time-dependent, pressure-induced effect by means of the same method as that developed for the SBE 43 (Edwards et al., 2010). The calibration coefficients, H1 (amplitude of hysteresis correction), H2 (curvature function for hysteresis), and H3 (time constant for hysteresis) were determined empirically as follows.

H1 = 0.0055 (for S/N 0024)

H2 = 5000 dbar

H3 = 2000 seconds

Outputs from RINKO are the raw phase shift data. The RINKO can be calibrated by the modified Stern-Volmer equation slightly modified from a method by Uchida et al. (2010):

$$O_2\ (\mu mol/l) = [(V_0 / V)^E - 1] / K_{sv}$$

where V is voltage, V_0 is voltage in the absence of oxygen, K_{sv} is Stern-Volmer constant. The coefficient E corrects nonlinearity of the Stern-Volmer equation. The V_0 and the K_{sv} are assumed to be functions of temperature as follows.

$$K_{sv} = C_0 + C_1 \times T + C_2 \times T^2$$

$$V_0 = 1 + C_3 \times T$$

$$V = C_4 + C_5 \times V_b$$

where T is CTD temperature (°C) and V_b is raw output (volts). V_0 and V are normalized by the output in the absence of

oxygen at 0°C. The oxygen concentration is calculated using accurate temperature data from the CTD temperature sensor instead of temperature data from the RINKO. The pressure-compensated oxygen concentration O_{2c} can be calculated as follows.

$$O_{2c} = O_2 (1 + C_p p / 1000)$$

where p is CTD pressure (dbar) and C_p is the compensation coefficient. Since the sensing foil of the optode is permeable only to gas and not to water, the optode oxygen must be corrected for salinity. The salinity-compensated oxygen can be calculated by multiplying the factor of the effect of salt on the oxygen solubility (Garcia and Gordon, 1992).

Pre-cruise sensor calibrations were performed at RCGC/JAMSTEC.

S/N 0024, 10 May 2015

viii. Fluorometer

The Seapoint Chlorophyll Fluorometer (Seapoint Sensors, Inc., Kingston, New Hampshire, USA) provides in-situ measurements of chlorophyll-a at depths up to 6000 m. The instrument uses modulated blue LED lamps and a blue excitation filter to excite chlorophyll-a. The fluorescent light emitted by the chlorophyll-a passes through a red emission filter and is detected by a silicon photodiode. The low level signal is then processed using synchronous demodulation circuitry, which generates an output voltage proportional to chlorophyll-a concentration.

ix. Transmissometer

The C-Star Transmissometer (WET Labs, Inc., Philomath, Oregon, USA) measures light transmittance at a single wavelength (650 nm) over a know path (25 cm). In general, losses of light propagating through water can be attributed to two primary causes: scattering and absorption. By projecting a collimated beam of light through the water and placing a focused receiver at a known distance away, one can quantify these losses. The ratio of light gathered by the receiver to the amount originating at the source is known as the beam transmittance. Suspended particles, phytoplankton, bacteria and dissolved organic matter contribute to the losses sensed by the instrument. Thus, the instrument provides information both for an indication of the total concentrations of matter in the water as well as for a value of the water clarity.

Light transmission T_r (in %) and beam attenuation coefficient c_p are calculated from the sensor output (V in volt) as follows.

$$T_r = (c_0 + c_1 V) \times 100$$

$$c_p = -(1 / 0.25) \ln(T_r / 100)$$

The calibration coefficients were determined by using the data obtained in the R/V Mirai MR15-03 cruise.

x. PAR

Photosynthetically Active Radiation (PAR) sensors (Satlantic, LP, Halifax, Nova Scotia, Canada) provide highly accurate measurements of PAR (400 – 700 nm) for a wide range of aquatic and terrestrial applications. The ideal spectral response for a PAR sensor is one that gives equal emphasis to all photons between 400 – 700 nm. Satlantic PAR sensors use a high quality filtered silicon photodiode to provide a near equal spectral response across the entire wavelength range of the measurement.

Pre-cruise sensor calibration was performed at Satlantic, LP.

S/N 0049, 22 January 2009

xi. CDOM

The Environmental Characterization Optics (ECO) miniature fluorometer (WET Labs, Inc., Philomath, Oregon, USA) allows the user to measure relative Colored Dissolved Organic Matter (CDOM) concentrations by directly measuring the amount of fluorescence emission in a sample volume of water. The CDOM fluorometer uses an UV LED to provide the excitation source. An interference filter is used to reject the small amount of out-of-band light emitted by the LED. The light from the source enters the water volume at an angle of approximately 55-60 degrees with respect to the end face of the unit. Fluoresced light is received by a detector positioned where the acceptance angle forms a 140-degree intersection with the source beam. An interference filter is used to discriminate against the scattered excitation light.

CDOM (Quinine Dihydrate Equivalent) concentration expressed in ppb can be derived using the equation as follows.

CDOM = Scale Factor * (Output – Dark Counts)

Pre-cruise sensor calibration was performed at WET Labs.

S/N FLCDRTD-2014, 1 September 2015

Dark Counts: 0.025 V

Scale Factor: 106 ppb/V

(5) Data collection and processing

i. Data collection

CTD system was powered on at least 20 minutes in advance of the data acquisition to stabilize the pressure sensor and was powered off at least two minutes after the operation in order to acquire pressure data on the ship's deck.

The package was lowered into the water from the starboard side and held 10 m beneath the surface in order to activate the pump. After the pump was activated, the package was lifted to the surface and lowered at a rate of 1.0 m/s to 200 m (or 300 m when significant wave height was high) then the package was stopped to operate the heave compensator of the crane. The package was lowered again at a rate of 1.2 m/s to the bottom. For the up cast, the package was lifted at a rate of 1.1 m/s except for bottle firing stops. As a rule, the bottle was fired after waiting from the stop for 30 seconds and the package was stayed at least 5 seconds for measurement of the SBE 35 at each bottle firing stops. For depths where vertical gradient of water properties were expected to be large (from surface to thermocline), the bottle was exceptionally fired after waiting from the stop for 60 seconds to enhance exchanging the water between inside and outside of the bottle. At 200 m (or 300 m) from the surface, the package was stopped to stop the heave compensator of the crane.

Water samples were collected using a 36-bottle SBE 32 Carousel Water Sampler with 12-litre Niskin-X bottles. Before a cast taken water for CFCs, the bottle frame and Niskin-X bottles were wiped with acetone. At station 001_1, 012_1, 022_1, 022_2, 030_1 and 037_1, specially washed Niskin-X bottles were used for #2 and #3, since samples for

incubation were collected from the bottles.

Data acquisition software

SEASAVE-Win32, version 7.23.2

ii. Data collection problems

(a) Miss trip, miss fire, and remarkable leak

Niskin bottles did not trip correctly at the following stations.

Miss trip	Miss fire	Leak
none	none	007_1 #14 stopcock: O-ring of the stopcock replaced
		025_1 #30 stopcock: O-ring of the end closure replaced
		033_3 #27 end closure: O-ring of the end closure replaced

(b) Failure of the slip ring swivel

The slip ring swivel failed by sea water immersion from the nipple joints at beginning of station 011_1. Therefore, the slip ring swivel was detached from the CTD cast.

(d) Cable replacement

Cables for sensors were replaced after the following stations.

900_1: noise of the secondary temperature

010_2: noise of fluorometer

035_1: noise of transmissometer at station 034_1 and 035_1

(e) Noise in down cast data

Secondary conductivity data were noisy at station 043_1 from 698 dbar of down cast due to a jellyfish. Transmissometer data were noisy at station 016_1 (from 1484 to 2556 dbar), 034_1 (from 539 to 544 dbar), and the data were removed and linearly interpolated. CDOM data were flagged as 4 (bad measurement) for depths deeper than about 4500 m due to noise and large shift of the data

iii. Data processing

SEASOFT consists of modular menu driven routines for acquisition, display, processing, and archiving of oceanographic data acquired with SBE equipment. Raw data are acquired from instruments and are stored as unmodified data. The conversion module DATCNV uses instrument configuration and calibration coefficients to create a converted engineering unit data file that is operated on by all SEASOFT post processing modules. The following are the SEASOFT and original software data processing module sequence and specifications used in the reduction of CTD data in this cruise.

Data processing software

SBEDataProcessing-Win32, version 7.23.2

DATCNV converted the raw data to engineering unit data. DATCNV also extracted bottle information where scans were marked with the bottle confirm bit during acquisition. The duration was set to 4.4 seconds, and the offset was set to 0.0 second. The hysteresis correction for the SBE 43 data (voltage) was applied for both profile and bottle information data.

TCORP (original module, version 1.1) corrected the pressure sensitivity of the SBE 3 for both profile and bottle information data.

RINKOCOR (original module, version 1.0) corrected the time-dependent, pressure-induced effect (hysteresis) of the RINKO for both profile data.

RINKOCORROS (original module, version 1.0) corrected the time-dependent, pressure-induced effect (hysteresis) of the RINKO for bottle information data by using the hysteresis-corrected profile data.

BOTTLESUM created a summary of the bottle data. The data were averaged over 4.4 seconds.

ALIGNCTD converted the time-sequence of sensor outputs into the pressure sequence to ensure that all calculations were made using measurements from the same parcel of water. For a SBE 9plus CTD with the ducted temperature and conductivity sensors and a 3000-rpm pump, the typical net advance of the conductivity relative to the temperature is 0.073 seconds. So, the SBE 11plus deck unit was set to advance the primary and the secondary conductivity for 1.73 scans (1.75/24 = 0.073 seconds). Oxygen data are also systematically delayed with respect to depth mainly because of the long time constant of the oxygen sensor and of an additional delay from the transit time of water in the pumped plumbing line. This delay was compensated by 5 seconds advancing the SBE 43 oxygen sensor output (voltage) relative to the temperature data. Delay of the RINKO data was also compensated by 1 second advancing sensor output (voltage) relative to the temperature data. Delay of the transmissometer data was also compensated by 2 seconds advancing sensor output (voltage) relative to the temperature data.

WILDEDIT marked extreme outliers in the data files. The first pass of WILDEDIT obtained an accurate estimate of the true standard deviation of the data. The data were read in blocks of 1000 scans. Data greater than 10 standard deviations were flagged. The second pass computed a standard deviation over the same 1000 scans excluding the flagged values. Values greater than 20 standard deviations were marked bad. This process was applied to pressure, temperature, conductivity, and SBE 43 output.

CELLTM used a recursive filter to remove conductivity cell thermal mass effects from the measured conductivity. Typical values used were thermal anomaly amplitude alpha = 0.03 and the time constant 1/beta = 7.0.

FILTER performed a low pass filter on pressure with a time constant of 0.15 seconds. In order to produce zero phase lag (no time shift) the filter runs forward first then backwards.

WFILTER performed as a median filter to remove spikes in fluorometer, transmissometer, and CDOM data. A median value was determined by 49 scans of the window. For CDOM data, an additional box-car filter with a window of 361 scans was applied to remove noise.

SECTIONU (original module, version 1.1) selected a time span of data based on scan number in order to reduce a file size. The minimum number was set to be the start time when the CTD package was beneath the sea-surface after activation of the pump. The maximum number was set to be the end time when the depth of the package was 1 dbar below the surface. The minimum and maximum numbers were automatically calculated in the module.

LOOPEDIT marked scans where the CTD was moving less than the minimum velocity of 0.0 m/s (traveling backwards due to ship roll).

DESPIKE (original module, version 1.0) removed spikes of the data. A median and mean absolute deviation was calculated in 1-dbar pressure bins for both down- and up-cast, excluding the flagged values. Values greater than 4 mean absolute deviations from the median were marked bad for each bin. This process was performed 2 times for temperature, conductivity, SBE 43, and RINKO output.

DERIVE was used to compute oxygen (SBE 43).

BINAVG averaged the data into 1-dbar pressure bins. The center value of the first bin was set equal to the bin size. The bin minimum and maximum values are the center value plus and minus half the bin size. Scans with pressures greater than the minimum and less than or equal to the maximum were averaged. Scans were interpolated so that a data record exist every dbar.

BOTTOMCUT (original module, version 0.1) deleted the deepest pressure bin when the averaged scan number of the deepest bin was smaller than the average scan number of the bin just above.

DERIVE was re-used to compute salinity, potential temperature, and density (σ_θ).

SPLIT was used to split data into the down cast and the up cast.

Remaining spikes in the CTD data were manually eliminated from the 1-dbar-averaged data. The data gaps resulting from the elimination were linearly interpolated with a quality flag of 6.

(6) Post-cruise calibration

i. Pressure

The CTD pressure sensor offset in the period of the cruise was estimated from the pressure readings on the ship deck. For best results the Paroscientific sensor was powered on for at least 20 minutes before the operation. In order to get the calibration data for the pre- and post-cast pressure sensor drift, the CTD deck pressure was averaged over first and last one minute, respectively. Then the atmospheric pressure deviation from a standard atmospheric pressure (14.7 psi) was subtracted from the CTD deck pressure to check the pressure sensor time drift. The atmospheric pressure was measured at the captain deck (20 m high from the base line) and sub-sampled one-minute interval as a meteorological data.

The pre- and the post-casts deck pressure data showed temperature dependency for the pressure sensor (Fig. 3.1.2). To correct the temperature dependency, the manufacturer's calibration coefficients were slightly modified on board as follows:

$T1 = 29.88499$

$T2 = -2.565740e^{-4}$

$T3 = 4.799030e^{-6}$

$Offset = 0.0$

Time series of the CTD deck pressure is shown in Fig. 3.1.3. The CTD pressure sensor offset was estimated from the deck pressure. Mean of the pre- and the post-casts data over the whole period gave an estimation of the pressure sensor offset (–0.01 dbar) from the pre-cruise calibration. The post-cruise correction of the pressure data is not deemed necessary for the pressure sensor.

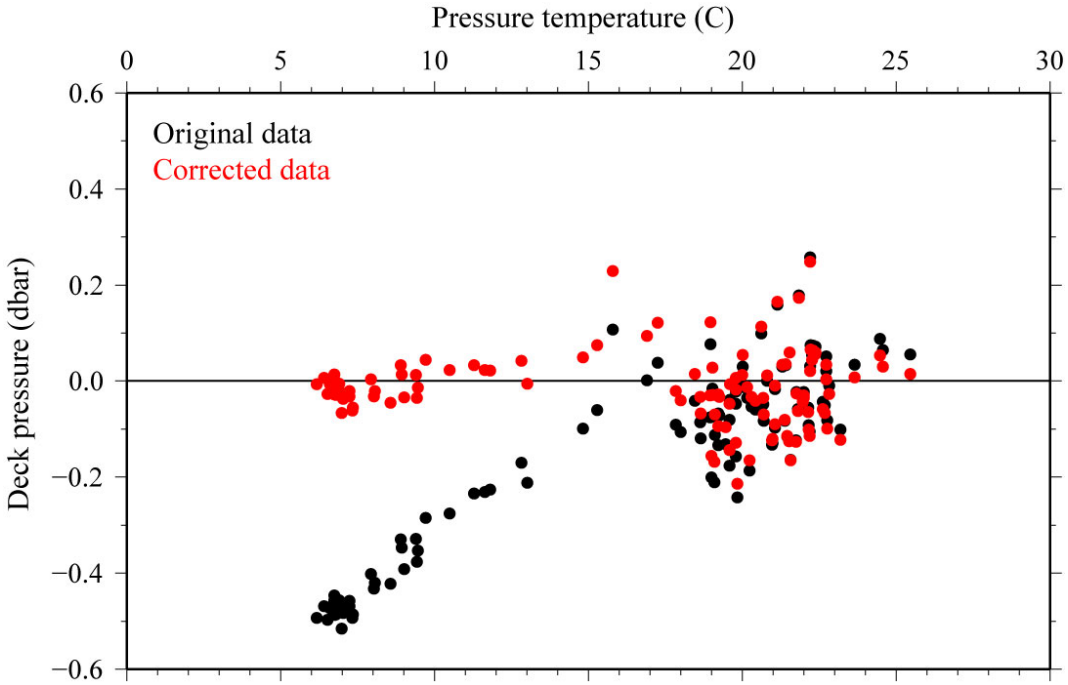

Fig. 3.1.2 Pre- and post-casts CTD deck pressure. Atmospheric pressure deviation from a standard atmospheric pressure was subtracted from the CTD deck pressure. Black dots show the original data and red dots show the data corrected for the temperature dependency of the sensor.

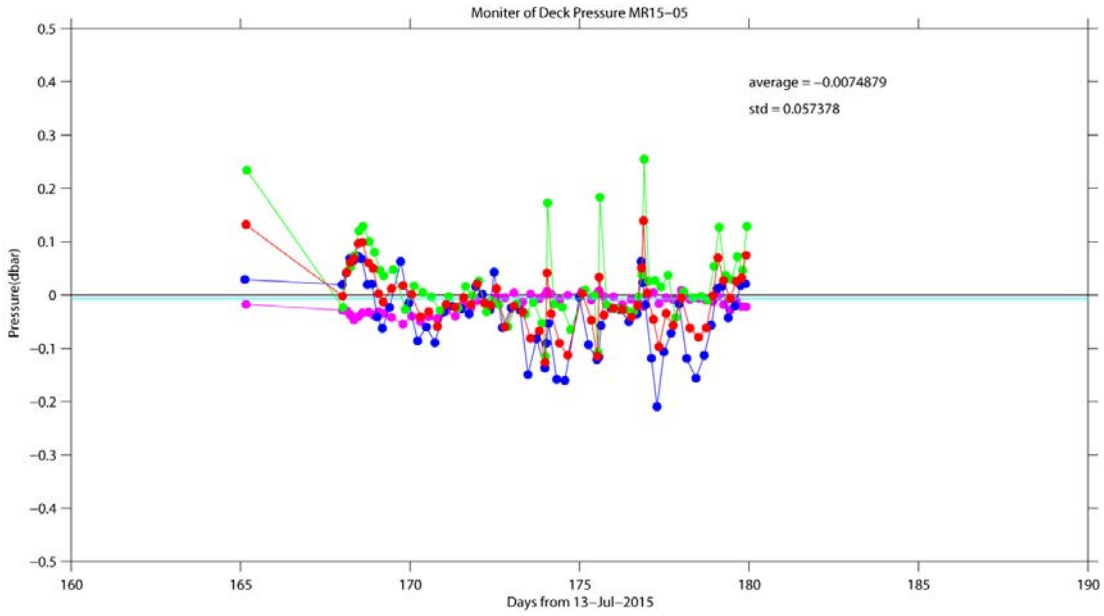

Fig. 3.1.3 Time series of the CTD deck pressure. Atmospheric pressure deviation (magenta dots) from a standard atmospheric pressure was subtracted from the CTD deck pressure. Blue and green dots indicate pre- and post-cast deck pressures, respectively. Red dots indicate averages of the pre- and the post-cast deck pressures.

ii. Temperature

The CTD temperature sensors (SBE 3) were calibrated with the SBE 35 under the assumption that discrepancies between SBE 3 and SBE 35 data were due to pressure sensitivity, the viscous heating effect, and time drift of the SBE 3, according to a method by Uchida et al. (2007).

Post-cruise sensor calibration for the SBE 35 will be performed at SBE, Inc in 2016

The CTD temperature was preliminary calibrated as

$$\text{Calibrated temperature} = T - (c_0 \times P + c_1 \times t + c_2)$$

where T is CTD temperature in °C, P is pressure in dbar, t is time in days from pre-cruise calibration date of the CTD temperature and c_0, c_1, and c_2 are calibration coefficients. The coefficients were determined using the data for the depths deeper than 1950 dbar. The coefficient c_1 was set to zero for this cruise.

The primary temperature data were basically used for the post-cruise calibration. The secondary temperature sensor was also calibrated and used instead of the primary temperature data when the data quality of the primary temperature data was bad. The calibration coefficients are listed in Table 3.1.1. The results of the post-cruise calibration for the CTD temperature are summarized in Table 3.1.2 and shown in Fig. 3.1.4.

Table 3.1.1 Calibration coefficients for the CTD temperature sensors.

Serial number	c_0 (°C/dbar)	c_1 (°C/day)	c_2 (°C)
3P4815	–4.79962e–8	0.0	–0.0007

Table 3.1.2 Difference between the CTD temperature and the SBE 35 after the post-cruise calibration. Mean and standard deviation (Sdev) are calculated for the data below and above 1950 dbar. Number of data used is also shown.

Serial number	Pressure ≥ 1950 dbar			Pressure < 1950 dbar		
	Number	Mean (mK)	Sdev (mK)	Number	Mean (mK)	Sdev (mK)
3P4815	467	0.0	0.2	854	–0.0	6.8

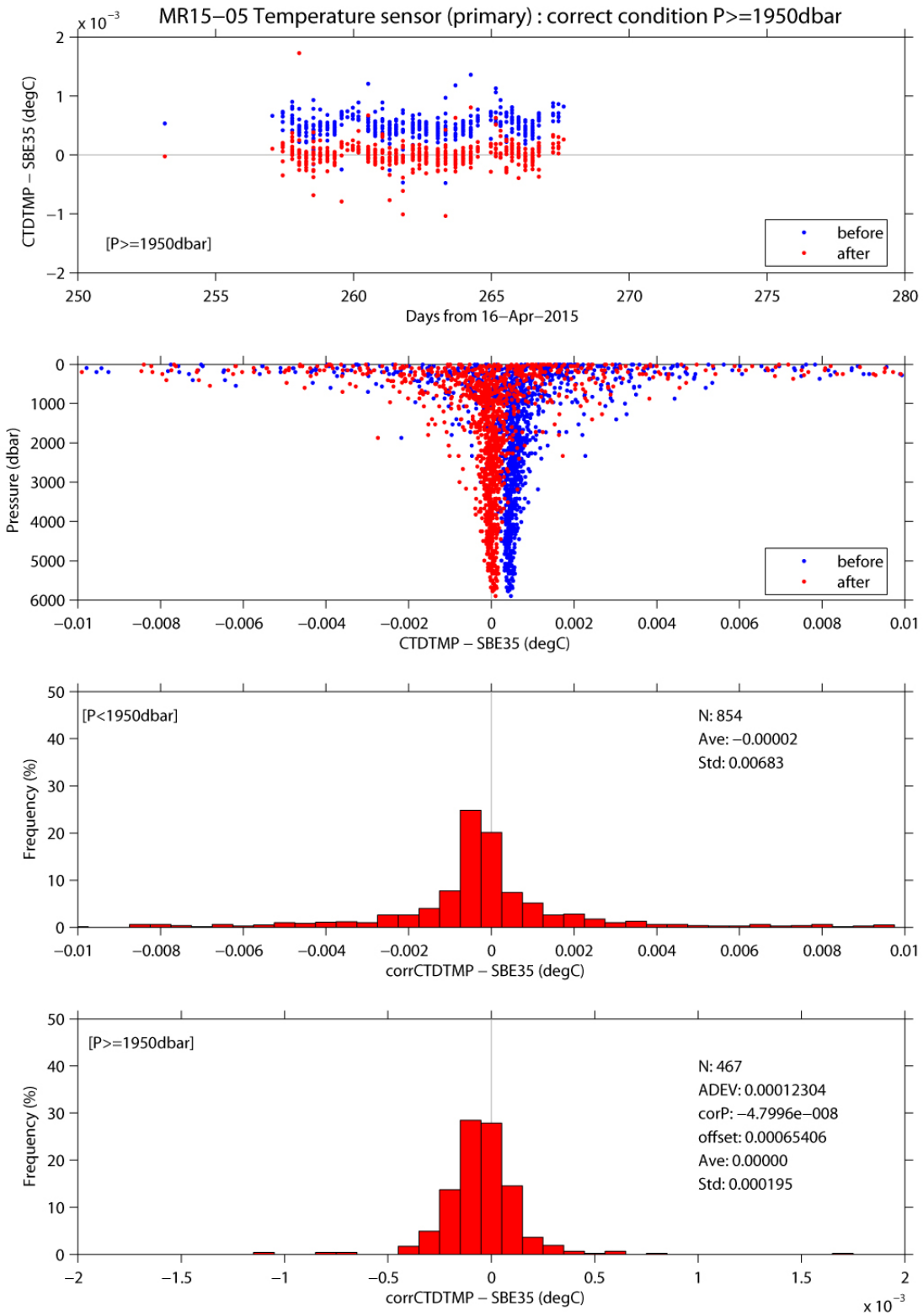

Fig. 3.1.4 Difference between the CTD temperature (primary) and the SBE 35. Blue and red dots indicate before and after the post-cruise calibration using the SBE 35 data, respectively. Lower two panels show histogram of the difference after the calibration.

iii. Salinity

The discrepancy between the CTD conductivity and the conductivity calculated from the bottle salinity data with the CTD temperature and pressure data is considered to be a function of conductivity, pressure and time. The CTD conductivity was calibrated as

$$\text{Calibrated conductivity} = c_0 \times C + c_1 \times P + c_2 \times C \times P + c_3 \times C^2 + c_4 \times t + c_5$$

where C is CTD conductivity in S/m, P is pressure in dbar, t is time in days, and c_0, c_1, c_2, c_3, c_4 and c_5 are calibration coefficients. The best fit sets of coefficients were determined by a least square technique to minimize the deviation from the conductivity calculated from the bottle salinity data. The coefficient c_4 was set to zero for this cruise.

The primary conductivity data created by the software module ROSSUM were used after the post-cruise calibration for the temperature data. The calibration coefficients are listed in Table 3.1.3. The results of the post-cruise calibration for the CTD salinity are summarized in Table 3.1.4 and shown in Fig. 3.1.5.

Table 3.1.3 Calibration coefficients for the CTD conductivity sensors.

Serial Number	c_0	c_1 [S/(m dbar)]	c_2 (1/dbar)	c_3 [1/(S/m)]	c_4 (S/m)
042435	–1.51687e–4	1.09232e–7	–3.67361e–8	4.72348e–12	5.09192e–4

Table 3.1.4 Difference between the CTD salinity and the bottle salinity after the post-cruise calibration. Mean and standard deviation (Sdev) (in 10^{-3}) are calculated for the data below and above 1950 dbar. Number of data used is also shown.

Serial number	Pressure ≥ 1950 dbar			Pressure < 1950 dbar		
	Number	Mean	Sdev	Number	Mean	Sdev
042435	493	–0.0	0.4	861	0.2	4.5

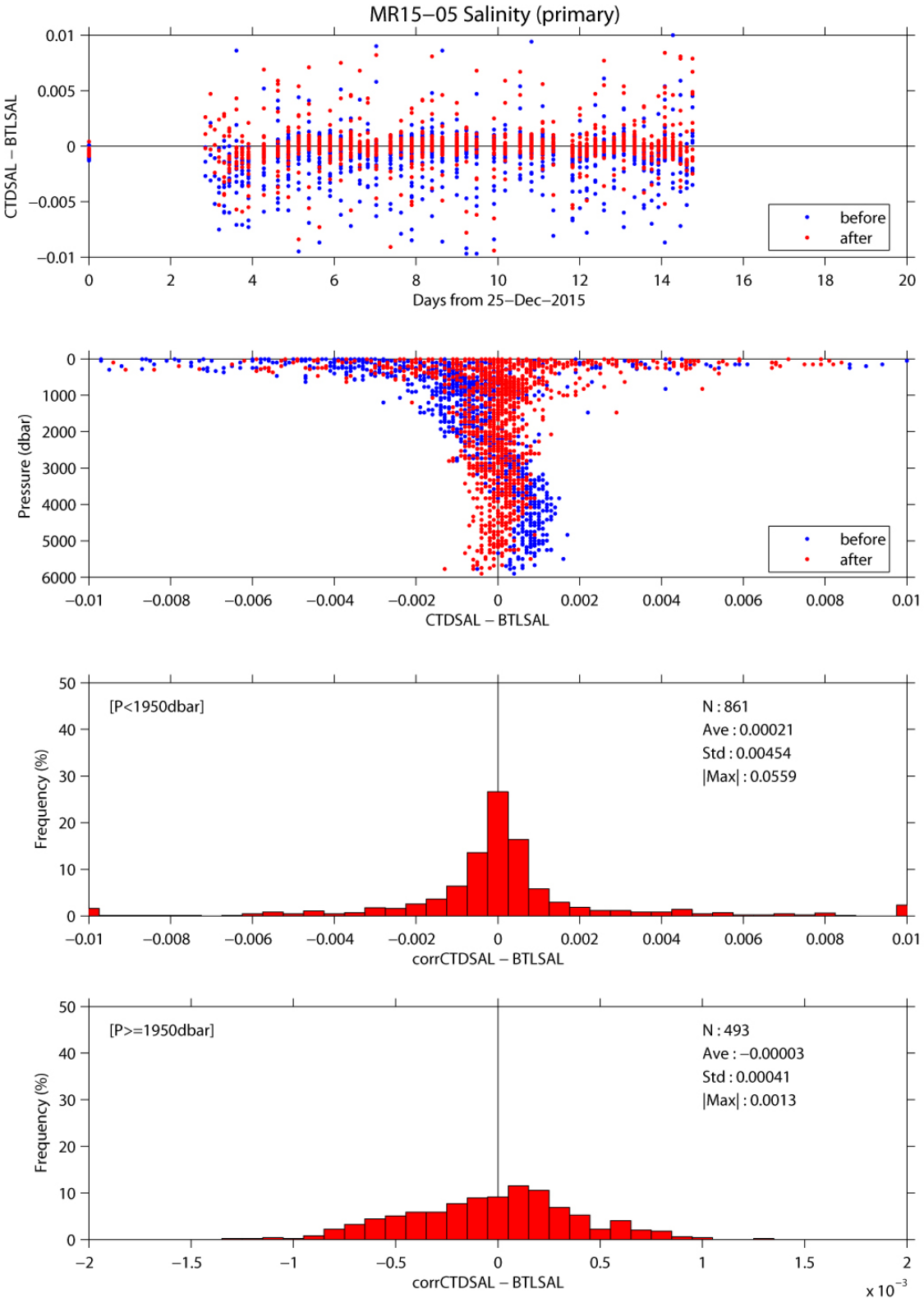

Fig. 3.1.5 Difference between the CTD salinity (primary) and the bottle salinity. Blue and red dots indicate before and after the post-cruise calibration, respectively. Lower two panels show histogram of the difference after the calibration.

iv. Oxygen

The RINKO oxygen optode (S/N 0024) was calibrated and used as the CTD oxygen data, since the RINKO has a fast time response. The pressure-hysteresis corrected RINKO data was calibrated by the modified Stern-Volmer equation, basically according to a method by Uchida et al. (2010) with slight modification:

$$[O_2]\ (\mu mol/l) = [(V_0 / V)^{1.5} - 1] / K_{sv}$$

and

$$K_{sv} = C_0 + C_1 \times T + C_2 \times T^2$$

$$V_0 = 1 + C_3 \times T$$

$$V = C_4 + C_5 \times V_b + C_6 \times t + C_7 \times t \times V_b$$

where V_b is the RINKO output (voltage), V_0 is voltage in the absence of oxygen, T is temperature in °C, and t is exciting time (days) integrated from the first CTD cast. Time drift of the RINKO output was corrected. The calibration coefficients were determined by minimizing the sum of absolute deviation with a weight from the bottle oxygen data. The revised quasi-Newton method (DMINF1) was used to determine the sets.

The post-cruise calibrated temperature and salinity data were used for the calibration. The calibration coefficients are listed in Table 3.1.5. The results of the post-cruise calibration for the RINKO oxygen are summarized in Table 3.1.6 and shown in Fig. 3.1.6.

Table 3.1.5 Calibration coefficients for the RINKO oxygen sensors.

Coefficient	S/N 0024
c_0	5.56160e–3
c_1	2.16834e–4
c_2	2.72251e–6
c_3	–1.03972e–3
c_4	–2.07308e–2
c_5	0.326691
c_6	1.52604e–4
c_7	1.29920e–5
C_p	0.015

Table 3.1.6 Difference between the RINKO oxygen and the bottle ooxygen after the post-cruise calibration. Mean and standard deviation (Sdev) are calculated for the data below and above 1950 dbar. Number of data used is also

shown.

Serial number	Pressure ≥ 1950 dbar			Pressure < 1950 dbar		
	Number	Mean [μmol/kg]	Sdev	Number	Mean [μmol/kg]	Sdev
0024	502	0.11	0.39	859	0.02	0.57

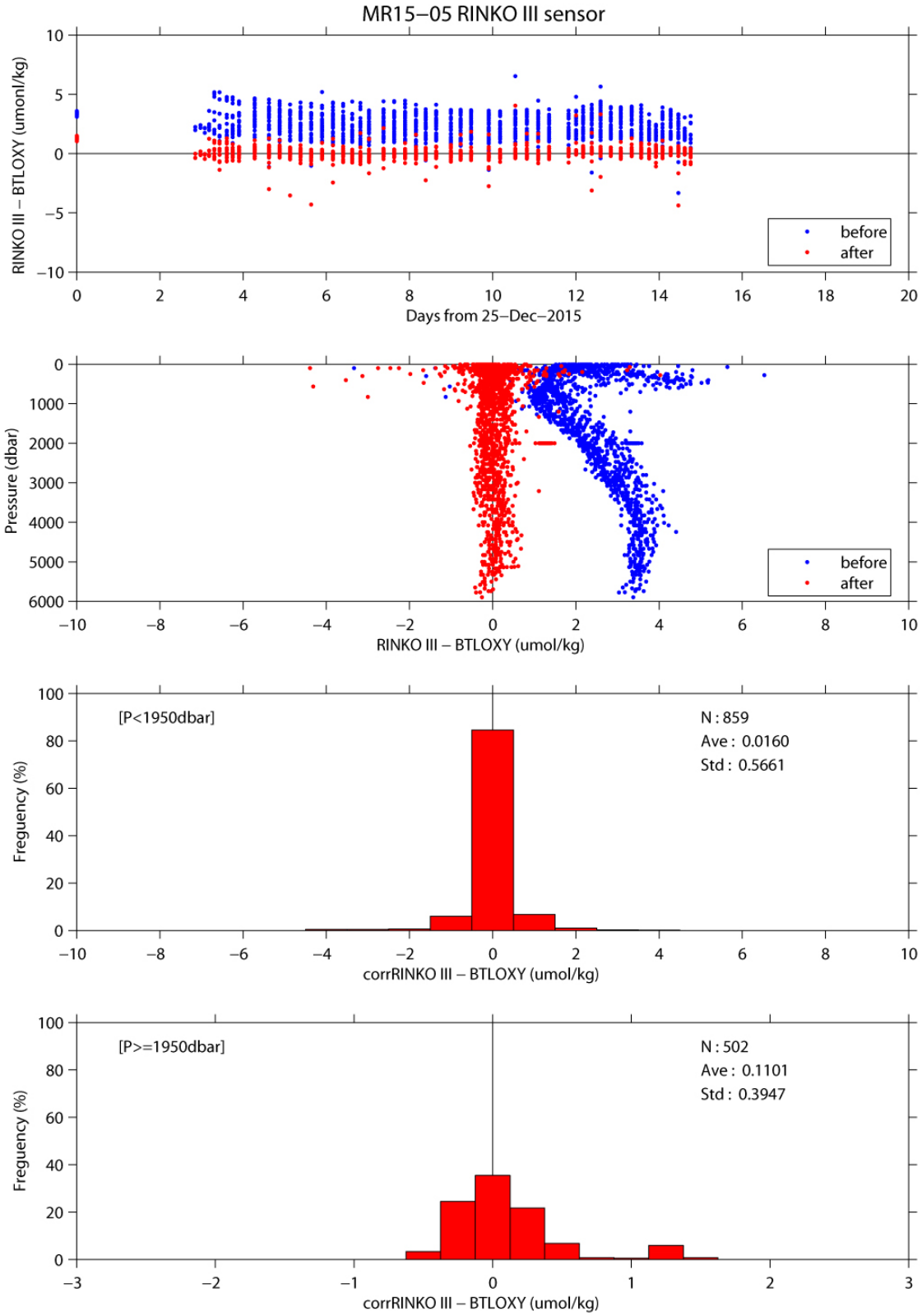

Fig. 3.1.6 Difference between the CTD oxygen and the bottle oxygen. Blue and red dots indicate before and after the post-cruise calibration, respectively. Lower two panels show histogram of the difference after the calibration.

v. Fluorometer

The CTD fluorometer (FLUOR in µg/L) was calibrated by comparing with the bottle sampled chlorophyll-a as

$$FLUORc = c_0 + c_1 \times FLUOR$$

where c_0 and c_1 are calibration coefficients. The CTD fluorometer data is slightly noisy so that the up cast profile data which was averaged over one decibar agree with the bottle sampled data better than the discrete CTD fluorometer data obtained at bottle-firing stop. Therefore, the CTD fluorometer data at water sampling depths extracted from the up cast profile data were compared with the bottle sampled chlorophyll-a data. The bottle sampled data obtained at dark condition [PAR (Photosynthetically Available Radiation) < 50 µE/(m^2 sec)] were used for the calibration, since sensitivity of the fluorometer to chlorophyll *a* is different at nighttime and daytime (Section 2.4 in Uchida et al., 2015) (Fig. 3.1.7). The calibration coefficients are listed in Table 3.1.7. The results of the post-cruise calibration for the fluorometer are summarized in Table 3.1.8 and shown in Fig. 3.1.8.

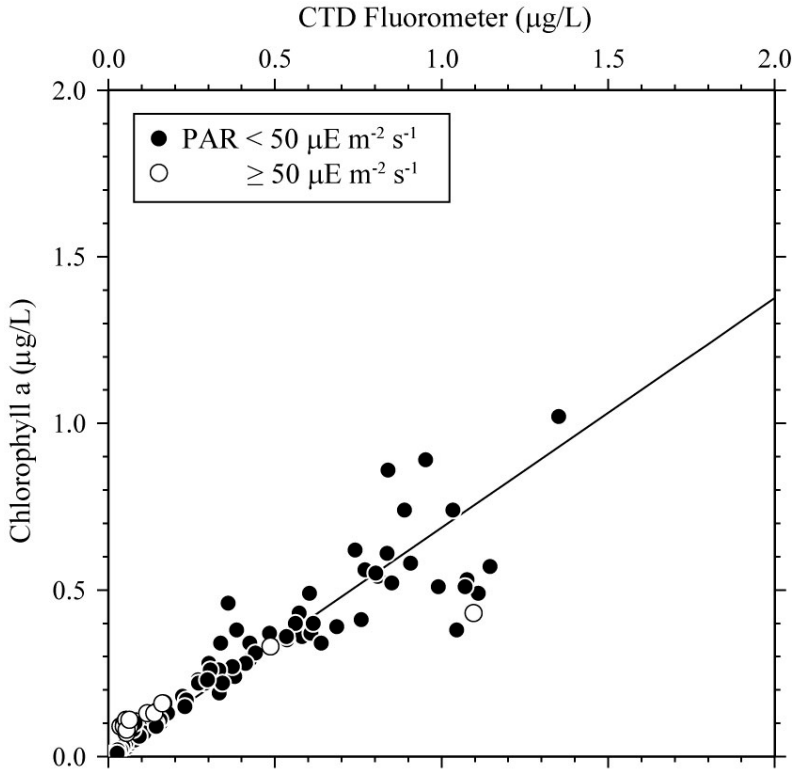

Fig. 3.1.7. Comparison of the CTD fluorometer and the bottle sampled chlorophyll-a. The regression lines are also shown.

Table 3.1.7. Calibration coefficients for the CTD fluorometer.

c_0	c_1	Note
–2.35932e–3	0.689112	

Table 3.1.8. Difference between the CTD fluorometer and the bottle chlorophyll-a after the post-cruise calibration. Mean, standard deviation (Sdev), and number of data used are shown. Data obtained at daytime are also used in this calculation.

Number	Mean	Sdev
156	–0.00 µg/L	0.07 µg/L

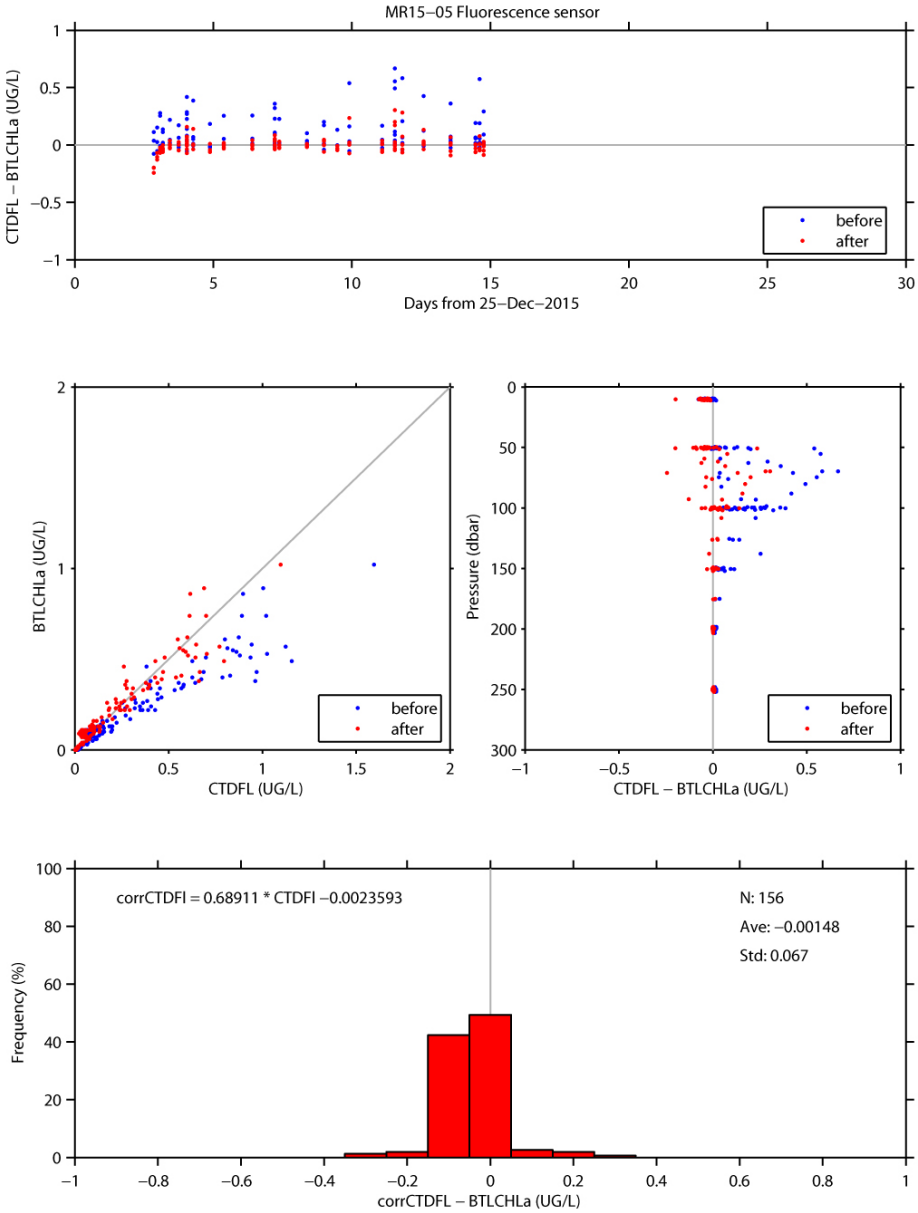

Fig. 3.1.8. Comparison of the CTD fluorometer and the bottle sampled chlorophyll-a. Blue and red dots indicate before and after the post-cruise calibration, respectively. Lower panel shows histogram of the difference after the calibration. Data obtained at daytime are also shown in this figure.

vi. Transmissometer

The transmissometer (T_r in %) is calibrated as

$$T_r = (V - V_d) / (V_r - V_d) \times 100$$

wehre V is the measured signal (voltage), V_d is the dark offset for the instrument, and V_r is the signal for clear water. V_d can be obtained by blocking the light path. V_d and V_{air}, which is the signal for air, were measured on deck before each cast after wiping the optical windows with ethanol. V_d was constant (0.0012) during the cruise. Vr is estimated from the measured maximum signal in the deep ocean at each cast. Since the transmissometer drifted in time (Fig. 3.1.9), Vr is expressed as

$$V_r = c_0 + c_1 \times t + c_2 \times t^2$$

where t is working time (in days) of the transmissometer, and c_0, c_1, and c_2 are calibration coefficients.

Maximum signal was extracted for each cast (Fig. 3.1.9). Data whose depth of the maximum signal was shallower than 200 dbar were not used to estimate V_r (black dots in Fig. 3.1.9). Fits were made iteratively, removing negatively deviated outliers (red dots in Fig. 3.1.9) greater than 2 standard deviations until no more outliers remain. The calibration coefficients thus determined are listed in Table 3.1.9. The coefficient c_2 was set to zero for this cruise.

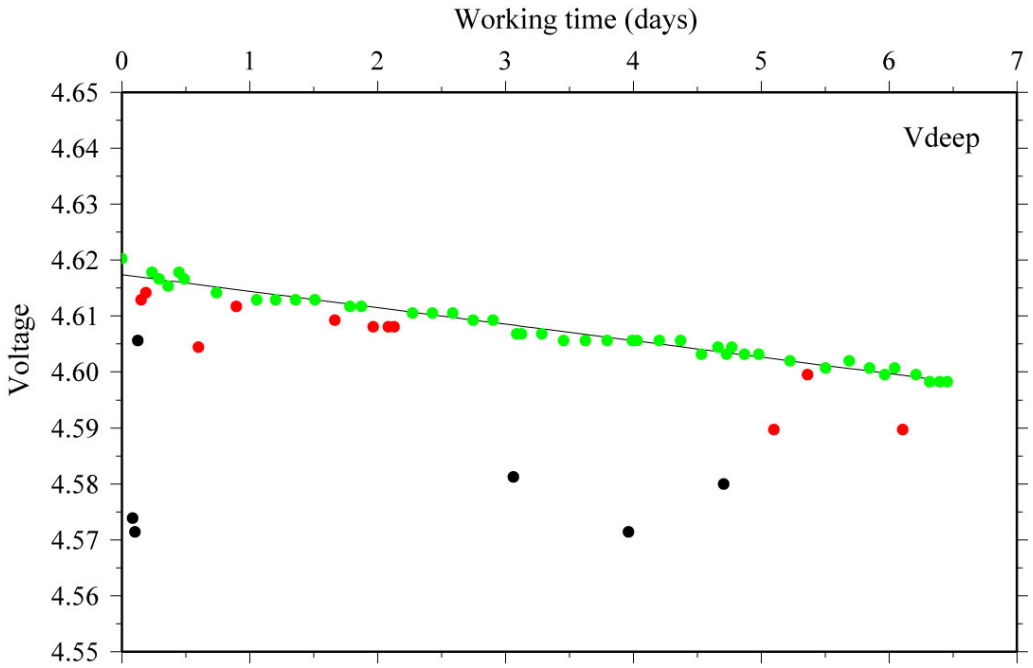

Fig. 3.1.9. Time series of an output signal (voltage) from transmissometer at deep ocean (Vdeep). The black solid line indicates the modeled signal in the deep clear ocean. Black and red dots were not used to estimate the final calibration coefficients (see text for detail).

Table 3.1.9 Calibration coefficients for the CTD transmissometer.

Leg	c_0	c_1	V_d
1	4.61740	–2.94693e–3	0.0012

vii. PAR

The PAR sensor was calibrated with an offset correction. The offset was estimated from the data measured in the deep ocean during the cruise. The corrected data (PARc) is calculated from the raw data (PAR) as follows:

PARc [$\mu E\ m^{-2}\ s^{-1}$] = PAR – 0.046.

vii. CDOM

The CDOM sensor wasn't calibrated, since the reference data (see Section 3.9) was not adequate for the in-situ calibration. The data were low-pass filtered by a running mean with a window of 15 seconds (about 13 m) in the data processing mentioned above, since the data was noisy.

(7) References

Edwards, B., D. Murphy, C. Janzen and N. Larson (2010): Calibration, response, and hysteresis in deep-sea dissolved oxygen measurements, *J. Atmos. Oceanic Technol.*, 27, 920–931.

Fukasawa, M., T. Kawano and H. Uchida (2004): Blue Earth Global Expedition collects CTD data aboard Mirai, BEAGLE 2003 conducted using a Dynacon CTD traction winch and motion-compensated crane, *Sea Technology*, 45, 14–18.

García, H. E. and L. I. Gordon (1992): Oxygen solubility in seawater: Better fitting equations. *Limnol. Oceanogr.*, 37 (6), 1307–1312.

Uchida, H., G. C. Johnson, and K. E. McTaggart (2010): CTD oxygen sensor calibration procedures, The GO-SHIP Repeat Hydrography Manual: A collection of expert reports and guidelines, IOCCP Rep., No. 14, ICPO Pub. Ser. No. 134.

Uchida, H., K. Katsumata, and T. Doi (2015): WHP P14S, S04I Revisit Data Book, JASTEC, Yokosuka, 187 pp.

Uchida, H., T. Nakano, J. Tamba, J. V. Widiatmo, K. Yamazawa, S. Ozawa and T. Kawano (2015): Deep ocean temperature measurement with an uncertainty of 0.7 mK, J. Atmos. Oceanic Technol., 32, 2199–2210.

Uchida, H., K. Ohyama, S. Ozawa, and M. Fukasawa (2007): In situ calibration of the Sea-Bird 9plus CTD thermometer, *J. Atmos. Oceanic Technol.*, 24, 1961–1967.

3.2 Bottle Salinity

January 27, 2016

(1) Personnel

Hiroshi Uchida (JAMSTEC)

Sonoka Wakatsuki (MWJ)

Hiroki Ushiromura (MWJ)

(2) Objectives

Bottle salinities were measured to calibrate CTD salinity data.

(3) Instrument and Method

Salinity measurement was conducted basically based on a method by Kawano (2010).

i. Salinity Sample Collection

The bottles in which the salinity samples were collected and stored were 250 ml brown borosilicate glass bottles with screw caps (PTFE packing). Each bottle was rinsed three times with sample water and was filled to the shoulder of the bottle. The caps were also thoroughly rinsed. Salinity samples were stored more than 24 hours in the same laboratory as the salinity measurement was made.

ii. Instruments and Methods

Salinity of water samples was measured with a salinometer (Autosal model 8400B; Guildline Instruments Ltd., Ontario, Canada; S/N 62556), which was modified by adding an peristaltic-type intake pump (Ocean Scientific International Ltd., Hampshire, UK) and two platinum thermometers (Guildline Instruments Ltd., model 9450). One thermometer monitored an ambient temperature and the other monitored a salinometer's bath temperature. The resolution of the thermometers was 0.001 °C. The measurement system was almost same as Aoyama et al. (2002). The salinometer was operated in the air-conditioned laboratory of the ship at a bath temperature of 24 °C.

The ambient temperature varied from approximately 22.3 to 24.3 °C, while the bath temperature was stable and varied within ±0.006 °C. A measure of a double conductivity ratio of a sample was taken as a median of 31 readings. Data collection was started after 10 seconds and it took about 10 seconds to collect 31 readings by a personal computer. Data were sampled for the sixth and seventh filling of the cell. In case where the difference between the double conductivity ratio of this two fillings was smaller than 0.00002, the average value of the two double conductivity ratios was used to calculate the bottle salinity with the algorithm for practical salinity scale, 1978 (UNESCO, 1981). When the difference was greater than or equal to the 0.00003, we measured another additional filling of the cell. In case where the double conductivity ratio of the additional filling did not satisfy the criteria above, we measured other additional fillings of the cell within 10 fillings in total. In case where the number of fillings was 10 and those fillings did not satisfy the criteria above, the median of the double conductivity ratios of five fillings were used to calculate the bottle salinity.

The measurement was conducted about from 2 to 19 hours per day and the cell was cleaned with soap (50 times diluted solution of S-CLEAN WO-23 [Neutral], Sasaki Chemical Co. Ltd., Kyoto, Japan) after the measurement for each day. A total of 1672 water samples were measured during the cruise.

(4) Results

i. Standard Seawater

Standardization control was set to 715. The value of STANDBY was 5216±0001 and that of ZERO was 0.00000 or ±0.00001. We used IAPSO Standard Seawater batch P157 whose conductivity ratio is 0.99985 (double conductivity ratio is 1.99970) as the standard for salinity measurement. We measured 66 bottles of the Standard Seawater during the cruise. History of double conductivity ratio measurement of the Standard Seawater is shown in Fig. 3.2.1.

Time drift of the salinometer was corrected by using the Standard Seawater measurements. Linear time drift of the salinometer was estimated from the Standard Seawater measurement by using the least square method (thin black line in Fig. 3.2.1). No remarkable time drift was estimated from the Standard Seawater measurement. The average of double conductivity ratio was 1.99968 and the standard deviation was 0.00001, which is equivalent to 0.0002 in salinity.

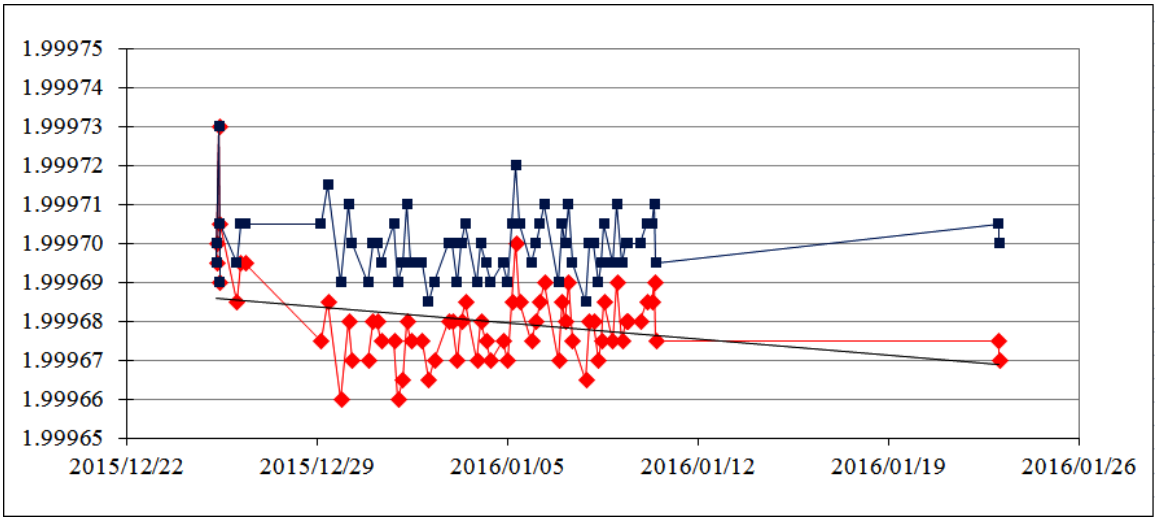

Fig. 3.2.1. History of double conductivity ratio measurement of the Standard Seawater (P157). Horizontal and vertical axes represents date and double conductivity ratio, respectively. Red dots indicate raw data and blue dots indicate corrected data.

ii. Sub-Standard Seawater

We also used sub-standard seawater which was deep-sea water filtered by pore size of 0.45 μm and stored in a 20 liter cubitainer made of polyethylene and stirred for at least 24 hours before measuring. It was measured every 6-8 samples in order to check the possible sudden drift of the salinometer. During the whole measurements, there was no detectable sudden drift of the salinometer.

iii. Replicate Samples

We took 257 pairs of replicate samples collected from the same Niskin bottle. Histogram of the absolute difference between replicate samples is shown in Fig. 3.2.2. The root-mean-square for 256 pairs of replicate samples which are acceptable-quality data was 0.0002.

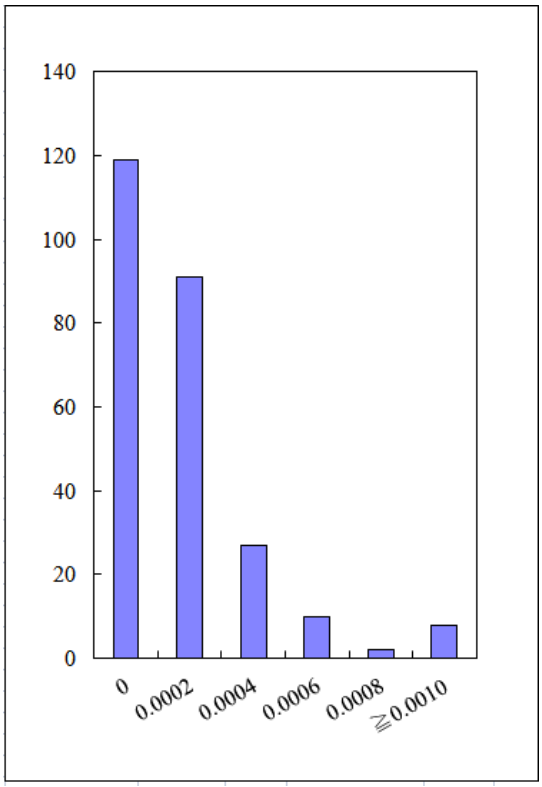

Fig. 3.2.2. Histogram of the absolute difference between replicate samples. Horizontal axis is absolute difference in salinity and vertical axis is frequency.

iv. Duplicate Samples

In this cruise, we took 36 samples collected from the different Niskin bottles at same depth (2000 dbar) of station 900, instead of taking duplicate samples. The average of salinity with the standard deviation was 34.7300 ± 0.0002.

(5) References

Aoyama, M., T. Joyce, T. Kawano and Y. Takatsuki (2002): Standard seawater comparison up to P129. Deep-Sea Research, I, Vol. 49, 1103-1114.

Kawano (2010): Salinity. The GO-SHIP Repeat Hydrography Manual: A collection of Expert Reports and Guidelines, IOCCP Report No. 14, ICPO Publication Series No. 134, Version 1.

UNESCO (1981): Tenth report of the Joint Panel on Oceanographic Tables and Standards. UNESCO Tech. Papers in Mar. Sci., 36, 25 pp.

3.3 Density

February 18, 2016

(1) Personnel

Hiroshi Uchida (JAMSTEC)

(2) Objectives

The objective of this study is to collect absolute salinity (also called "density salinity") data, and to evaluate an algorithm to estimate absolute salinity provided along with TEOS-10 (the International Thermodynamic Equation of Seawater 2010) (IOC et al., 2010).

(3) Materials and methods

Seawater densities were measured during the cruise with an oscillation-type density meter (DMA 5000M, serial no. 80570578, Anton-Paar GmbH, Graz, Austria) with a sample changer (Xsample 122, serial no. 80548492, Anton-Paar GmbH). The sample changer was used to load samples automatically from up to ninety-six 12-mL glass vials.

The water samples were collected in 100-mL aluminum bottles (Mini Bottle Can, Daiwa Can Company, Japan). The bottles were stored at room temperature (~23 ºC) upside down usually for 12 to 24 hours to make the temperature of the sample equal to the room temperature. The water sample was filled in a 12-mL glass vial and the glass vial was sealed with Parafilm M (Pechiney Plastic Packaging, Inc., Menasha, Wisconsin, USA) immediately after filling. Densities of the samples were measured at 20 ºC by the density meter two times for each bottle and averaged to estimate the density. When the difference between the two measurements was greater than 0.002, additional measurements were conducted until two samples satisfying the above criteria were obtained.

Time drift of the density meter was monitored by periodically measuring the density of ultra-pure water (Milli-Q water, Millipore, Billerica, Massachusetts, USA) prepared from Yokosuka (Japan) tap water in October 2012. The true density at 20 ºC of the Milli-Q water was estimated to be 998.2042 kg m^{-3} from the isotopic composition ($\delta D = -8.76$ ‰, $\delta^{18}O = -56.86$ ‰) and International Association for the Properties of Water and Steam (IAPWS)-95 standard. An offset correction was applied to the measured density by using the Milli-Q water measurements ($\rho_{Milli\text{-}Q}$) with a slight modification of the density dependency (Uchida et al., 2011). The offset (ρ_{offset}) of the measured density (ρ) was reevaluated in November 2014 as follows:

$$\rho_{offset} = (\rho_{Milli\text{-}Q} - 998.2042) - (\rho - 998.2042) \times 0.000411 \text{ [kg m}^{-3}\text{]}.$$

The offset correction was verified by measuring Reference Material for Density in Seawater (prototype Dn-RM1) developing with Marine Works Japan, Ltd., Kanagawa, Japan, and produced by Kanso Technos Co., Ltd., Osaka, Japan, along with the Milli-Q water.

Density salinity can be back calculated from measured density and temperature (20 ºC) with TEOS-10.

(4) Results

Results of density measurements of the Reference Material for Density in Seawater (Dn-RM1) were shown in Table 3.3.1.

A total of 32 pairs of replicate samples were measured. The root-mean square of the absolute difference of replicate samples was 0.0009 g/kg.

The measured density salinity anomalies (δS_A) are shown in Fig. 3.3.1. The measured δS_A well agree with calculated δS_A from Pawlowicz et al. (2011) which exploits the correlation between δS_A and nutrient concentrations and

carbonate system parameters based on mathematical investigation using a model relating composition, conductivity and density of arbitrary seawaters.

(5) References

IOC, SCOR and IAPSO (2010): The international thermodynamic equation of seawater – 2010: Calculation and use of thermodynamic properties. Intergovernmental Oceanographic Commission, Manuals and Guides No. 56, United Nations Educational, Scientific and Cultural Organization (English), 196 pp.

Pawlowicz, R., D. G. Wright and F. J. Millero (2011): The effects of biogeochemical processes on ocean conductivity/salinity/density relationships and the characterization of real seawater. *Ocean Science*, 7, 363–387.

Uchida, H., T. Kawano, M. Aoyama and A. Murata (2011): Absolute salinity measurements of standard seawaters for conductivity and nutrients. *La mer*, 49, 237–244.

Table 3.3.1. Result of density measurements of the Reference Material for Density in Seawater (prototype Dn-RM1).

Date	Stations	Mean density of Dn-RM1 (kg/m^3)	Note
2015/12/29	1,2,3,4,6,10	1024.2631	
2015/12/31	14	1024.2637	
2016/01/01	18	1024.2628	
2016/01/02	22	1024.2627	
2016/01/03	26	1024.2631	
2016/01/04	31	1024.2619	
	33	1024.2622	
2016/01/06	37	1024.2638	
2016/01/07	41	1024.2634	
	42	1024.2624	
2016/01/08	43	1024.2597	
	45	1024.2601	
2016/01/08	46,47	1024.2609	
	48,50	1024.2602	
2016/01/09	51,52	1024.2640	
	Average:	1024.2623 ± 0.0014	

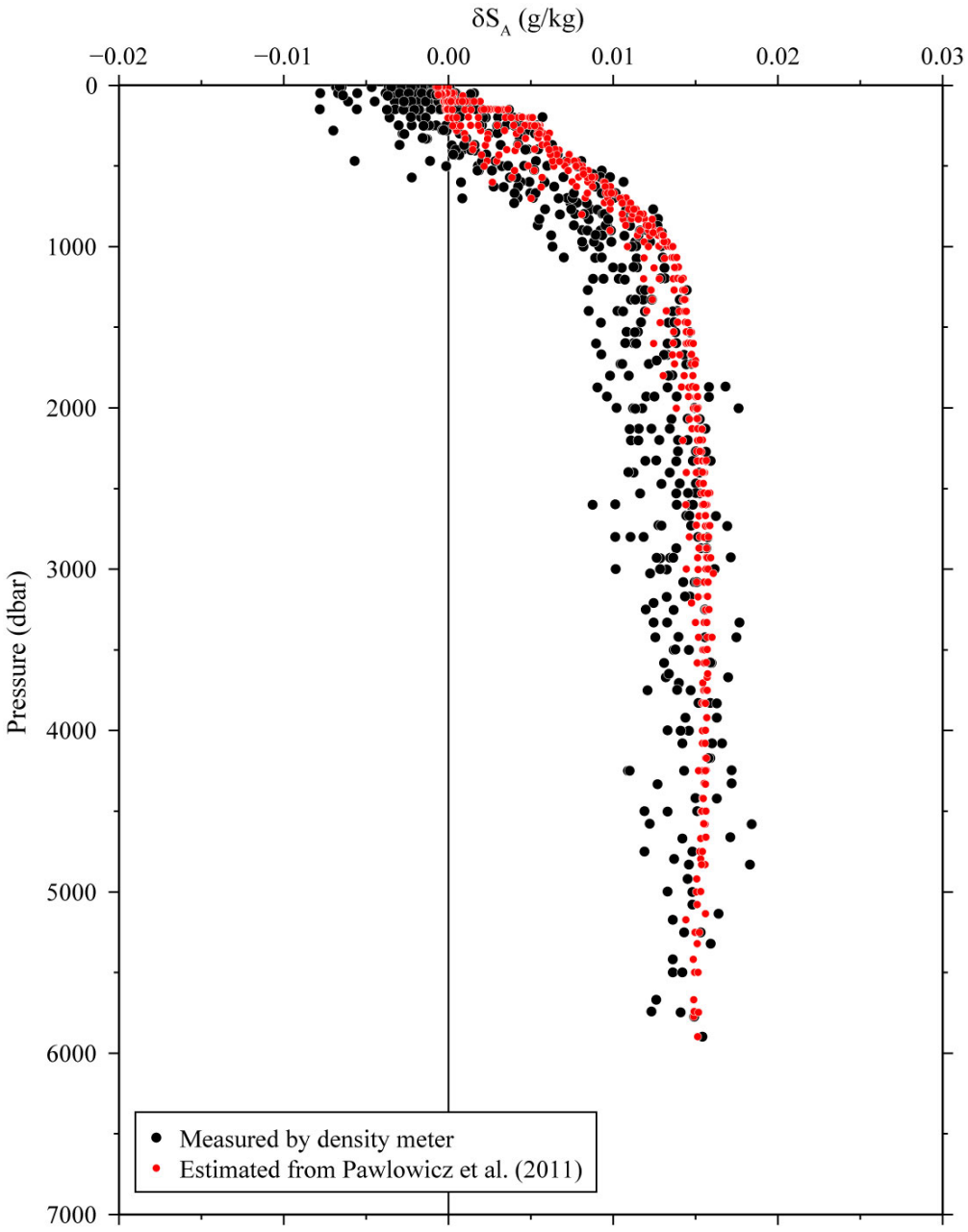

Figure 3.3.1. Vertical distribution of density salinity anomaly measured by the density meter. Absolute Salinity anomaly estimated from nutrients and carbonate parameters (Pawlowicz et al., 2011) are also shown for comparison.

3.4 Oxygen

January 27, 2016
Yuichiro Kumamoto
Japan Agency for Marine-Earth Science and Technology

(1) Personnel

Yuichiro Kumamoto [1)], ***Misato Kuwahara*** [2)], ***Keitaro Matsumoto*** [2)], ***Masahiro Orui*** [2)], **and** ***Haruka Tamada*** [2)]

1) Japan Agency for Marine-Earth Science and Technology

2) Marine Works Japan Co. Ltd

(2) Objectives

Dissolved oxygen is one of good tracers for the ocean circulation. Climate models predict a decline in oceanic dissolved oxygen concentration and a consequent expansion of the oxygen minimum layers under global warming conditions, which results mainly from decreased interior advection and ongoing oxygen consumption by remineralization. The mechanism of the decrease, however, is still unknown. During MR15-05 cruise, we measured dissolved oxygen concentration from surface to bottom layers at all the hydrocast stations in the eastern Indian Ocean. All the stations reoccupied the WOCE Hydrographic Program I10 stations in 1995. Our purpose is to evaluate temporal change in dissolved oxygen concentration in the North Pacific Ocean during the past decades.

(3) Reagents

Pickling Reagent I: Manganous chloride solution (3M)

Pickling Reagent II: Sodium hydroxide (8M) / sodium iodide solution (4M)

Sulfuric acid solution (5M)

Sodium thiosulfate (0.025M)

Potassium iodate (0.001667M): NMIJ CRM 3006-a No.028, Mass fraction: 99.973 ± 0.018 % (expanded uncertainty)

CSK standard of potassium iodate: Lot KPG6393, Wako Pure Chemical Industries Ltd., 0.0100N

(4) Instruments

Burette for sodium thiosulfate and potassium iodate;

APB-620 and APB-510 manufactured by Kyoto Electronic Co. Ltd. / 10 cm^3 of titration vessel

Detector;

Automatic photometric titrator, DOT-01X manufactured by Kimoto Electronic Co. Ltd.

(5) Seawater sampling

Following procedure is based on a determination method in the WHP Operations Manual (Dickson, 1996). Seawater samples were collected from 12-liters Niskin sampler bottles attached to the CTD-system. Seawater for bottle oxygen measurement was transferred from the Niskin sampler bottle to a volume calibrated glass flask (ca. 100 cm^3). Three times

volume of the flask of seawater was overflowed. Sample temperature was measured using a thermometer. Then two reagent solutions (Reagent I, II) of 0.5 cm^3 each were added immediately into the sample flask and the stopper was inserted carefully into the flask. The sample flask was then shaken vigorously to mix the contents and to disperse the precipitate finely throughout. After the precipitate has settled at least halfway down the flask, the flask was shaken again to disperse the precipitate. The sample flasks containing pickled samples were stored in a laboratory until they were titrated.

(6) Sample measurement

At least two hours after the re-shaking, the pickled samples were measured on board. A magnetic stirrer bar and 1 cm^3 sulfuric acid solution were added into the sample flask and stirring began. Samples were titrated by sodium thiosulfate solution whose molarity was determined by potassium iodate solution. Temperature of sodium thiosulfate during titration was recorded by a thermometer. We measured dissolved oxygen concentration using two sets of the titration apparatus, named DOT-6 and DOT-8. Dissolved oxygen concentration ($\mu mol\ kg^{-1}$) was calculated by the sample temperature during the sampling, CTD salinity, flask volume, and titrated volume of the sodium thiosulfate solution.

(7) Standardization

Concentration of sodium thiosulfate titrant (ca. 0.025M) was determined by potassium iodate solution. Pure potassium iodate was dried in an oven at 130°C. 1.7835 g potassium iodate weighed out accurately was dissolved in deionized water and diluted to final volume of 5 dm^3 in a calibrated volumetric flask (0.001667M). 10 cm^3 of the standard potassium iodate solution was added to a flask using a volume-calibrated dispenser. Then 90 cm^3 of deionized water, 1 cm^3 of sulfuric acid solution, and 0.5 cm^3 of pickling reagent solution II and I were added into the flask in order. Amount of titrated volume of sodium thiosulfate (usually 5 times measurements average) gave the molarity of the sodium thiosulfate titrant. Table 3.4.1 shows result of the standardization during this cruise. Coefficient of variation (C.V.) for the standardizations was 0.016 ± 0.005 % (standard deviation, n = 16), c.a. 0.05 $\mu mol\ kg^{-1}$.

(8) Determination of the blank

The oxygen in the pickling reagents I (0.5 cm^3) and II (0.5 cm^3) was assumed to be 3.8×10^{-8} mol (Murray *et al.*, 1968). The blank from the presence of redox species apart from oxygen in the reagents (the pickling reagents I, II, and the sulfuric acid solution) was determined as follows. 1 and 2 cm^3 of the standard potassium iodate solution were added to two flasks respectively. Then 100 cm^3 of deionized water, 1 cm^3 of sulfuric acid solution, and 0.5 cm^3 of pickling reagent solution II and I each were added into the two flasks in order. The blank was determined by difference between the two times of the first (1 cm^3 of KIO_3) titrated volume of the sodium thiosulfate and the second (2 cm^3 of KIO_3) one. The results of 3 times blank determinations were averaged (Table 3.4.1). The averaged blank values for DOT-6 and DOT-8 were 0.002 ± 0.002 (standard deviation, n=8) and 0.000 ± 0.002 (standard deviation, n=8) cm^3, respectively.

Table 3.4.1 Results of the standardization (End point, E.P.) and the blank determinations (cm^3).

Date (UTC)	KIO_3 No.	$Na_2S_2O_3$ No.	DOT-6		DOT-8		Stations
			E.P.	blank	E.P.	blank	
2015/12/27	K1504E02	T1505A	3.962	0.002	3.963	0.000	001-015
2015/12/30	K1504E03	T1505A	3.965	0.003	3.965	0.001	016-026
2016/01/03	K1504E04	T1505B	3.957	0.000	3.959	0.001	027-041
2016/01/06	K1504E05	T1505B	3.957	0.002	3.958	0.000	042-052

(9) Replicate sample measurement

From a routine CTD cast at all the stations, a pair of replicate samples was collected at four layers of 50, 400, 1800, and 3500 dbars. The total number of the replicate sample pairs in good measurement (flagged 2) was 170 (Fig. 3.4.1). The standard deviation of the replicate measurement was 0.60 μmol kg^{-1} calculated by a procedure (SOP23) in DOE (1994).

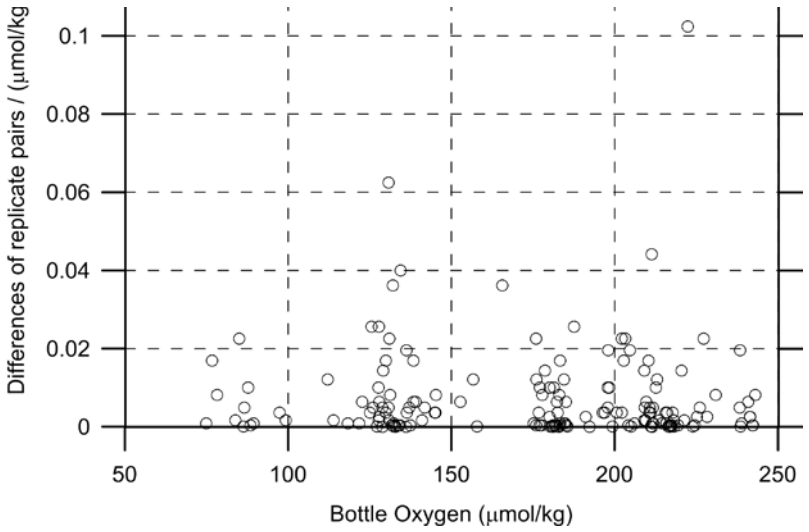

Figure 3.4.1 Oxygen difference between measurements of a replicate pair against oxygen concentration.

Duplicated Niskin #	Niskin	Pres.(db)	Oxygen (μmol kg^{-1})
1	X12J01	2000	139.67
2	X12J02	2000	139.74
3	X12J03	2001	139.73
4	X12104	2001	139.91
5	X12J05	2000	139.78
6	X12J06	2000	139.91

Table 3.4.2 Results of duplicate sample measurements.

7	X12J07	2000	139.85
8	X12J08	2000	139.93
9	X12J09	2000	139.87
10	X12J10	2000	139.85
11	X12J11	2001	139.96
12	X12J12	2001	139.87
13	X12J13	2001	140.02
14	X12J14	2001	139.86
15	X12J15	2001	139.89
16	X12J16	2001	139.92
17	X12J17	2000	139.97
18	X12J18	1999	139.86
19	X12J19	2000	139.97
20	X12J20	1999	139.99
21	X12J21	2000	139.94
22	X12J22	2001	139.90
23	X12J23	2001	139.97
24	X12J24	2001	139.98
25	X12J25	2000	139.91
26	X12J26	2001	139.94
27	X12J27	2000	139.93
28	X12J28	2001	139.70
29	X12J29	2001	139.89
30	X12J30	2001	139.78
31	X12J31	2001	139.88
32	X12J32	2001	139.79
33	X12J33	2001	140.02
34	X12J34	2001	139.92
35	X12J35	2000	139.77
36	X12J36	2000	139.85

(10) Duplicate sample measurement

At Station 900 (test), duplicate sampling were taken at 2000 dbar for all the Niskin bottles (36 bottles, Table 3.4.2). The standard deviation of the duplicate measurements were calculated to be 0.09 μmol kg^{-1}, which were nearly equivalent with that of the replicate measurements (0.06 μmol kg^{-1}, see section 9). **(11) CSK standard measurements**

The CSK standard is a commercial potassium iodate solution (0.0100 N) for analysis of dissolved oxygen. We titrated the CSK standard solution (Lot KPG6393) against our KIO_3 standard solution (Lot K1504E01) as samples before the cruise on 25 Dec. 2016. Concentration of the CSK solution against that of our KIO_3 solution was calculated to be 0.010006 ± 0.000002 N and 0.010006 ± 0.000002 N for DOT-6 and DOT-8, respectively.

(12) Quality control flag assignment

Quality flag values were assigned to oxygen measurements using the code defined in Table 0.2 of WHP Office Report WHPO 91-1 Rev.2 section 4.5.2 (Joyce *et al.*, 1994). Measurement flags of 2 (good), 3 (questionable), 4 (bad), and 5 (missing) have been assigned (Table 3.4.3). For the choice between 2, 3, or 4, we basically followed a flagging procedure as listed below:

a. Bottle oxygen concentration at the sampling layer was plotted against sampling pressure. Any points not lying on a generally smooth trend were noted.
b. Difference between bottle oxygen and CTD oxygen was then plotted against sampling pressure. If a datum deviated from a group of plots, it was flagged 3.
c. Vertical sections against pressure and potential density were drawn. If a datum was anomalous on the section plots, datum flag was degraded from 2 to 3, or from 3 to 4.
d. If there was problem in the measurement, the datum was flagged 4.
e. If the bottle flag was 4 (did not trip correctly), a datum was flagged 4 (bad). In case of the bottle flag 3 (leaking) or 5 (unknown problem), a datum was flagged based on steps a, b, c, and d.

Table 3.4.3 Summary of assigned quality control flags.

Flag	Definition	Number*
2	Good	1363
3	Questionable	0
4	Bad	0
5	Not report (missing)	0
	Total	1363

*Replicate samples (n = 170) were not included.

References

Dickson, A. (1996) Determination of dissolved oxygen in sea water by Winkler titration, in WHPO Pub. 91-1 Rev. 1, November 1994, Woods Hole, Mass., USA.

DOE (1994) Handbook of methods for the analysis of the various parameters of the carbon dioxide system in sea water; version 2. A.G. Dickson and C. Goyet (eds), ORNL/CDIAC-74.

Joyce, T., and C. Corry, eds., C. Corry, A. Dessier, A. Dickson, T. Joyce, M. Kenny, R. Key, D. Legler, R. Millard, R. Onken, P. Saunders, M. Stalcup (1994) Requirements for WOCE Hydrographic Programme Data Reporting, WHPO Pub. 90-1 Rev. 2, May 1994 Woods Hole, Mass., USA.

Murray, C.N., J.P. Riley, and T.R.S. Wilson (1968) The solubility of oxygen in Winkler reagents used for determination of dissolved oxygen, Deep-Sea Res., 15, 237-238

3.5 Nutrients

(1) Personnel

Michio AOYAMA(JAMSTEC/Fukushima Univ. , Principal Investigator)

LEG 1

Elena HAYASHI (Department of Marine & Earth Science, Marine Works Japan Ltd.)

Tomomi SONE (Department of Marine & Earth Science, Marine Works Japan Ltd.)

Kohei MIURA (Department of Marine& Earth Science, Marine Works Japan Ltd.)

Minoru KAMATA (Department of Marine & Earth Science, Marine Works Japan Ltd.)

LEG 2

Elena HAYASHI (Department of Marine & Earth Science, Marine Works Japan Ltd.)

Minoru KAMATA (Department of Marine & Earth Science, Marine Works Japan Ltd.)

(2) Objectives

The objectives of nutrients analyses during the R/V Mirai MR1505 cruise, GO-SHIP I10 repeat cruise in 2015-2016, in the Eastern Indian Ocean are as follows;

- Describe the present status of nutrients concentration with excellent comparability.
- The determinants are nitrate, nitrite, silicate, phosphate and Ammonium.
- Study the temporal and spatial variation of nutrients concentration based on the previous high quality experiments data of WOCE previous I10 cruises in 1995, GEOSECS, IGY and so on.
- Study of temporal and spatial variation of nitrate: phosphate ratio, so called Redfield ratio.
- Obtain more accurate estimation of total amount of nitrate, silicate and phosphate in the interested area.
- Provide more accurate nutrients data for physical oceanographers to use as tracers of water mass movement.

(3) Summary of nutrients analysis

We made 50 QuAAtro 2-HR runs for the samples at 56 casts, 52 stations in MR1505. The total amount of layers of the seawater sample reached up to 2484 for MR1505. We made duplicate measurement at all layers at all stations.

(4) Instrument and Method

(4.1) Analytical detail using QuAAtro 2-HR systems (BL-Tech)

We applied two units of QuAAtro in this cruise. Unit 1 and Unit 2 were put for R/V Mirai equipment. Configurations of all units are completely same for five parameters, Nitrate, Nitrite, Silicate, Phosphate, and Ammonium.

Nitrate + nitrite and nitrite were analyzed according to the modification method of Grasshoff (1970). The sample nitrate was reduced to nitrite in a cadmium tube inside of which was coated with metallic

copper. The sample streamed with its equivalent nitrite was treated with an acidic, sulfanilamide reagent and the nitrite forms nitrous acid which reacted with the sulfanilamide to produce a diazonium ion. N-1-Naphthylethylene-diamine added to the sample stream then coupled with the diazonium ion to produce a red, azo dye. With reduction of the nitrate to nitrite, both nitrate and nitrite reacted and were measured; without reduction, only nitrite reacted. Thus, for the nitrite analysis, no reduction was performed and the alkaline buffer was not necessary. Nitrate was computed by difference.

The silicate method was analogous to that described for phosphate. The method used was essentially that of Grasshoff et al. (1983), wherein silicomolybdic acid was first formed from the silicate in the sample and added molybdic acid; then the silicomolybdic acid was reduced to silicomolybdous acid, or "molybdenum blue" using ascorbic acid as the reductant. The analytical methods of the nutrients, nitrate, nitrite, silicate and phosphate, during this cruise were same as the methods used in (Kawano et al. 2009).

The phosphate analysis was a modification of the procedure of Murphy and Riley (1962). Molybdic acid was added to the seawater sample to form phosphomolybdic acid which was in turn reduced to phosphomolybdous acid using L-ascorbic acid as the reductant.

The details of modification of analytical methods for four parameters, Nitrate, Nitrite, Silicate and Phosphate, used in this cruise are also compatible with the methods described in nutrients section in GO-SHIP repeat hydrography manual (Hydes et al., 2010), while an analytical method of ammonium is compatible with Determination of ammonia in seawater using a vaporization membrane permeability method (Kimura, 2000). The flow diagrams and reagents for each parameter are shown in Figures 3.5.1 to 3.5.5.

(4.2) Nitrate Reagents

Imidazole (buffer), 0.06 M (0.4 % w/v)

Dissolve 4 g imidazole, $C_3H_4N_2$, in 1000 mL DIW, add 2 mL concentrated HCl. After mixing, 1 mL Triton^{TM} X-100 (50 % solution in ethanol) is added.

Sulfanilamide, 0.06 M (1 % w/v) in 1.2 M HCl

Dissolve 10 g sulfanilamide, 4-$NH_2C_6H_4SO_3H$, in 900 mL of DIW, add 100 ml concentrated HCl. After mixing, 2 mL Triton^{TM} X-100 (50 %f solution in ethanol) is added.

N-1-Napthylethylene-diamine dihydrochloride, 0.004 M (0.1 %f w/v)

Dissolve 1 g NEDA, $C_{10}H_7NHCH_2CH_2NH_2$•2HCl, in 1000 mL of DIW and add 10 mL concentrated HCl. After mixing, 1 mL Triton^{TM} X-100 (50 %f solution in ethanol) is added.

Stored in a dark bottle.

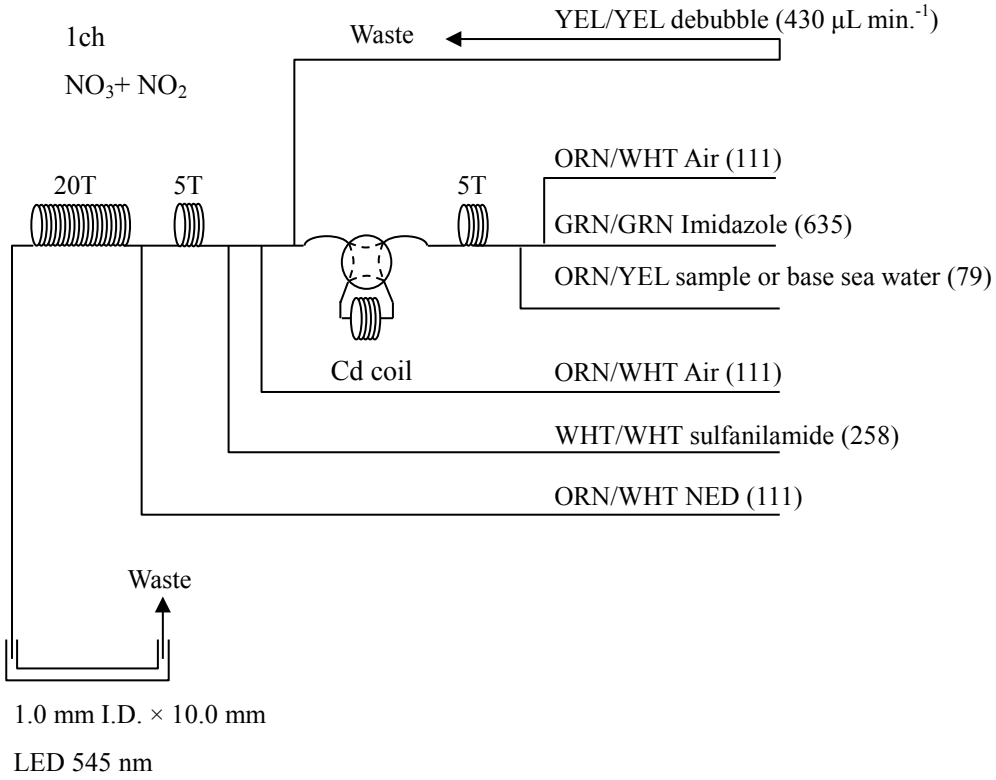

Figure 3.5.1 NO_3 + NO_2 (1ch.) Flow diagram.

(4.3) Nitrite Reagents

Sulfanilamide, 0.06 M (1% w/v) in 1.2 M HCl

Dissolve 10 g sulfanilamide, 4-$NH_2C_6H_4SO_3H$, in 900 mL of DIW, add 100 mL concentrated HCl. After mixing, 2 mL Triton™ X-100 (50% solution in ethanol) is added.

N-1-Napthylethylene-diamine dihydrochloride, 0.004 M (0.1% w/v)

Dissolve 1 g NEDA, $C_{10}H_7NHCH_2CH_2NH_2$•2HCl, in 1000 mL of DIW and add 10 mL concentrated HCl. After mixing, 1 mL Triton™ X-100 (50% solution in ethanol) is added. This reagent was stored in a dark bottle.

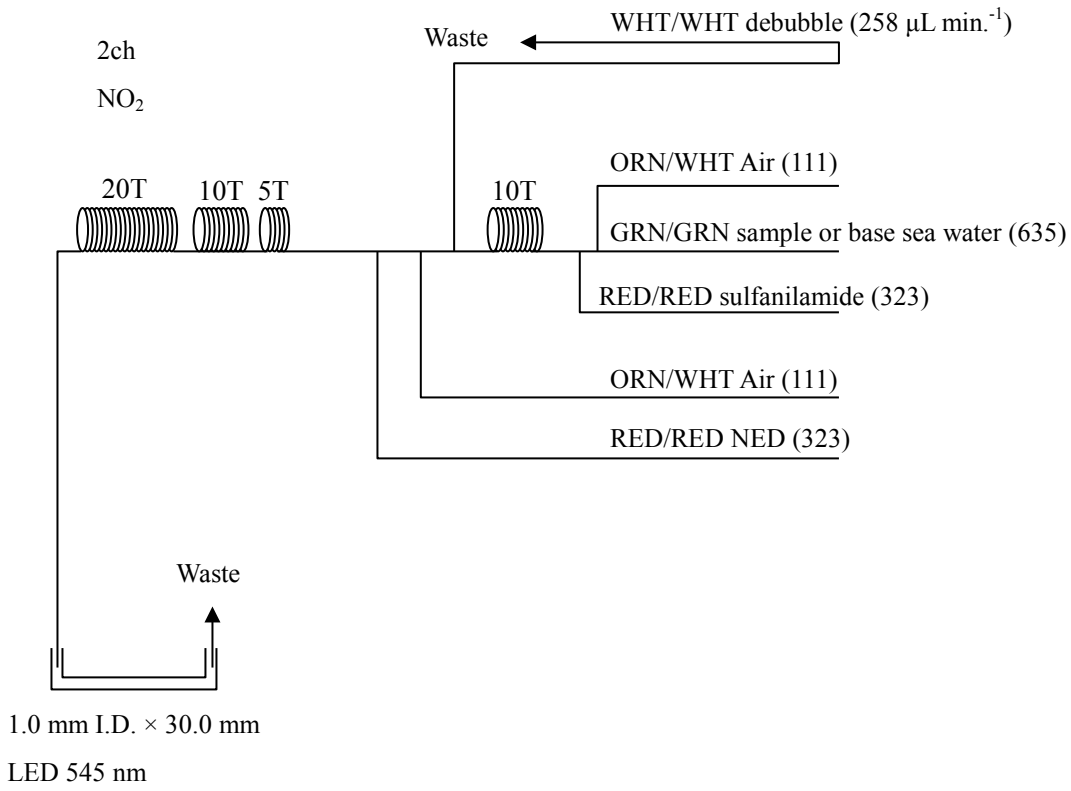

Figure 3.5.2 NO_2 (2ch.) Flow diagram.

(4.4) Silicate Reagents

Molybdic acid, 0.06 M (2% w/v)

Dissolve 15 g disodium Molybdate(VI) dihydrate, $Na_2MoO_4 \cdot 2H_2O$, in 980 mL DIW, add 8 mL concentrated H_2SO_4. After mixing, 20 mL sodium dodecyl sulphate (15% solution in water) is added.

Oxalic acid, 0.6 M (5% w/v)

Dissolve 50 g oxalic acid anhydrous, HOOC: COOH, in 950 mL of DIW.

Ascorbic acid, 0.01 M (3% w/v)

Dissolve 2.5g L(+)-ascorbic acid, $C_6H_8O_6$, in 100 mL of DIW. This reagent was freshly prepared at every day.

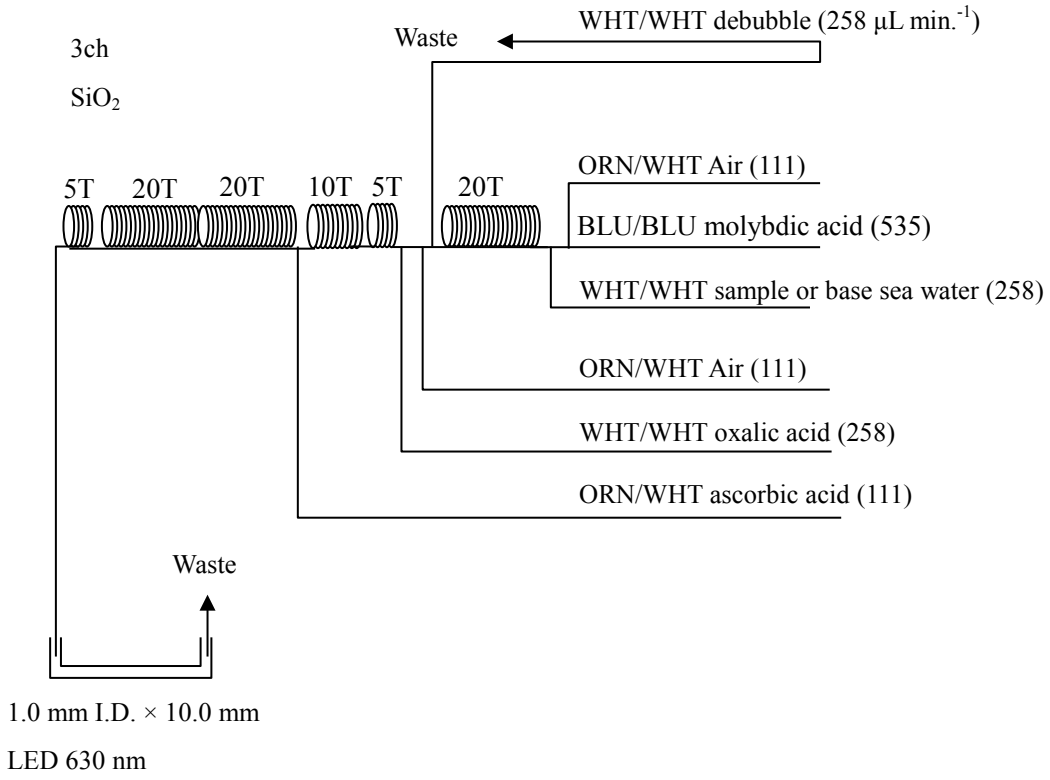

Figure 3.5.3 SiO_2 (3ch.) Flow diagram.

(4.5) Phosphate Reagents

Stock molybdate solution, 0.03 M (0.8% w/v)

Dissolve 8 g disodium molybdate(VI) dihydrate, $Na_2MoO_4 \cdot 2H_2O$, and 0.17 g antimony potassium tartrate, $C_8H_4K_2O_{12}Sb_2 \cdot 3H_2O$, in 950 mL of DIW and added 50 ml concentrated H_2SO_4.

Mixed Reagent

Dissolve 1.2 g L(+)-ascorbic acid, $C_6H_8O_6$, in 150 mL of stock molybdate solution. After mixing, 3 mL sodium dodecyl sulphate (15% solution in water) was added. This reagent was freshly prepared before every measurement.

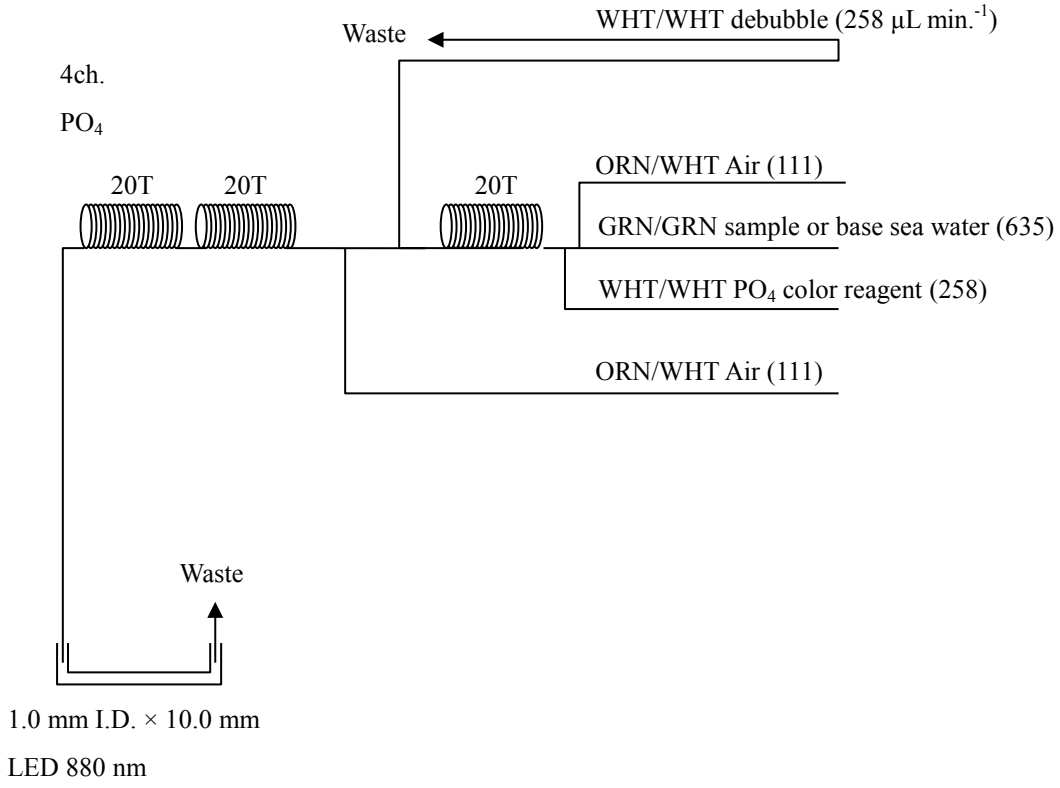

Figure 3.5.4 PO_4 (4ch.) Flow diagram.

(4.6) Ammonium Reagents

EDTA

Dissolve 41 g EDTA (ethylenediaminetetraacetatic acid tetrasodium salt), $C_{10}H_{12}N_2O_8Na_4 \cdot 4H_2O$, and 2 g boric acid, H_3BO_3, in 200 mL of DIW. After mixing, 1 mL Triton™ X-100 (30% solution in DIW) is added. This reagent is prepared at a week about.

NaOH

Dissolve 5 g sodium hydroxide, NaOH, and 16 g EDTA in 100 mL of DIW. This reagent is prepared at a week about.

Stock Nitroprusside

Dissolve 0.25 g sodium pentacyanonitrosylferrate(II), $Na_2[Fe(CN)_5NO]$, in 100 mL of DIW and add 0.2 mL 1N H_2SO_4. Stored in a dark bottle and prepared at a month about.

Nitroprusside solution

Mixed 4 mL stock nitroprusside and 5 mL 1N H_2SO_4 in 500 mL of DIW. After mixing, 2 mL Triton™ X-100 (30% solution in DIW) is added. This reagent is stored in a dark bottle and prepared at every 2 or 3 days.

Alkaline phenol

Dissolve 10 g phenol, C_6H_5OH, 5 g sodium hydroxide and citric acid, $C_6H_8O_7$, in 200 mL DIW. Stored in a dark bottle and prepared at a week about.

NaClO solution

Mix 3 mL sodium hypochlorite solution, NaClO, in 47 mL DIW. Stored in a dark bottle and fleshly prepared before every measurement. This reagent is prepared 0.3% available chlorine.

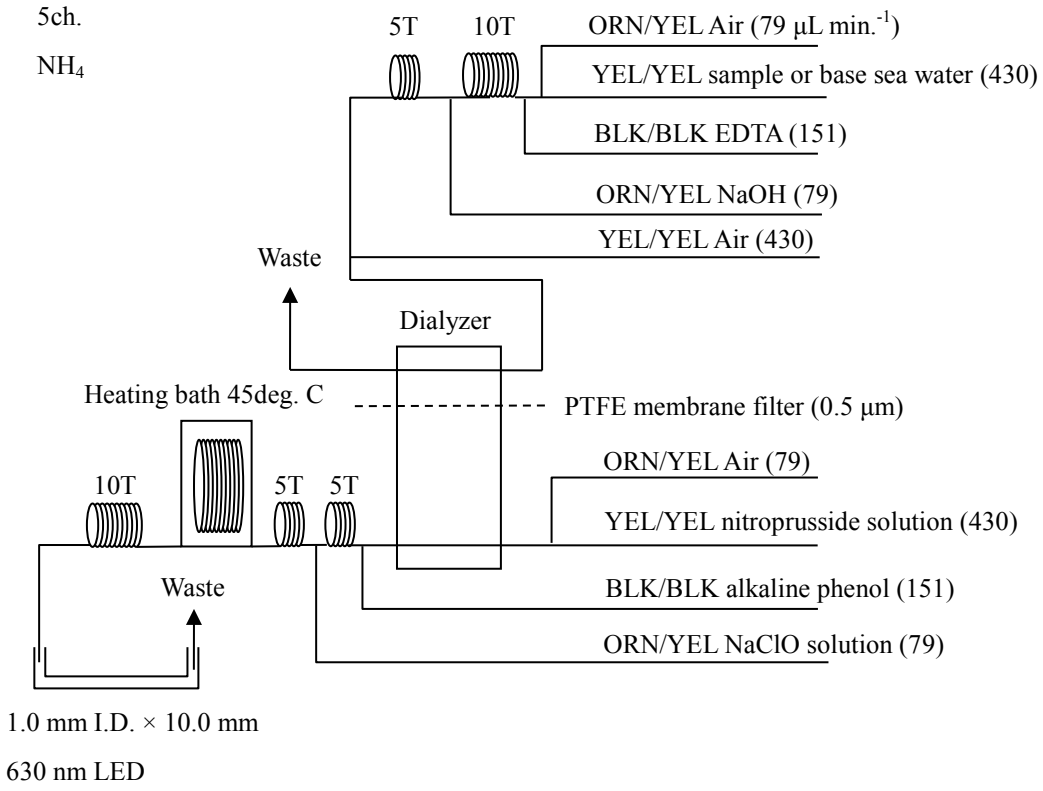

Figure 3.5.5 NH_4 (5ch.) Flow diagram.

(4.7) Sampling procedures

Sampling of nutrients followed that oxygen, salinity and trace gases. Samples were drawn into two of virgin 10 mL polyacrylates vials without sample drawing tubes. These were rinsed three times before filling and then vials were capped immediately after the drawing. The vials were put into water bath adjusted to ambient temperature, 23 ± 2 deg. C, in about 30 minutes before use to stabilize the temperature of samples in MR1505.

No transfer was made and the vials were set an auto sampler tray directly. Samples were analyzed after collection basically within 24 hours in principal.

(4.8) Data processing

Raw data from QuAAtro 2-HR was treated as follows:

- Checked baseline shift.
- Checked the shape of each peak and positions of peak values taken, and then changed the positions of peak values taken if necessary.
- Carry-over correction and baseline drift correction were applied to peak heights of each samples followed by sensitivity correction.
- Baseline correction and sensitivity correction were done basically using liner regression.
- Loaded pressure and salinity from CTD data to calculate density of seawater. In case of bucket sample, we generally used bottle salinity from AUTOSAL, while in case of bio-cast we used surface CTD data.
- Calibration curves to get nutrients concentration were assumed second order equations.

(5) Nutrients standards

(5.1) Volumetric laboratory ware of in-house standards

All volumetric glass ware and polymethylpentene (PMP) ware were gravimetrically calibrated. These volumetric flasks were gravimetrically calibrated at the temperature of using in the laboratory within 0 to 4 K.

Volumetric flasks

Volumetric flasks of Class quality (Class A) are used because their nominal tolerances are 0.05 % or less over the size ranges likely to be used in this work. Class A flasks are made of borosilicate glass, and the standard solutions were transferred to plastic bottles as quickly as possible after they are made up to volume and well mixed in order to prevent excessive dissolution of silicate from the glass. High quality plastic (polymethylpentene, PMP, or polypropylene) volumetric flasks were gravimetrically calibrated and used only within 0 to 4 K of the calibration temperature.

The computation of volume contained by glass flasks at various temperatures other than the calibration temperatures were done by using the coefficient of linear expansion of borosilicate crown glass.

Because of their larger temperature coefficients of cubical expansion and lack of tables constructed for these materials, the plastic volumetric flasks were gravimetrically calibrated over the temperature range of intended use and used at the temperature of calibration within 0 to 4 K. The weights obtained in the calibration weightings were corrected for the density of water and air buoyancy.

Pipettes and pipettors

All pipettes have nominal calibration tolerances of 0.1 % or better. These were gravimetrically calibrated in order to verify and improve upon this nominal tolerance.

(5.2) Reagents, general considerations

Specifications

For nitrate standard, "potassium nitrate 99.995 suprapur®" provided by Merck, Lot. B0771365211, CAS No. 7757-91-1, was used.

For nitrite standard, nitrite ion standard solution of JCSS (NO_2 1000mg/L) provided by Wako, Lot. ECP4122, CAS No. 7632-00-0, was used. The nitrite concentration was assigned by ion chromatography method using secondary standard solution of nitrite ion. ECP4122 was certified as 999mg L^{-1} (± 0.7 % k=2).

For phosphate standard, "potassium dihydrogen phosphate anhydrous 99.995 suprapur®" provided by Merck, Lot. B0691108204, CAS No.: 7778-77-0, was used.

For the silicate standard, we use "Silicon standard solution SiO_2 in NaOH 0.5 mol/l CertiPUR®" provided by Merck, CAS No. 1310-73-2, of which lot number is HC41358736 are used. The silicate concentration is certified by NIST-SRM3150. HC41358736 was certified as 982 mg kg^{-1} with the expanded uncertainty of ± 5 mg kg^{-1} (k=2). In the previous cruises, we assigned correction factor of merck solutions are shown in table 3.5.1 to ensure internal comparability among WOCE/CLIVAR cruises, we however used merck certified concentration to keep traceability to SI for silicate concentration throughout MR1505 and in the future cruises.

For ammonium standard, we use certified reference material of "ammonium chloride" provided by NMIJ, CAS No. 12125-02-9, of which lot number is NMIJ CRM 3011-a with the expanded uncertainty of ± 0.065 mass fraction % (k=2).

Table 3.5.1 A history of assigned factor of Merck solutions

Lot	Factor	Date	Reference
Merck OC551722	**1.001**	**2006/5/24**	
Merck HC623465	**1.000**		
Merck HC751838	**0.998**	**2007/4/13**	
Merck HC814662	**0.999**	**2008/8/27**	
Merck HC074650	**0.975**	**2010/11/5**	
Merck HC097572	**0.976**	**2011/06/20**	**RM Lot. BA, AY, BD, BE, BF**
Merck HC382250	**0.973**	**2013/9/14**	**RM Lot. BS, BU, BT, BD**

Treatment of silicate standard due to high alkalinity

Since the silicon standard solution Merck CertiPUR® is in NaOH 0.5 mol/l, we need to dilute and neutralize to avoid make precipitation of $MgOH_2$ etc. When we make B standard, silicon standard solution is diluted by factor 12 with pure water and neutralized by HCl 1.0 mol L^{-1} to be about 7. After that B standard solution is used to prepare C standards.

Ultra pure water

Ultra pure water (MilliQ water) freshly drawn was used for preparation of reagents, standard solutions and for measurement of reagent and system blanks.

Low-Nutrient Seawater (LNSW)

Surface water having low nutrient concentration was taken and filtered using 0.20 μm pore size capsule cartridge filter. This water was stored in 20 liter cubitainer with paper box. After stored for 5 month, a 1000 liter bag were filled with this LNSW filtering once more using 0.20 μm pore size capsule cartridge filter and irradiating by ultraviolet light in August 2015. After circulation of filtering and irradiating for 24 hours, LNSW was drawn into 20 liter cubitainer with paper box. The concentrations of nutrients of this LNSW were measured carefully in September 2015.

Although LNSW was sterilized by filtration and UV irradiation, in-house standard solution prepared with this LNSW showed that concentrations of nitrate, nitrite and phosphate decreased about 2 % after 2 days in November 2015. This should be caused by micro-organismal activity.

Therefore, LNSW was pasteurized at low temperature with 75 deg. C more than 12 hours to suspend micro-organismal activity in December 2015 on board. The concentrations of nutrients of in-house standard solution using pasteurized LNSW became not to decrease after 2 days of preparation as expected. The concentrations of nutrients of pasteurized LNSW were measured again in December 2015.

(5.3) Concentrations of nutrient for A, B and C standards

Concentrations of nutrients for A, B, C and D standards are set as shown in Table 3.5.2. The C standard is prepared according recipes as shown in Table 3.5.3. All volumetric laboratory tools were calibrated prior the cruise as stated in chapter (5.1). Then the actual concentration of nutrients in each fresh standard was calculated based on the ambient, solution temperature and determined factors of volumetric laboratory wares.

The calibration curves for each run were obtained using 6 levels, C-1, C-2, C-3, C-4, C-5 and C-6. C-1, C-2, C-3, C-4 and C-5 were the certified reference material of nutrients in seawater (hereafter CRM) and C-6 was in-house standard.

Table 3.5.2 Nominal concentrations of nutrients for A, B and C standards.

	A	B	D	C-1	C-2	C-3	C-4	C-5	C-6	C-7	C-8
NO_3(μM)	22500	900	900	BY	BU	CA	BW	BZ	54	-	-
NO_2(μM)	21700	26	865	BY	BU	CA	BW	BZ	1.0	-	-
SiO_2(μM)	35000	2760		BY	BU	CA	BW	BZ	172	-	-
PO_4(μM)	3000	60		BY	BU	CA	BW	BZ	3.7	-	-
NH_4(μM)	4000	200		-	-	-	-	-	6.0	2.0	0

Table 3.5.3 Working calibration standard recipes.

C std.	B-1 std.	B-2 std.	B-3 std
C-6	30 mL	20 mL	15 mL
C-7	-	-	5 mL
C-8	-	-	0 mL

B-1 std.: Mixture of nitrate, silicate and phosphate

B-2 std.: Nitrite

B-3 std: Ammonium

(5.4) Renewal of in-house standard solutions.

In-house standard solutions as stated in paragraph (5.2) were renewed as shown in Table 3.5.4 (a) to (c).

Table 3.5.4(a) Timing of renewal of in-house standards.

NO_3, NO_2, SiO_2, PO_4, NH_4	Renewal
A-1 std. (NO_3)	maximum a month
A-2 std. (NO_2)	commercial prepared solution
A-3 std. (SiO_2)	commercial prepared solution
A-4 std. (PO_4)	maximum a month
A-5 std. (NH_4)	maximum a month
B-1 std. (mixture of A-1, A-3 and A-4 std.)	maximum 8 days
B-2 std. (dilute D-2 std.)	maximum 8 days
B-3 std. (dilute A-5 std.)	maximum 8 days

Table 3.5.4(b) Timing of renewal of in-house standards.

Working standards	Renewal
C-6 std. (mixture of B-1, B-2 and B-3 std.) C-7 std. (dilute B-3 std.) C-8 (LNSW)	every 24 hours

Table 3.5.4(c) Timing of renewal of in-house standards for reduction estimation.

Reduction estimation	Renewal
D-1 std. (900 µM NO_3)	maximum 8 days
D-2 std. (870 µM NO_2)	maximum 8 days
36 µM NO_3	when C Std. renewed
34 µM NO_2	when C Std. renewed

(6) CRM

To get the more accurate and high quality nutrients data to achieve the objectives stated above, huge numbers of the bottles of the reference material of nutrients in seawater were prepared and used during the previous cruises (Aoyama et al., 2006, 2007, 2008, 2009, 2012, 2014). In the previous worldwide expeditions, such as WOCE cruises, the higher reproducibility and precision of nutrients measurements were required (Joyce and Corry, 1994). Since no standards were available for the measurement of nutrients in seawater at that time, the requirements were described in term of reproducibility. The required reproducibility was 1%, 1 to 2%, 1 to 3% for nitrate, phosphate and silicate, respectively. Although nutrient data from the WOCE one-time survey was of unprecedented quality and coverage due to much care in sampling and measurements, the differences of nutrients concentration at crossover points are still found among the expeditions (Aoyama and Joyce, 1996, Mordy et al., 2000, Gouretski and Jancke, 2001). For instance, the mean offset of nitrate concentration at deep waters was 0.5 µmol kg^{-1} for 345 crossovers at world oceans, though the maximum was 1.7 µmol kg^{-1} (Gouretski and Jancke, 2001). At the 31 crossover points in the Pacific WHP one-time lines, the WOCE standard of reproducibility for nitrate of 1 % was fulfilled at about half of the crossover points and the maximum difference was 7 % at deeper layers below 1.6 deg. C in potential temperature (Aoyama and Joyce, 1996).

During the period from 2003 to 2014, RMNS were used to keep comparability of nutrients measurement among the 8 cruises of CLIVAR project (Sato et al., 2010), MR1005 cruise for Arctic research (Aoyama et al., 2010) and MR1006 cruise for “Change in material cycles and ecosystem by the climate change and its feedback” (Aoyama et al., 2011).

In this MR1505 cruises, we used 6 lots of CRM (Lot BY, BU, CA, BW, BV, BZ) to ensure comparability and traceability to SI.

(6.1) CRMs for this cruise

5 lot of CRMs were used as calibration standards together with the C-6. Certified concentrations of these lots as shown in table 3.5.4 were used. These bottles were stored at a room in the ship, REAGENT STORE, where the temperature was maintained around 16 - 25 deg. C.

(6.2) Certified concentration for CRMs

The concentrations for CRM lots BY, BU, CA, BW, BZ, and BV are shown in Table 3.5.4.

Table 3.5.4 Certified concentration and uncertainty (k=2) of CRMs.

unit: µmol kg^{-1}

	Nitrate	Phosphate	Silicate	Nitrite
BY	**0.02 ± 0.02**	**0.039 ± 0.010**	**1.76 ± 0.06**	**0.02 ± 0.01**
BU	**3.94 ± 0.05**	**0.345 ± 0.009**	**20.92 ± 0.49**	**0.07 ± 0.01**
CA	**19.66 ± 0.15**	**1.407 ± 0.014**	**36.58 ± 0.22**	**0.06 ± 0.01**
BW	**24.59 ± 0.20**	**1.541 ± 0.014**	**60.01 ± 0.42**	**0.07 ± 0.01**
BZ	**43.35 ± 0.33**	**3.056 ± 0.033**	**161.0 ± 0.93**	**0.22 ± 0.01**
BV	**35.36 ± 0.35**	**2.498 ± 0.023**	**102.2 ± 1.10**	**0.05 ± 0.01**

(7) Quality control

(7.1) Precision of nutrients analyses during this cruise

Precision of nutrients analyses during this cruise was evaluated based on the 7 to 11 measurements, which are measured every 8 to 13 samples, during a run at the concentration of C-6 std. Summary of precisions are shown as Table 3.5.5 and Figures 3.5.6 to 3.5.8, the precisions for each parameter are generally good considering the analytical precisions during the R/V Mirai cruses conducted in 2009 - 2014. During this cruise, analytical precisions were 0.11% for nitrate, 0.11% for phosphate and 0.10% for silicate in terms of median of precision, respectively.

Table 3.5.5 Summary of precision based on the replicate analyses for all unit.

	Nitrate CV%	Nitrite CV%	Silicate CV%	Phosphate CV %	Ammonium CV %
Median	**0.11**	**0.17**	**0.10**	**0.11**	**0.36**
Mean	**0.11**	**0.18**	**0.10**	**0.11**	**0.39**
Maximum	**0.19**	**0.34**	**0.20**	**0.21**	**0.83**
Minimum	**0.03**	**0.07**	**0.03**	**0.04**	**0.12**
N	**49**	**49**	**49**	**49**	**11**

Table 3.5.5a Summary of precision based on the replicate analyses for unit 1.

	Nitrate CV%	Nitrite CV%	Silicate CV%	Phosphate CV %	Ammonium CV %
Median	**0.10**	**0.17**	**0.10**	**0.09**	**0.42**
Mean	**0.11**	**0.17**	**0.10**	**0.10**	**0.41**
Maximum	**0.17**	**0.27**	**0.20**	**0.14**	**0.83**
Minimum	**0.03**	**0.07**	**0.03**	**0.05**	**0.12**
N	**24**	**24**	**24**	**24**	**9**

Table 3.5.5b Summary of precision based on the replicate analyses for unit 2.

	Nitrate CV%	Nitrite CV%	Silicate CV%	Phosphate CV %	Ammonium CV %
Median	**0.11**	**0.18**	**0.10**	**0.13**	**0.27**
Mean	**0.12**	**0.18**	**0.10**	**0.13**	**0.27**
Maximum	**0.19**	**0.34**	**0.15**	**0.21**	**0.27**
Minimum	**0.07**	**0.07**	**0.07**	**0.04**	**0.26**
N	**25**	**25**	**25**	**25**	**2**

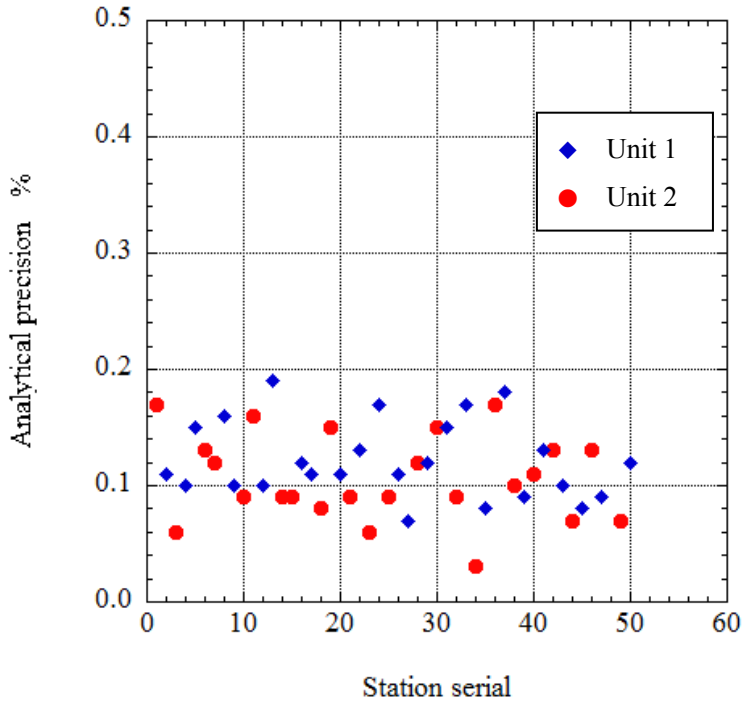

Figure 3.5.6 Time series of precision of nitrate in MR1505.

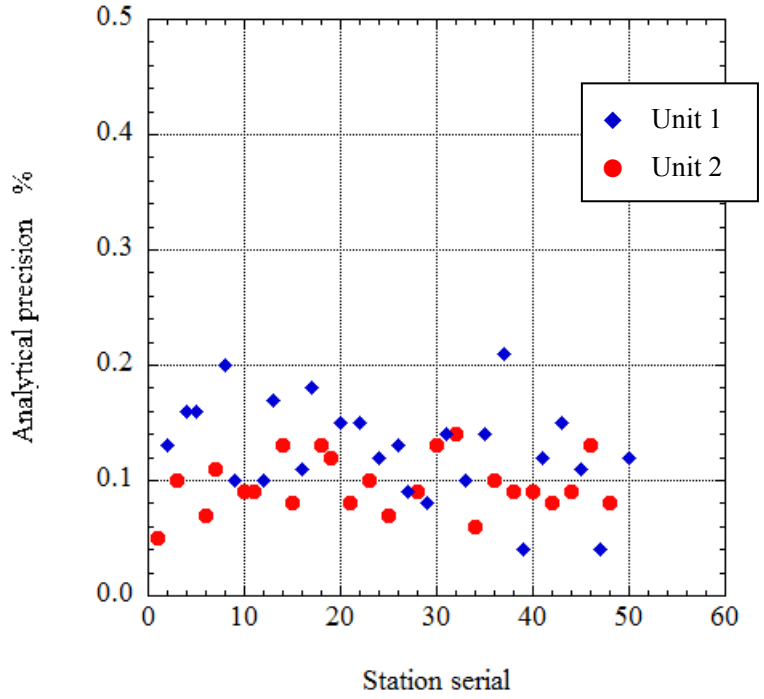

Figure 3.5.7 Time series of precision of phosphate in MR1505.

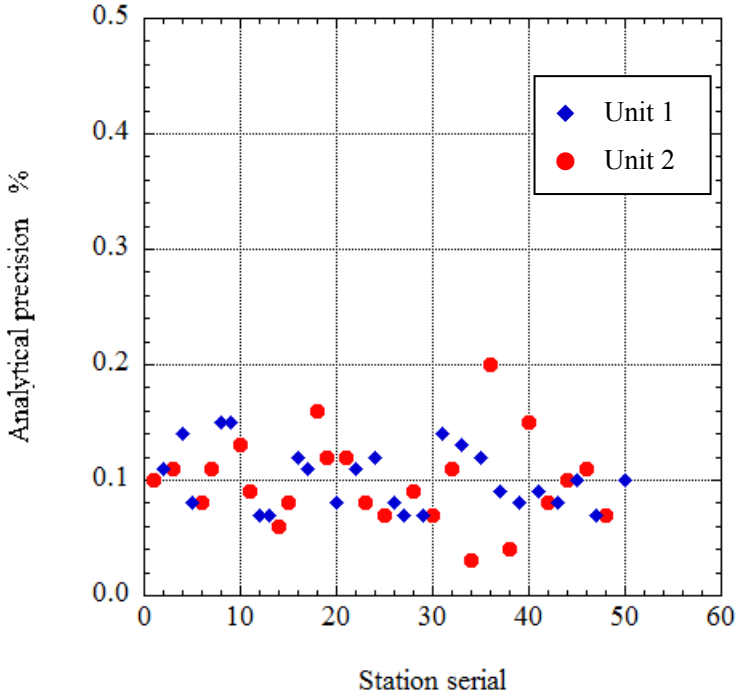

Figure 3.5.8 Time series of precision of silicate in MR1505.

(7.2) CRM lot. BV measurement during this cruise

CRM lot. BV was measured every run to monitor the comparability among runs. The results of lot. BV during this cruise are shown as Figures 3.5.9 to 3.5.11. Error bars represent analytical precision in figure 3.5.6 to 3.5.8.

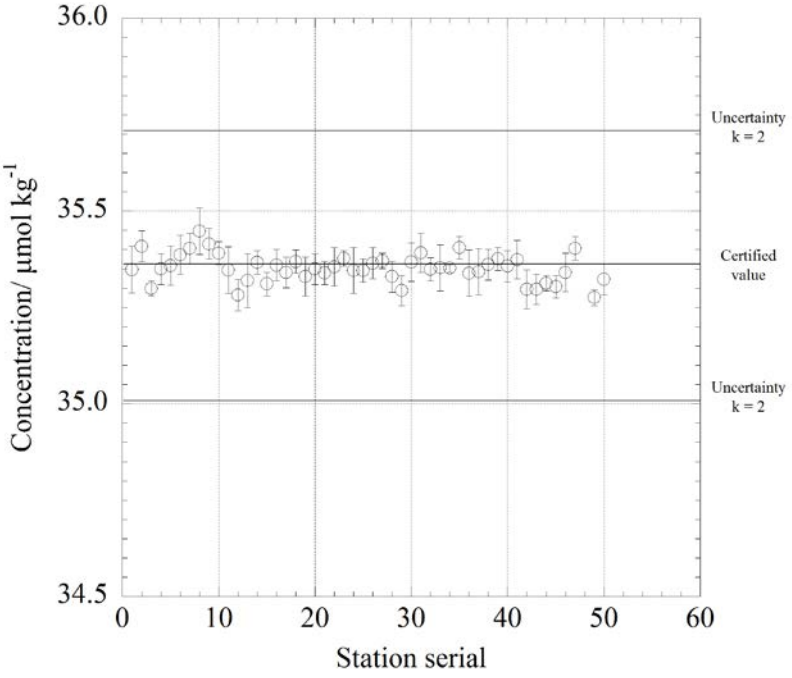

Figure3.5.9 Time series of CRM-BV of nitrate in MR1505.

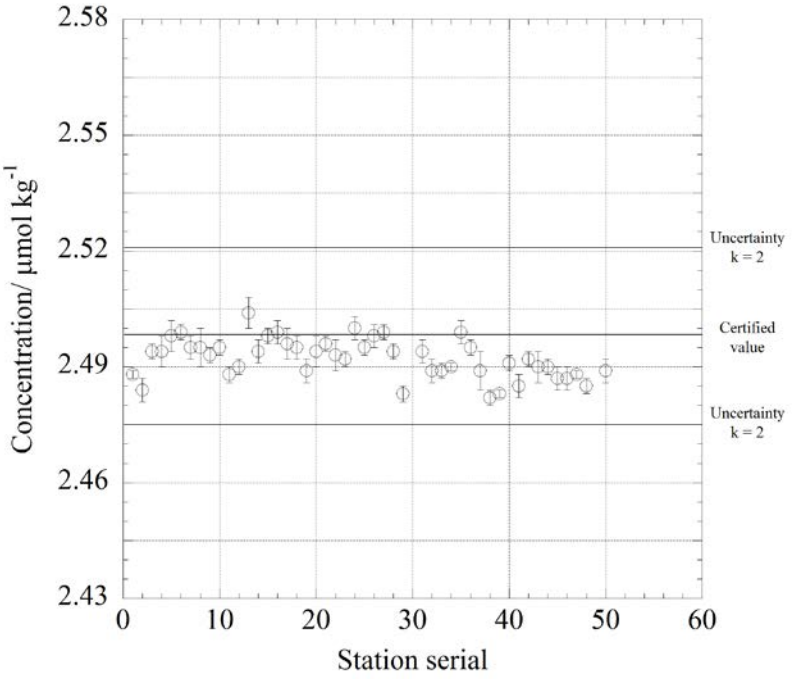

Figure 3.5.10 Time series of CRM-BV of phosphate in MR1505.

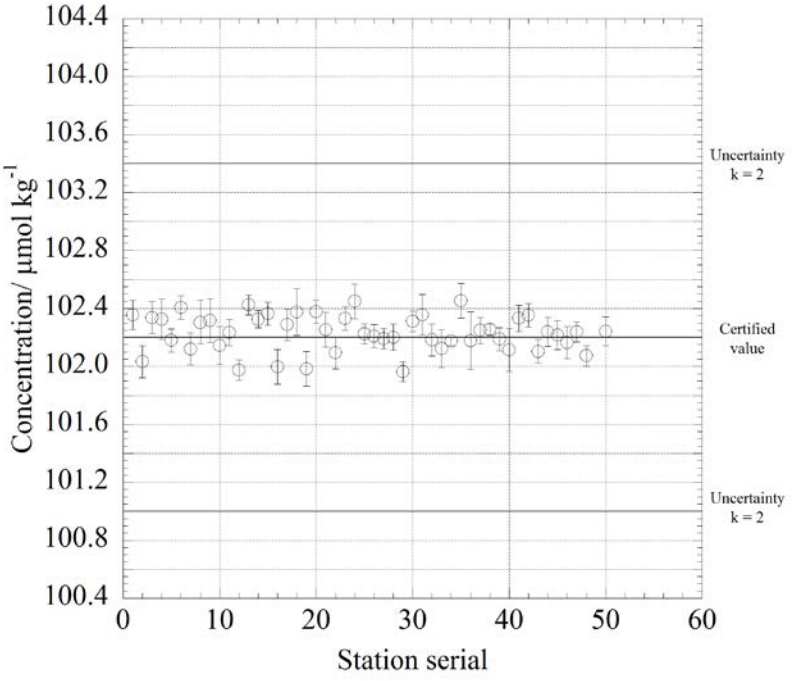

Figure 3.5.11 Time series of CRM-BV of silicate in MR1505.

(7.3) Carryover

We can also summarize the magnitudes of carryover throughout the cruise. These are small enough within acceptable levels as shown in Table 3.5.8 and Figures 3.5.12 to 3.5.14. The carryover in nitrate and silicate had a bias by equipments. It was 0.06% and 0.05%, mean value, at Unit 2. The other hand, it was 0.17% and 0.13 %, mean value, at Unit 1. We carried out the maintenance for Unit 1 by changing for new glass coils and new transmission tube before the stn. 22. The bias was clearly solved by the maintenance.

Table 3.5.6 Summary of carry over throughout MR1505.

	Nitrate CV%	Nitrite CV%	Silicate CV%	Phosphate CV %	Ammonium CV %
Median	**0.10**	**0.11**	**0.07**	**0.10**	**0.42**
Mean	**0.12**	**0.10**	**0.09**	**0.11**	**0.39**
Maximum	**0.28**	**0.40**	**0.23**	**0.17**	**0.67**
Minimum	**0.03**	**0.00**	**0.03**	**0.05**	**0.08**
N	**49**	**49**	**49**	**49**	**11**

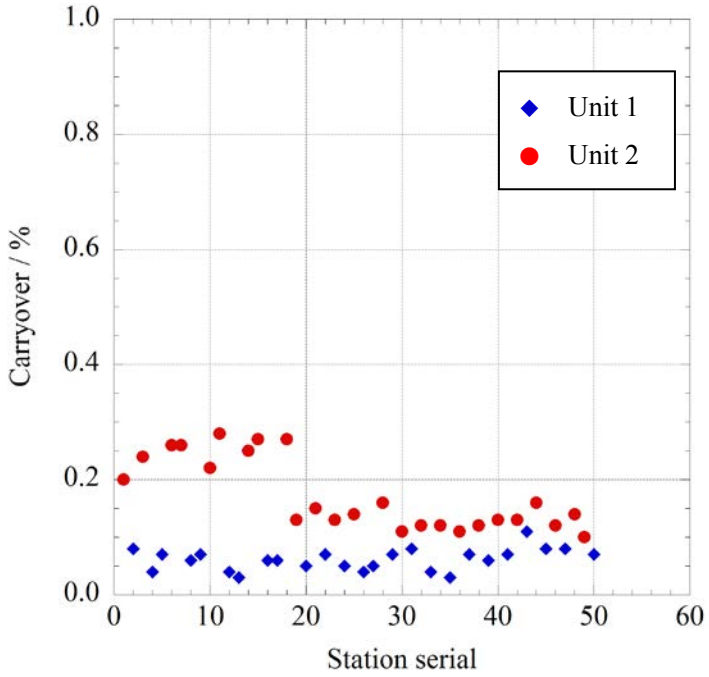

Figure 3.5.12 Time series of carryover of nitrate in MR1505.

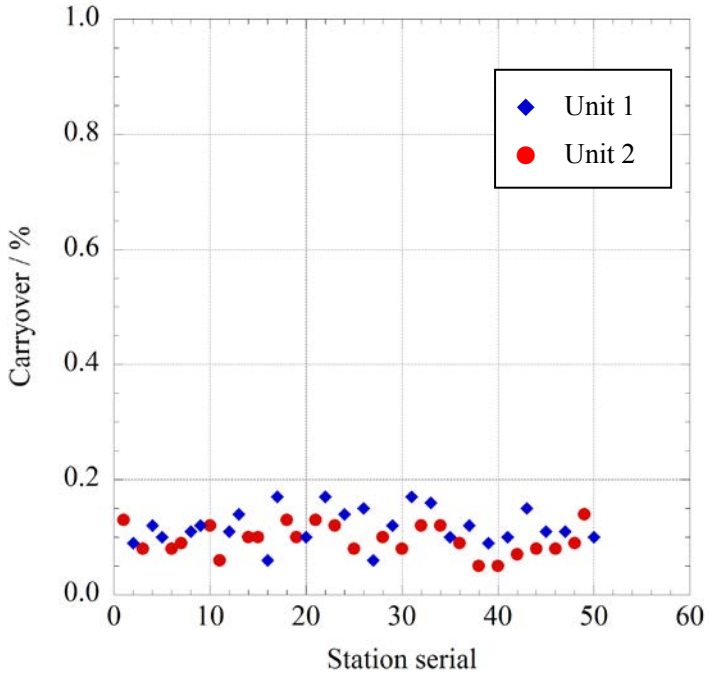

Figure 3.5.13 Time series of carryover of phosphate in MR1505.

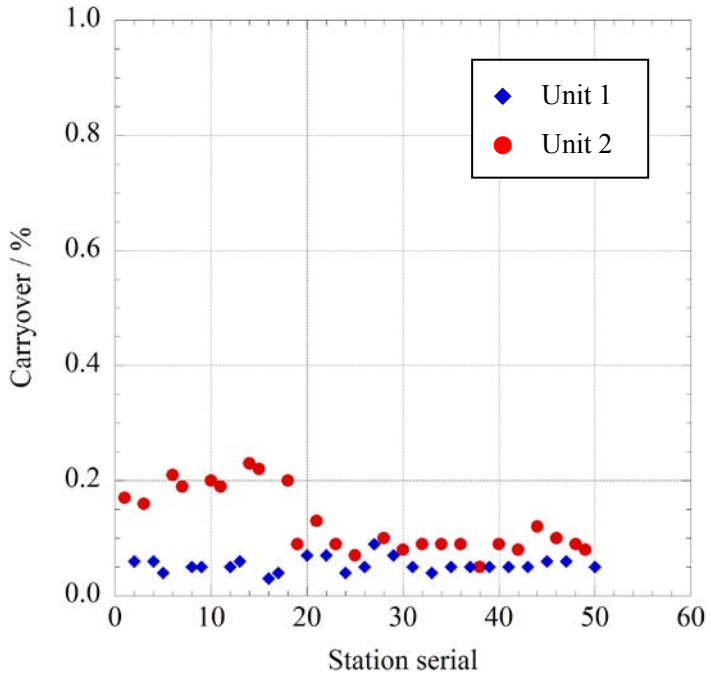

Figure 3.5.14 Time series of carryover of silicate in MR1505.

(7.4) Estimation of uncertainty of phosphate, nitrate and silicate concentrations

Empirical equations, eq. (1), (2) and (3) to estimate uncertainty of measurement of phosphate, nitrate and silicate are used based on measurements of 24 sets of CRMs during this cruise. Empirical equations, eq. (4) and (5) to estimate uncertainty of measurement of nitrite and ammonium are used based on duplicate measurements of the samples. These empirical equations and graphic presentation of equations are as follows, respectively.

Phosphate Concentration Cp in μmol kg^{-1}:
Uncertainty of measurement of phosphate (%) =
$0.142 + 0.136 * (1 / Cp) + 0.005 * (1 / Cp) * (1 / Cp)$ --- (1)
where Cp is phosphate concentration of sample.

Nitrate Concentration Cno_3 in μmol kg^{-1}:
Uncertainty of measurement of nitrate (%) =
$0.08 + 1.49 * (1 / Cno_3) + 0.02 * (1 / Cno_3) * (1 / Cno_3)$ --- (2)
where Cno_3 is nitrate concentration of sample.

Silicate Concentration Cs in μmol kg^{-1}:

Uncertainty of measurement of silicate (%) =

$0.11 + 0.96 * (1 / Cs) + 3.74 * (1 / Cs) * (1 / Cs)$ --- (3)

where Cs is silicate concentration of sample.

Nitrite Concentration Cno_2 in μmol kg^{-1}:

Uncertainty of measurement of nitrite (%) =

$- 0.10 + 0.18 * (1 / Cno_2) + 0.000022 * (1 / Cno_2) * (1 / Cno_2)$ --- (4)

where Ca is ammonium concentration of sample.

Ammonium Concentration Ca in μmol kg^{-1}:

Uncertainty of measurement of ammonium (%) =

$10.8 + 0.9 * (1 / Ca) + 0.003 * (1 / Ca) * (1 / Ca)$ --- (5)

where Ca is ammonium concentration of sample.

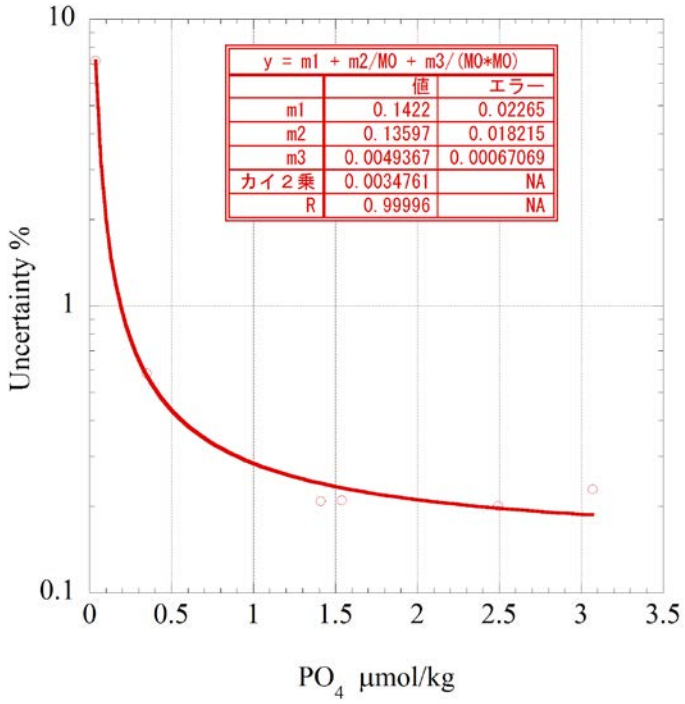

Figure 3.5.15 Estimation of uncertainty for phosphate in MR1505.

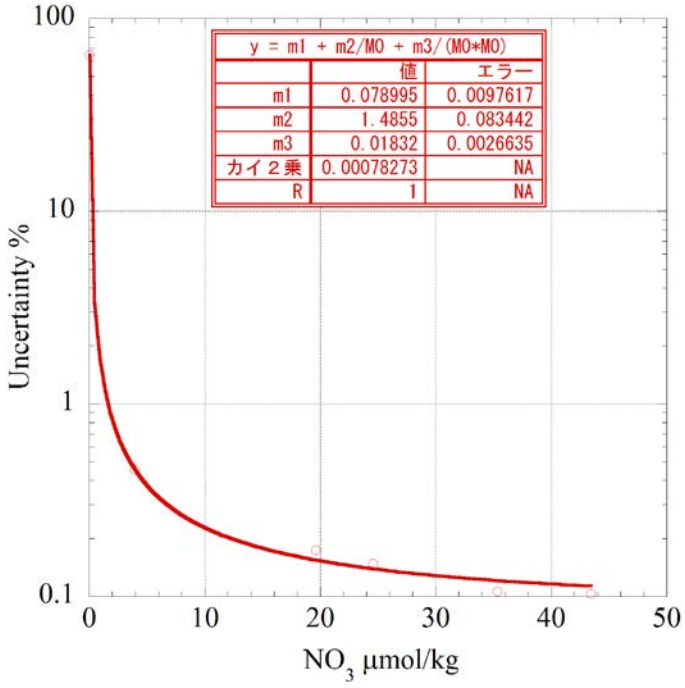

Figure 3.5.16 Estimation of uncertainty for nitrate in MR1505.

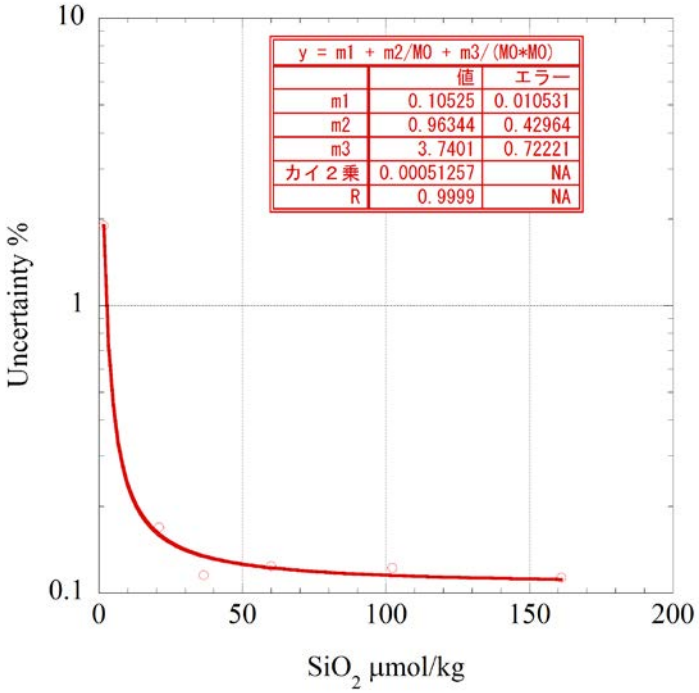

Figure 3.5.17 Estimation of uncertainty for silicate in MR1505.

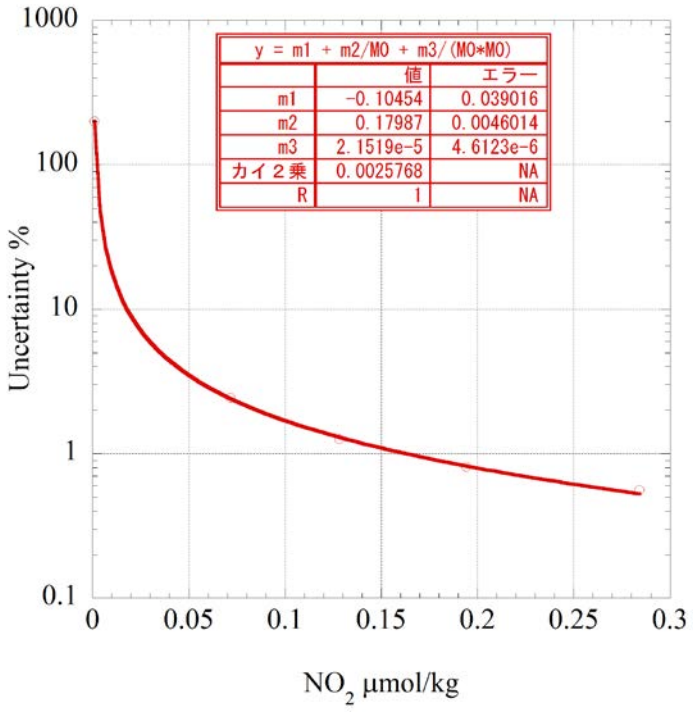

Figure 3.5.18 Estimation of uncertainty for nitrite in MR1505.

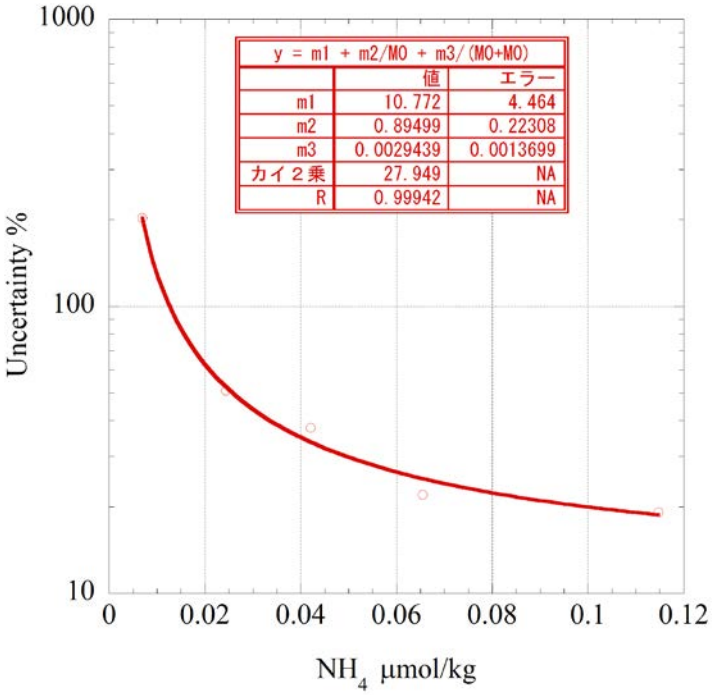

Figure 3.5.19 Estimation of uncertainty for ammonium in MR1505.

(8) Problems / improvements occurred and solutions

(8.1) squashed air tube

We found that peak shape at 1ch became broad in the middle of run for stn. 50. And segment air into inlet were too small. Then we found air tube to inlet was squashed by manifold cover. Because samples concentration of broad peak shape were lower than same samples of normal peak shape, we analysed again all samples of stn. 50. We accepted NO_3 data of second run and others of first run for stn. 50.

(8.2) Phosphate channel

Phosphate channel we observe slightly higher concentration of 0.015 μmol kg^{-1} for lot BZ in terms of average of 49 runs, and slightly lower concentration of 0.006 μmol kg^{-1} for lot BV in terms of average of 50 runs respectively. Most likely reason of these differences we found state above is optics/electronics malfunction of this channel of this analyzers.

(8.3) Improvement of reduction rate at nitrate measurement

Because of decrease of absorbance of maximum concentration of in-house standard solution, we changed a kind of pumptube of sample line at 1ch from ORG/WHT to ORG/YEL. In using ORG/WHT pumptube, absorbance of maximum concentration of In-house standard solution was nearly 0.2. after changed, absorbance was 1.2. As flow rate of sample became more slowly, we achieved a good stable and high reduction rate which was 99.7% (+ 0.4% - 0.7%) in terms of mean of 50 runs during this cruise.

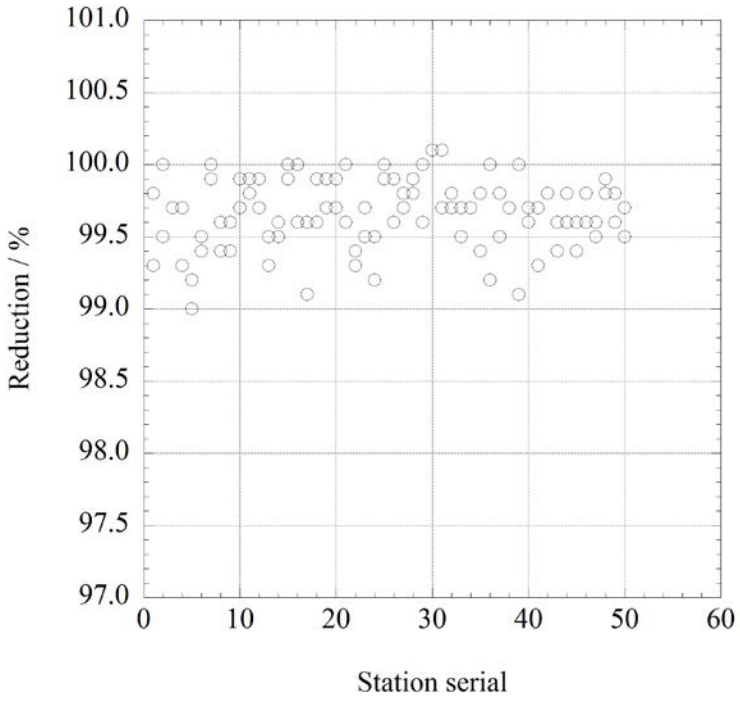

Figure 3.5.20 Time series of reduction of nitrate in MR1505.

(9) Data archive

All data will be submitted to Data Management Group of JAMSTEC (DMG) and is currently under its control.

References

Aminot, A. and Kerouel, R. 1991. Autoclaved seawater as a reference material for the determination of nitrate and phosphate in seawater. Anal. Chim. Acta, 248: 277-283.

Aminot, A. and Kirkwood, D.S. 1995. Report on the results of the fifth ICES intercomparison exercise for nutrients in sea water, ICES coop. Res. Rep. Ser., 213.

Aminot, A. and Kerouel, R. 1995. Reference material for nutrients in seawater: stability of nitrate, nitrite, ammonia and phosphate in autoclaved samples. Mar. Chem., 49: 221-232.

Aoyama M., and Joyce T.M. 1996, WHP property comparisons from crossing lines in North Pacific. In Abstracts, 1996 WOCE Pacific Workshop, Newport Beach, California.

Aoyama, M., 2006: 2003 Intercomparison Exercise for Reference Material for Nutrients in Seawater in a Seawater Matrix, Technical Reports of the Meteorological Research Institute No.50, 91pp, Tsukuba, Japan.

Aoyama, M., Susan B., Minhan, D., Hideshi, D., Louis, I. G., Kasai, H., Roger, K., Nurit, K., Doug, M., Murata, A., Nagai, N., Ogawa, H., Ota, H., Saito, H., Saito, K., Shimizu, T., Takano, H., Tsuda, A., Yokouchi, K., and Agnes, Y. 2007. Recent Comparability of Oceanographic Nutrients Data: Results of a 2003 Intercomparison Exercise Using Reference Materials. Analytical Sciences, 23: 1151-1154.

Aoyama M., J. Barwell-Clarke, S. Becker, M. Blum, Braga E. S., S. C. Coverly,E. Czobik, I. Dahllof, M. H. Dai, G. O. Donnell, C. Engelke, G. C. Gong, Gi-Hoon Hong, D. J. Hydes, M. M. Jin, H. Kasai, R. Kerouel, Y. Kiyomono, M. Knockaert, N. Kress, K. A. Krogslund, M. Kumagai, S. Leterme, Yarong Li, S. Masuda, T. Miyao, T. Moutin, A. Murata, N. Nagai, G.Nausch, M. K. Ngirchechol, A. Nybakk, H. Ogawa, J. van Ooijen, H. Ota, J. M. Pan, C. Payne, O. Pierre-Duplessix, M. Pujo-Pay, T. Raabe, K. Saito, K. Sato, C. Schmidt, M. Schuett, T. M. Shammon, J. Sun, T. Tanhua, L. White, E.M.S. Woodward, P. Worsfold, P. Yeats, T. Yoshimura, A.Youenou, J. Z. Zhang, 2008: 2006 Intercomparison Exercise for Reference Material for Nutrients in Seawater in a Seawater Matrix, Technical Reports of the Meteorological Research Institute No. 58, 104pp.

Aoyama, M., Nishino, S., Nishijima, K., Matsushita, J., Takano, A., Sato, K., 2010a. Nutrients, In: R/V Mirai Cruise Report MR10-05. JAMSTEC, Yokosuka, pp. 103-122.

Aoyama, M., Matsushita, J., Takano, A., 2010b. Nutrients, In: MR10-06 preliminary cruise report. JAMSTEC, Yokosuka, pp. 69-83

Gouretski, V.V. and Jancke, K. 2001. Systematic errors as the cause for an apparent deep water property variability: global analysis of the WOCE and historical hydrographic data・REVIEW ARTICLE, Progress In Oceanography, 48: Issue 4, 337-402.

Grasshoff, K., Ehrhardt, M., Kremling K. et al. 1983. Methods of seawater anylysis. 2nd rev. Weinheim: VerlagChemie, Germany, West.

Hydes, D.J., Aoyama, M., Aminot, A., Bakker, K., Becker, S., Coverly, S., Daniel, A., Dickson, A.G., Grosso, O., Kerouel, R., Ooijen, J. van, Sato, K., Tanhua, T., Woodward, E.M.S., Zhang, J.Z., 2010. Determination of Dissolved Nutrients (N, P, Si) in Seawater with High Precision and

Inter-Comparability Using Gas-Segmented Continuous Flow Analysers, In: GO-SHIP Repeat Hydrography Manual: A Collection of Expert Reports and Guidelines. IOCCP Report No. 14, ICPO Publication Series No 134.

Joyce, T. and Corry, C. 1994. Requirements for WOCE hydrographic programmed data reporting. WHPO Publication, 90-1, Revision 2, WOCE Report No. 67/91.

Kawano, T., Uchida, H. and Doi, T. WHP P01, P14 REVISIT DATA BOOK, (Ryoin Co., Ltd., Yokohama, 2009).

Kimura, 2000. Determination of ammonia in seawater using a vaporization membrane permeability method. 7th auto analyzer Study Group, 39-41.

Kirkwood, D.S. 1992. Stability of solutions of nutrient salts during storage. Mar. Chem., 38 : 151-164.

Kirkwood, D.S. Aminot, A. and Perttila, M. 1991. Report on the results of the ICES fourth intercomparison exercise for nutrients in sea water. ICES coop. Res. Rep. Ser., 174.

Mordy, C.W., Aoyama, M., Gordon, L.I., Johnson, G.C., Key, R.M., Ross, A.A., Jennings, J.C. and Wilson. J. 2000. Deep water comparison studies of the Pacific WOCE nutrient data set. Eos Trans-American Geophysical Union. 80 (supplement), OS43.

Murphy, J., and Riley, J.P. 1962. Analyticachim. Acta 27, 31-36.

Sato, K., Aoyama, M., Becker, S., 2010. CRM as Calibration Standard Solution to Keep Comparability for Several Cruises in the World Ocean in 2000s. In: Aoyama, M., Dickson, A.G., Hydes, D.J., Murata, A., Oh, J.R., Roose, P., Woodward, E.M.S., (Eds.), Comparability of nutrients in the world's ocean. Tsukuba, JAPAN: MOTHER TANK, pp 43-56.

Uchida, H. &Fukasawa, M. WHP P6, A10, I3/I4 REVISIT DATA BOOK Blue Earth Global Expedition 2003 1, 2, (Aiwa Printing Co., Ltd., Tokyo, 2005).

3.6 Chlorofluorocarbons and Sulfur hexafluoride

Ken'ichi Sasaki[1)], Hironori Sato[2)], Katsunori Sagishima[2)], and Hiroshi Hoshino[2)]

1) Mutsu Institute for Oceanography, Japan Agency for Marine Earth Science and Technology

2) Marine Works Japan Ltd.

3.6.1 Objectives

Chlorofluorocarbons (CFCs) and sulfur hexafluoride (SF_6) are man-made stable gases. These atmospheric gases can slightly dissolve in sea surface water by air-sea gas exchange and then are spread into the ocean interior. So dissolved these gases could be used as chemical tracers for the ocean circulation. We measured concentrations of three chemical species of CFCs, CFC-11 (CCl_3F), CFC-12 (CCl_2F_2), and CFC-113 ($C_2Cl_3F_3$), and SF_6 in seawater on board, and made simultaneous analysis of dissolved nitrous oxide (N_2O) for a certain number of seawater samples on the trial base.

3.6.2 Apparatus

We use three measurement systems. One of them is CFCs analyzing system. Other two are SF_6/CFCs simultaneous analyzing system. Trial analysis of N_2O was made on latter systems. Both systems are based on purging and trapping gas chromatography.

Table 3-5-1 Instruments

SF_6/CFCs (&N2O) simultaneous analyzing system	
Gas Chromatograph:	GC-14B (Shimadzu Ltd.)
Detector 1:	ECD-14 (Shimadzu Ltd.)
Detector 2:	ECD-14 (Shimadzu Ltd.)
Analytical Column:	
Pre-column 1:	Silica Plot capillary column [i.d.: 0.53 mm, length: 6 m, film thickness: 6 μm]
Pre-column 2:	Molesive 5A Plot capillary column [i.d.: 0.53 mm, length: 5 m, film thickness: 15 μm]
Main column 1&2:	Connected two capillary columns (Pola Bond-Q [i.d.: 0.53mm, length: 9 m, film thickness: 10μm] followed by Silica Plot [i.d.: 0.53mm, length: 18 m, film thickness: 6μm])
Purging & trapping:	Developed in JAMSTEC. Cold trap columns are 30 cm length stainless steel tubing packed the section of 5cm with 80/100 mesh Porapak Q and followed by the section of 5cm of 100/120 mesh Carboxen 1000. Outer

	diameters of the main and focus trap columns are 1/8" and 1/16", respectively.
CFCs analyzing system	
Gas Chromatograph:	GC-14B (Shimadzu Ltd.)
Detector:	ECD-14 (Shimadzu Ltd.)
Analytical Column:	
Pre-column:	Silica Plot capillary column [i.d.: 0.53mm, length: 6 m, film thickness: 6μm]
Main column:	Connected two capillary columns (Pola Bond-Q [i.d.: 0.53mm, length: 9 m, film thickness: 10μm] followed by Silica Plot [i.d.: 0.53mm, length: 18 m, film thickness: 6μm])
Purging & trapping:	Developed in JAMSTEC. Cold trap columns are 1/16" SUS tubing packed the section of 5cm with 100/120 mesh Porapak T.

3.6.3 Procedures

3.6.3.1 Sampling

Seawater sub-samples were collected from 12 liter Niskin bottles to 450 ml of glass bottles developed in JAMSTEC. The glass bottles were filled by CFC free gas (pure nitrogen gas) before sampling. Two times of the bottle volume of seawater sample were overflowed. The seawater samples were kept in water bath controlled at 7ºC. The samples were taken to determination as soon as possible after sampling (usually within 12 hours).

In order to confirm CFC/SF_6 concentrations of standard gases and their stabilities and also to check saturation levels in sea surface water, mixing ratios in background air were periodically analyzed. Air samples were continuously led into laboratory by air pump. The end of 10 mm OD Dekaron tubing was put on a head of the compass deck and another end was connected onto the air pump in the laboratory. The tubing was relayed by a T-type union which had a small stop cock. Air sample was collected from the flowing air into a 200ml glass cylinder attached on the cock.

3.6.3.2 Analysis

SF_6/CFCs (/N_2O) simultaneous analyzing system

Constant volume of sample water (200 ml) is taken into a sample loop. The sample is send into stripping chamber and dissolved SF_6, CFCs and N_2O are de-gassed by N_2 gas purging for 8 minutes. The gas sample is dried by magnesium perchlorate desiccant and concentrated on a main trap column cooled down to -80 ºC. Stripping efficiencies are frequently confirmed by re-stripping of surface layer

samples and more than 99 % of dissolved SF_6 and CFCs and ~95 % of N_2O are extracted on the first purge. Following purging & trapping, the main trap column is isolated and electrically heated to 170 ºC. After 1 minute, the desorbed gases are sent onto focus trap cooled down to -80 ºC for 30 seconds. Gaseous sample on the focus trap are desorbed by same manner of the main trap, and lead onto the pre-column 1 (PC 1). Sample gases are roughly separated on the PC 1. Eluting SF_6, CFCs and N_2O onto pre-column 2 (PC 2), PC1 is connected onto cleaning line and high boiling point compounds are flushed by counter flow of pure nitrogen gas. SF_6 and CFCs are rapidly eluted from PC 2 onto main-column 1 (MC 1) and N_2O is retained on PC 2. Then PC 2 is connected back-flush carrier gas line and N_2O is sent onto main-column 2 (MC 2). SF_6 and CFCs are further separated on MC 1 and detected by ECD 1. N_2O sent onto MC 2 is detected by ECD 2.

CFCs analyzing system

Constant volume of sample water (50 ml) is taken into a sample loop. The sample is send into stripping chamber and dissolved CFCs are de-gassed by N_2 gas purging for 8 minutes. The gas sample is dried by magnesium perchlorate desiccant and concentrated on a trap column cooled down to -50 ºC. Stripping efficiencies are frequently confirmed by re-stripping of surface layer samples and more than 99.5 % of dissolved CFCs are extracted on the first purge. Following purging & trapping, the trap column is isolated and electrically heated to 140 ºC. The desorbed gases are lead into the pre-column. Sample gases are roughly separated in the pre-column. When CFC-113 eluted from pre-column onto main column, the pre-column is connected onto another line and flushed by counter flow of pure nitrogen gas. CFCs send on MC 1 are further separated and detected by ECD.

Nitrogen gases used in these systems was filtered by gas purifier column packed with Molecular Sieve 13X (MS-13X).

Table 3-5-2 Analytical conditions

SF_6/CFCs(N_2O) simultaneous analyses	
Temperature	
Analytical Column:	95 ºC
Detector (ECD):	300 ºC
Trap column:	-80 ºC (at adsorbing) & 170 ºC (at desorbing)
Mass flow rate of nitrogen gas (99.99995%)	
Carrier gas 1:	10 ml/min
Carrier gas 2:	10 ml/min
Detector make-up gas 1:	27 ml/min
Detector make-up gas 2:	27 ml/min

Back flush gas: 10 ml/min

Sample purge gas: 220 ml/min

CFCs analyses

Temperature

Analytical Column: 95 ºC

Detector (ECD): 240 ºC

Trap column: -50 ºC (at adsorbing) & 140 ºC (at desorbing)

Mass flow rate of nitrogen gas (99.99995%)

Carrier gas : 10 ml/min

Detector make-up gas : 27 ml/min

Back flush gas: 10 ml/min

Sample purge gas: 130 ml/min

Standard gas (Japan Fine Products co. Ltd.)

Cylinder No.	Base gas	CFC-11	CFC-12	CFC113	SF_6	N_2O	remarks
		ppt	ppt	ppt	ppt	ppm	
CPB28497	N_2	901	485	78.8	10.10	14.9	for SF_6/CFC
CPB26840	N_2	889	481	81.4	9.98	14.9	for SF_6/CFC
CPB16993	N_2	300	160	29.9	0.0	0.0	for CFC
CPB15651	N_2	300	161	29.8	0.0	0.0	Reference

3.6.4 Performance

The analytical precisions are estimated from replicate sample analyses. The estimated preliminary precisions were ± 0.005 pmol/kg (n = 143), ± 0.007 pmol/kg (n = 143), ± 0.003 pmol/kg (n = 121), and ± 0.021 fmol/kg (n = 96) for CFC-11, CFC-12, CFC-113, and SF_6, respectively. Analyses of N_2O had serious problems probably caused by error of standard gas composition. Evaluating the standard gas composition, we may report the N_2O data later (but as bad data).

3.6.5 Data archive

All data will be submitted to Data Management Group of JAMSTEC (DMG) and under its control.

3.7. Carbon items

(1) Personnel

Akihiko Murata (JAMSTEC)

Tomonori Watai (MWJ)

Makoto Takada (MWJ)

Atsushi Ono (MWJ)

Kanako Yoshida (MWJ)

(2) Objectives

Concentrations of CO_2 in the atmosphere are now increasing at a rate of about 2.0 ppmv y^{-1} owing to human activities such as burning of fossil fuels, deforestation, and cement production. It is an urgent task to estimate as accurately as possible the absorption capacity of the oceans against the increased atmospheric CO_2, and to clarify the mechanism of the CO_2 absorption, because the magnitude of the anticipated global warming depends on the levels of CO_2 in the atmosphere, and because the ocean currently absorbs 1/3 of the 6 Gt of carbon emitted into the atmosphere each year by human activities.

The eastern part of the Indian Ocean is one of the regions where uncertainty of uptake of anthropogenic CO_2 is large. In this cruise, therefore, we were aimed at quantifying how much anthropogenic CO_2 was absorbed in the ocean interior of the eastern part of the Indian Ocean. For the purpose, we measured CO_2-system parameters such as dissolved inorganic carbon (C_T), total alkalinity (A_T) and pH along the WHP I10 in the region.

(3) Apparatus

i. C_T

Measurement of C_T was made with a total CO_2 measuring system (called as System D, Nippon ANS, Inc.). The system comprised of a seawater dispensing system, a CO_2 extraction system and a coulometer. In this cruise, we used a coulometer Model 3000, which was constructed by Nippon ANS. The systems had a specification as follows:

The seawater dispensing system has an auto-sampler (6 ports), which dispenses seawater from a 300 ml borosilicate glass bottle into a pipette of about 15 ml volume by PC control. The pipette is kept at 20 °C by a water jacket, in which water from a water bath set at 20 °C is circulated. CO_2 dissolved in a seawater sample is extracted in a stripping chamber of the CO_2 extraction system by adding phosphoric acid (~ 10 % v/v) of about 2 ml. The stripping chamber is approx. 25 cm long and has a fine frit at the bottom. The acid is added to the stripping chamber from the bottom of the chamber by pressurizing an acid bottle for a given time to push out the right amount of acid. The pressurizing is made with nitrogen gas (99.9999 %). After the acid is transferred to the stripping chamber, a seawater

sample kept in a pipette is introduced to the stripping chamber by the same method as in adding an acid. The seawater reacted with phosphoric acid is stripped of CO_2 by bubbling the nitrogen gas through a fine frit at the bottom of the stripping chamber. The CO_2 stripped in the chamber is carried by the nitrogen gas (flow rates is 140 ml min^{-1}) to the coulometer through a dehydrating module. The module consists of two electric dehumidifiers (kept at ~4 °C) and a chemical desiccant ($Mg(ClO_4)_2$).

The measurement sequence such as system blank (phosphoric acid blank), 1.865 % CO_2 gas in a nitrogen base, sea water samples (6) is programmed to repeat. The measurement of 1.865 % CO_2 gas is made to monitor response of coulometer solutions purchased from UIC.

ii. A_T

Measurement of A_T was made based on spectrophotometry using a custom-made system (Nippon ANS, Inc.). The system comprises of a water dispensing unit, a HCl titration unit (Hamilton No.2), and a detection unit of a spectrophotometer (TM-UV/VIS C10082CAH, Hamamatsu Photonics, Japan) and an optical source (Mikropack, Germany). The system was automatically controlled by a PC. The water dispensing unit had a water-jacketed pipette and a water-jacketed glass titration cell.

A seawater of approx. 42 ml was transferred from a sample bottle (borosilicate glass bottle; 130 ml) into the water-jacketed (25 ºC) pipette by pressurizing the sample bottle (nitrogen gas), and was introduced into the water-jacketed (25 ºC) glass titration cell. The introduced seawater was used to rinse the titration cell. After dumping the seawater used for rinse, Milli-Q water was introduced into the titration cell to rinse it. This is repeated twice. Next, a seawater of approx. 42 ml was weighted again by the pipette, and was transferred into the titration cell. Then, for seawater blank, absorbances were measured at three wavelengths (750, 616 and 444 nm). After the measurement, an acid titrant, which was a mixture of approx. 0.05 M HCl in 0.65 M NaCl and bromocresol green (BCG), was added into the titration cell. The volume of acid titrant solution was changed according to expected values of A_T from approx. 2.2 ml to 2.0 ml. The seawater and acid titrant were mixed for 5 minutes by a stirring tip and bubbling by nitrogen gas in the titration cell. Then, absorbances at the three wavelengths were measured again.

Calculation of A_T was made by the following equation:

$$A_T = (-[H^+]_T V_{SA} + M_A V_A) / V_S,$$

where M_A is the molarity of the acid titrant added to the seawater sample, $[H^+]_T$ is the total excess hydrogen ion concentration in the seawater, and V_S, V_A and V_{SA} are the initial seawater volume, the added acid titrant volume, and the combined seawater plus acid titrant volume, respectively. $[H^+]_T$ is calculated

from the measured absorbances based on the following equation (Yao and Byrne, 1998):

$$pH_T = -\log[H^+]_T = 4.2699 + 0.002578(35 - S) + \log((R - 0.00131)/(2.3148 - 0.1299R)) - \log(1 - 0.001005S),$$

where S is the sample salinity, and R is the absorbance ratio calculated as:

$$R = (A_{616} - A_{750})/(A_{444} - A_{750}),$$

where A_i is the absorbance at wavelength *i* nm.

The HCl in the acid titrant was standardized on land. The concentrations of BCG were estimated to be approx. 2.0×10^{-6} M in the sample seawater, respectively.

iii. pH

Measurement of pH was made by a pH measuring system (Nippon ANS, Inc.). For the detection of pH, spectrophotometry was adopted. The system comprises of a water dispensing unit and a spectrophotometer (Bio 50 Scan, Varian). For an indicator, *m*-cresol purple (2 mM) was used.

Seawater is transferred from borosilicate glass bottle (300 ml) to a sample cell in the spectrophotometer. The length and volume of the cell are 8 cm and 13 ml, respectively, and the sample cell is kept at 25.00 ± 0.05 ºC in a thermostated compartment. First, absorbance of seawater only is measured at three wavelengths (730, 578 and 434 nm). Then the indicator is injected and circulated for about 4 minutes to mix the indicator and seawater sufficiently. After the pump is stopped, the absorbance of seawater + indicator is measured at the same wavelengths. The pH is calculated based on the following equation (Clayton and Byrne, 1993):

$$pH = pK_2 + \log\left(\frac{A_1/A_2 - 0.00691}{2.2220 - 0.1331(A_1/A_2)}\right),$$

where A_1 and A_2 indicate absorbance at 578 and 434 nm, respectively, and pK_2 is calculated as a function of water temperature and salinity.

(4) Results

Cross sections of C_T, pH, and A_T along WOCE I10 line are illustrated in Figs. 3.7.1, 3.7.2 and

3.7.3, respectively.

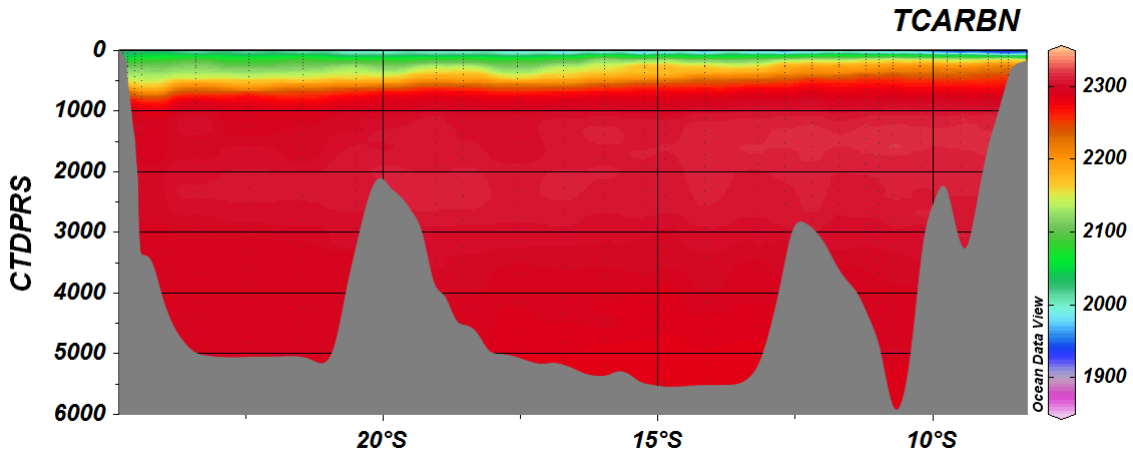

Fig. 3.7.1. Distributions of C_T along the I10 section.

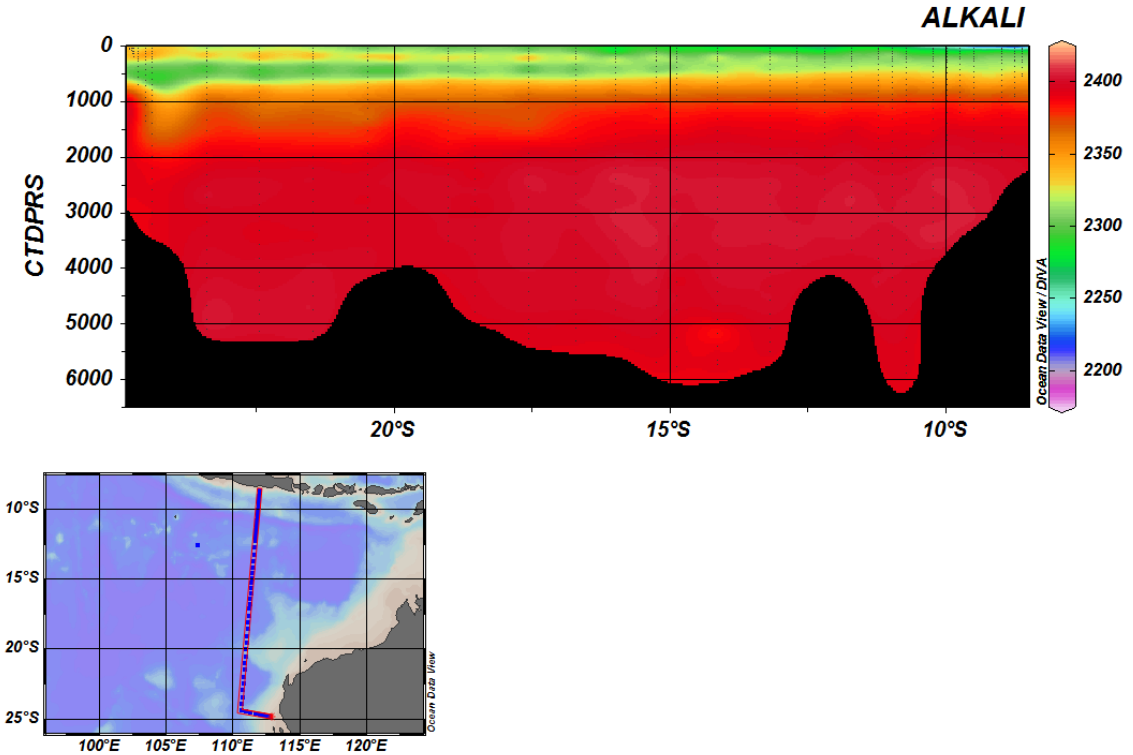

Fig. 3.7.2. Distributions of A_T along the I10 section.

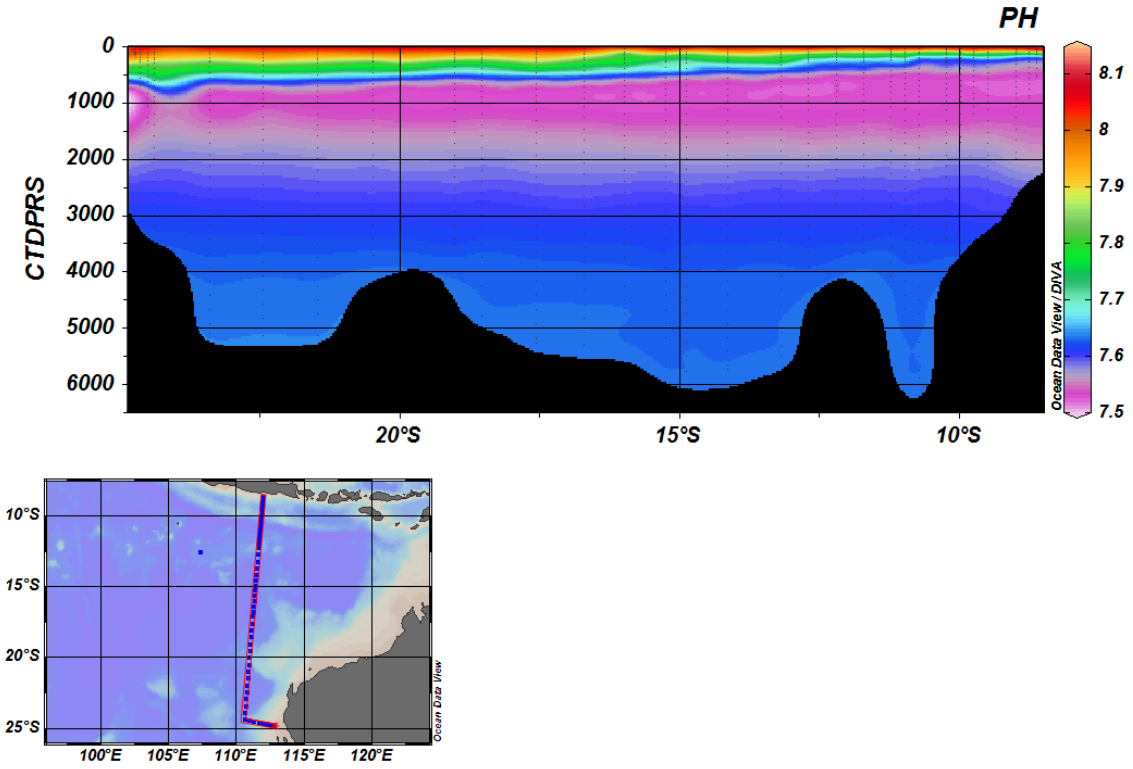

Fig. 3.7.3. Distributions of pH along the I10 section.

References

Clayton T.D. and R.H. Byrne (1993) Spectrophotometric seawater pH measurements: total hydrogen ion concentrtaion scale calibration of m-cresol purple and at-sea results. Deep-Sea Research 40, 2115-2129.

3.8 Calcium and Total alkalinity 2

Calcium

(1) Personnel

Etsuro Ono (JAMSTEC)

(2) Objectives

According to the recent IPCC report, concentrations of CO_2 in the atmosphere have increased by 40% since pre-industrial times, primarily from fossil fuel emissions and secondarily from net land use change. The ocean has absorbed about 30% of the emitted anthropogenic carbon dioxide, causing ocean acidification. Ocean acidification is characterized by an increase of H^+ (i.e., a decrease of pH) and a concurrent decrease of carbonate ion concentration (CO_3^{2-}). The decrease of CO_3^{2-} is unfavorable to marine calcifying organisms, which utilize CO_3^{2-}, together with Ca^{2+}, to produce their calcium carbonate ($CaCO_3$) shells and skeletons. To evaluate dissolution and precipitation of calcium carbonate, we measured directly the concentration of calcium in the sea water in the subtropical region of the eastern part of the Indian Ocean.

(3) Apparatus

Measurement of calcium was made by a modified Dissolved Oxygen Titrator DOT-01 (Kimoto Electronic Co. Ltd.). Bandpass filter was replaced to f0=620nm.

Added reagents are as follows.

NH_3/NH_4buffer: 0.4 mol/l NH_4Cl/ 0.4 mol/l NH_3 buffer

Masking agent: 0.05 mol/l 2,2',2"-nitrotriethanol solution

Zincon solution:

0.004 mol/l Zincon, 0.0925g Zincon was dissolved 0.8 ml 1M NaOH and was diluted to 50 ml

Zn/EGTA solution: 0.004 mol/l $ZnSO_4$/ 0.004 mol/l EGTA

EGTA titrant: 0.02 mol/l EGTA

The system comprises of a light source, photodiode detectors, auto-burette and control unit. Seawater of accurate 10ml was transferred from a sample bottle (60ml HDPE bottle) into 100 ml tall beaker by volumetric pipet. A magnetic stirrer bar was added into beaker. 1ml NH_3/NH_4buffer, 1ml masking agent, 1ml Zincon solution, 1ml Zn/EGTA solution and about 60ml H_2O were added into the beaker. The seawater samples were titrated by the EGTA titrant. The EGTA titrant was calibrated by 1000mg/l Ca standard solution (produced by Wako Pure Chemical Industries, Ltd.).

(4) Performances

The system worked well no troubles. The repeatability was estimated to be 0.0088±0.0080 (n=17 pairs) mmol kg^{-1}.

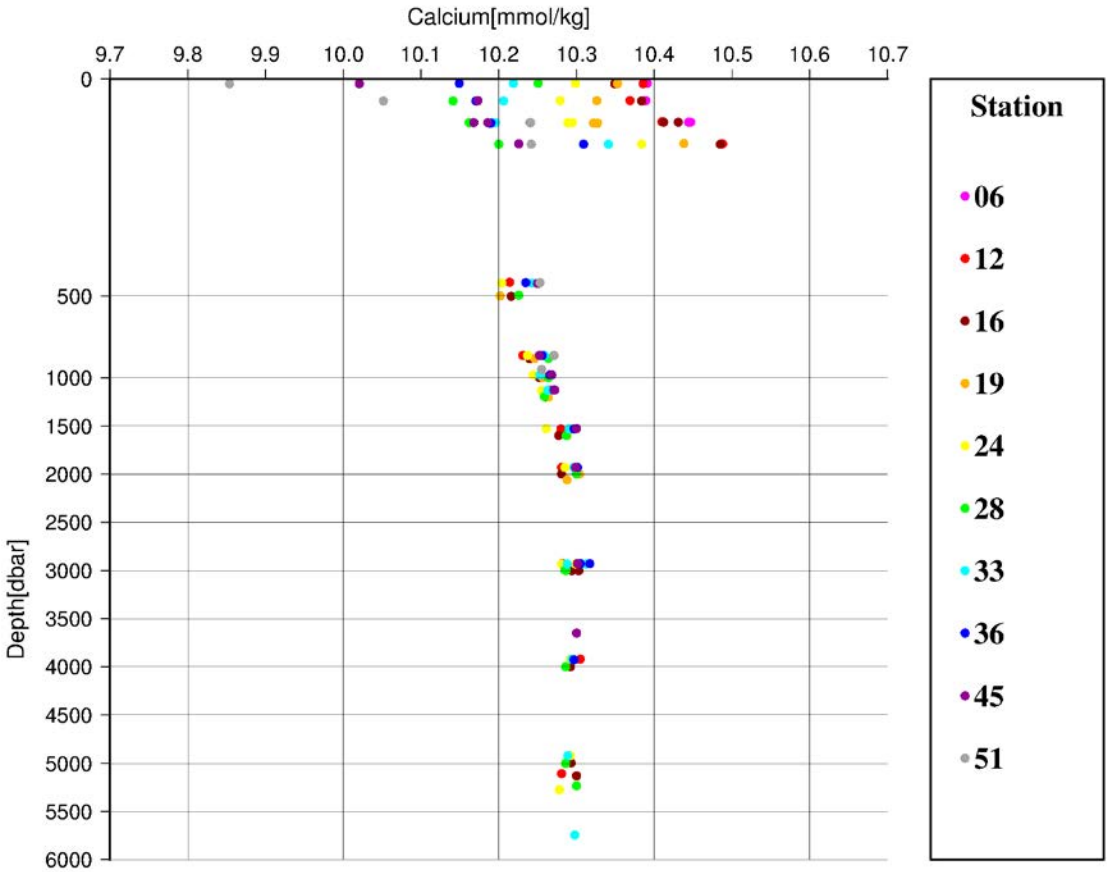

Fig.3.8.1 Vertical profiles of calcium.

Total alkalinity 2

(1) Personnel

Etsuro Ono (JAMSTEC)

(2) Objectives

Same as in "Carbon Items"

(3)Apparatus

Measurement of A_T was made based on potentiometry with Total Alkalinity Titrator ATT-05 (Kimoto Electronic Co. Ltd.). The system comprises of an auto-burette, combination electrode (pHC2001-8 S/N:13242-F17, S/N:13282-F11, Radiometer analytical) and control unit.

The in-house acid solution (approx.0.1 M HCl in 0.6 M NaCl) was prepared as a titrant in advance of cruise.

(4)Analysis

All measurements were carried out with open cell method.

Open cell method

Seawater of accurate 50ml was transferred from a sample bottle (glass bottle) into 100 ml tall beaker by volumetric pipet. A magnetic stirrer bar was added into beaker. The combination electrode and temperature sensor were immersed in sample. The seawater samples were titrated by the acid titrant. The acid titrant was calibrated by measuring Dickson's CRM (Batch 149). First, the acid titrant was added until pH of sample under 3.8 and stirred for 300 seconds. Second, the acid titrant was added by 20 μl at intervals of 15 seconds until reaching pH of 2.8. Values of A_T were computed with a program incorporated in the equipment.

The electrode of S/N:13242-17, at first, was used at station 06, 12, 16 and 24. However, S/N:13242-17 was replaced with S/N:13282-F11 after the measurements at station 24, because S/N:13242-17 showed such slow a response that some measured values were not computed accurate. The measurements worked well with S/N:13282-F11 at station 28, 33, 36, 45 and 51.

3.9. Dissolved organic carbon and total dissolved nitrogen

(1) Personnel

Masahito Shigemitsu	(JAMSTEC): Principal investigator
Chisato Yoshikawa	(JAMSTEC)
Masahide Wakita	(JAMSTEC)
Akihiko Murata	(JAMSTEC)

(2) Objectives

Dissolved organic carbon (DOC) and total dissolved nitrogen (TDN) are considered to be important reservoirs of carbon and nitrogen in the ocean. They can also be substrates for heterotrophic microbial communities and TDN can serve as a source of nitrogen to autotrophs in nitrogen-deficient regions.

In this cruise, we aimed to gain insights into the amount of DOC and TDN transported via the Indonesian throughflow from the Pacific to the Indian ocean, and interactions between dissolved organic materials like DOC and TDN and heterotrophic micro-organisms in the Indian Ocean.

(3) Material and methods

Seawater samples were obtained from Niskin bottles on a CTD-rosette system. Each sample taken in the upper 500 m was filtered using a pre-combusted (450℃ for 4 hours) Whatman 47-mm GF/F filter. The filtration was carried out by connecting a spigot of the Niskin bottle through silicone tube to an inline plastic filter holder. Filtrates were collected in acid-washed 60 mL High Density Polyethylene (HDPE) bottles in duplicates or triplicates, and were immediately stored frozen until analysis. Other samples taken below 500 m were unfiltered and stored in the same way.

In the analysis after the cruise, the frozen samples are thawed at room temperature, and acidified to pH < 2 with hydrochloric acid followed by being bubbled to remove dissolved inorganic carbon from the samples. Concentrations of DOC and TDN are, then, measured by using a total organic carbon analyzer equipped with a chemiluminescence detector unit (Shimadzu, Japan).

(4) Data archives

The data of DOC and TDN obtained in this cruise will be submitted to the Data Management Group of JAMSTEC, and will be open to the public via “Data Research System for Whole Cruise Information in JAMSTEC (DARWIN)” in JAMSTEC web site.

3.10 Chlorophyll *a*

(1) Personnel

Kosei Sasaoka (JAMSTEC)

Keitaro Matsumoto (MWJ)

Misato Kuwahara (MWJ)

Masahiro Orui (MWJ)

Haruka Tamada (MWJ)

(2) Objectives

Chlorophyll *a* is one of the most convenient indicators of phytoplankton stock, and has been used extensively for the estimation of phytoplankton abundance in various aquatic environments. In this study, we investigated horizontal and vertical distribution of phytoplankton along the I10 section in the Eastern Indian Ocean. The chlorophyll *a* data is also utilized for calibration of fluorometers, which were installed in the surface water monitoring and CTD profiler system.

(3) Instrument and Method

Seawater samples were collected in 250 ml brown Nalgene bottles without head-space. The whole samples were gently filtrated by low vacuum pressure (< 0.02 MPa) through Whatman GF/F filter (diameter = 25 mm) in the dark room. Whole volume of each sampling bottle was precisely measured in advance. After filtration, phytoplankton pigments were immediately extracted in 7 ml of N,N-dimethylformamide (DMF), and samples were stored at -20°C under the dark condition to extract chlorophyll *a* more than 24 hours. Chlorophyll *a* concentrations were measured by the Turner fluorometer (10-AU-005, TURNER DESIGNS), which was previously calibrated against a pure chlorophyll *a* (Sigma-Aldrich Co., LLC) (Fig. 3.10-1). To estimate the chlorophyll *a* concentrations, we applied to the fluorometric "Non-acidification method" (Welschmeyer, 1994).

(4) Results

Cross section of chlorophyll *a* concentrations along the I10 line during the cruise is shown in Fig. 3.10-2. To estimate the measurement precision, 48-pairs of replicate samples were obtained from hydrographic casts. All pairs of the replicate samples were collected in 250 ml bottles. Standard deviation calculated from 48-pairs of the replicate samples was 0.078 μg/L, although absolute difference values between 45-pairs of the replicate samples were smaller than 0.01 μg/L.

(5) Reference

Welschmeyer, N. A. (1994): Fluorometric analysis of chlorophyll a in the presence of chlorophyll b and pheopigments. Limnor. Oceanogr., 39, 1985-1992.

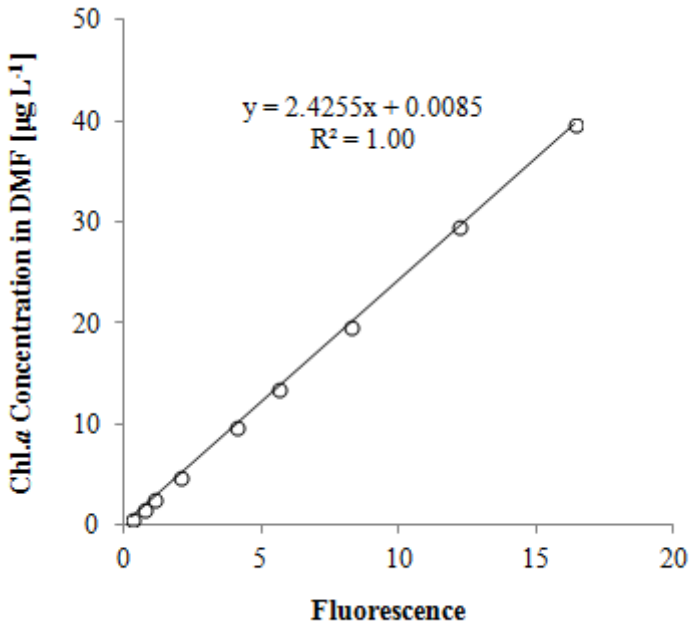

Figure 3.10-1 Relationships between pure chlorophyll *a* concentrations and fluorescence light intensity.

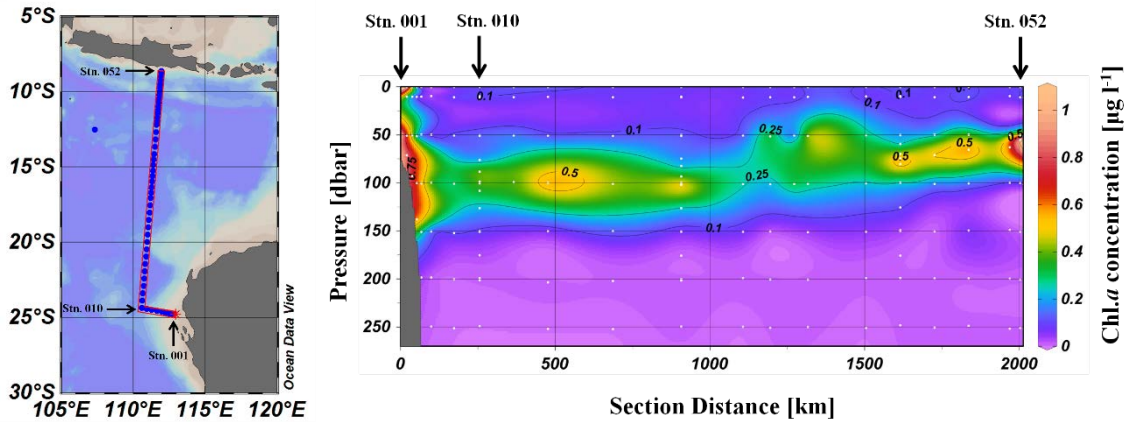

Figure 3.10-2 Cross section of chlorophyll *a* concentrations along the I10-line obtained from hydrographic casts.

3.11 Absorption coefficients of particulate matter and colored dissolved organic matter (CDOM)

(1) Personnel

Kosei Sasaoka (JAMSTEC)

(2) Objectives

Absorption coefficients of particulate matter (phytoplankton and non-phytoplankton particles, defined as 'detritus') and colored dissolved organic matter (CDOM) play an important role in determining the optical properties of seawater. In particular, light absorption by phytoplankton is a fundamental process of photosynthesis, and their chlorophyll *a* (Chl-*a*) specific coefficient, a^*_{ph}, can be essential factors for bio-optical models to estimate primary productivities. Absorption coefficients of CDOM are also important parameters to validate and develop the bio-optical algorithms for ocean color sensors, because the absorbance spectrum of CDOM overlaps that of Chl-*a*. The global colored detrital and dissolved materials (CDOM) distribution appears regulated by a coupling of biological, photochemical, and physical oceanographic processes all acting on a local scale, and greater than 50% of blue light absorption is controlled by CDOM (Siegel et al., 2002). Additionally, some investigators have reported that CDOM emerges as a unique tracer for diagnosing changes in biogeochemistry and the overturning circulation, similar to dissolved oxygen (e.g., Nelson et al., 2010). The objectives of this study are to understand the North-South variability of light absorption by phytoplankton and CDOM along the I10 section in the Indian Ocean.

(3) Methods

Seawater samples for absorption coefficient of total particulate matter ($a_p(\lambda)$) were performed using Niskin bottles and a bucket above 100m depth along the I10 section (Fig. 3.11-1, Table 3.11-1). Samples were collected in 3000ml dark bottles and filtered (500 - 3000 ml) through 25-mm What-man GF/F glass-fiber filters under a gentle vacuum (< 0.013 MPa) on board in the dark room. After filtration, the optical density of total particulate matter on filter ($OD_{fp}(\lambda)$) between 350 and 750 nm at a rate of 1.0 nm was immediately measured by an UV-VIS recording spectrophotometer (UV-2400, Shimadzu Co.), and absorption coefficient was determined from the OD according to the quantitative filter technique (QFT) (Mitchell, 1990). A blank filter with filtered seawater was used as reference. All spectra were normalized to 0.0 at 750nm to minimize difference between sample and reference filter. To determine the optical density of non-pigment detrital particles ($OD_{fd}(\lambda)$), the filters were then soaked in methanol for a few hours and rinsed with filtered seawater to extract and remove the pigments (Kishino et al., 1985), and its absorption coefficient was measured again by UV-2400. These measured optical densities on filters ($OD_{fp}(\lambda)$ and $OD_{fd}(\lambda)$) were converted to optical densities in suspensions ($OD_{sp}(\lambda)$ and $OD_{sd}(\lambda)$) using the pathlength amplification factor of Cleveland and Weidemann (1993) as follows:

$$OD_{sp}(\lambda) = 0.378\ OD_{fp}(\lambda) + 0.523\ OD_{fp}(\lambda)^2 \text{ and}$$
$$OD_{sd}(\lambda) = 0.378\ OD_{fd}(\lambda) + 0.523\ OD_{fd}(\lambda)^2.$$

The absorption coefficient of total particles ($a_p(\lambda)$ (m^{-1})) and non-pigment detrital particles ($a_d(\lambda)$ (m^{-1})) are computed from the corrected optical densities ($OD_s(\lambda)$):

$a_p(\lambda) = 2.303 \times OD_{sp}(\lambda) / L$ (L = V / S), and
$a_d(\lambda) = 2.303 \times OD_{sd}(\lambda) / L$ (L = V / S),

Where S is the clearance area of the filter (m^2) and V is the volume filtered (m^3). Absorption coefficient of phytoplankton ($a_{ph}(\lambda)$) was obtained by subtracting $a_d(\lambda)$ from $a_p(\lambda)$ as follows:

$$a_{ph}(\lambda) = a_p(\lambda) - a_d(\lambda).$$

Finally, we calculated chl-*a* normalized specific absorption spectra (a^*_{ph}) to divide a_{ph} by chl-*a* concentrations obtained from same hydrographic casts.

Seawater samples for absorption coefficient of CDOM ($a_y(\lambda)$) were collected in 250ml bottles using Niskin bottles and a bucket from surface to bottom (Fig. 3.11-1, Table 3.11-1). CDOM samples were filtered using 0.2 μm Nuclepore polycarbonate filters on board. Optical densities of the CDOM ($OD_y(\lambda)$) in this filtered seawater were recorded against UV-2400 in the range from 300 to 800 nm using 10-cm pathlength glass cells. Milli-Q water was used as a base line. A blank (Milli-Q water versus Milli-Q water) was subtracted from each wavelength of the spectrum. The absorption coefficient of CDOM ($a_y(\lambda)$ (m^{-1})) was calculated from measured optical densities ($OD_y(\lambda)$) as follows:

$a_y(\lambda) = 2.303 \times OD_y(\lambda) / L$ (L is the cuvette path-length (m)).

(4) Preliminary results

Some examples of chl-*a* normalized specific absorption spectra (a^*_{ph}) were shown in Fig.3.11-2. Cross section of CDOM (as absorption coefficient at 325 nm, unit = m^{-1}) along the I10 section were shown in Fig. 3.11-3.

(5) References

Cleveland, J.S. and Weidemann, A.D., 1993, Quantifying absorption by aquatic particles: a multiple scattering correction for glass fiber filters, Limnology and Oceanography, 38, 1321-1327.

Kishino, M., Takahashi, M., Okami, N. and Ichimura, S., 1985, Estimation of the spectral absorption coefficients of phytoplankton in the sea, Bulletin of Marine Science, 37, 634-642.

Mitchell, B.G., 1990, Algorithms for determining the absorption coefficient of aquatic particulates using the quantitative filter technique (QFT), Ocean Optics X, SPIE 1302, 137-148.

Nelson, N. B., D. A. Siegel, C. A. Carlson, and C. M. Swan, 2010, Tracing global biogeochemical cycles and meridional overturning circulation using chromophoric dissolved organic matter, Geophys. Res. Lett., 37, L03610, doi:10.1029/2009GL042325.

Siegel, D.A., Maritorena, S., Nelson, N.B., Hansell, D.A., Lorenzi-Kayser, M., 2002, Global distribution and dynamics of colored dissolved and detrital organic materials. J. Geophys. Res., 107, C12, 3228, doi:10.1029/2001JC000965.

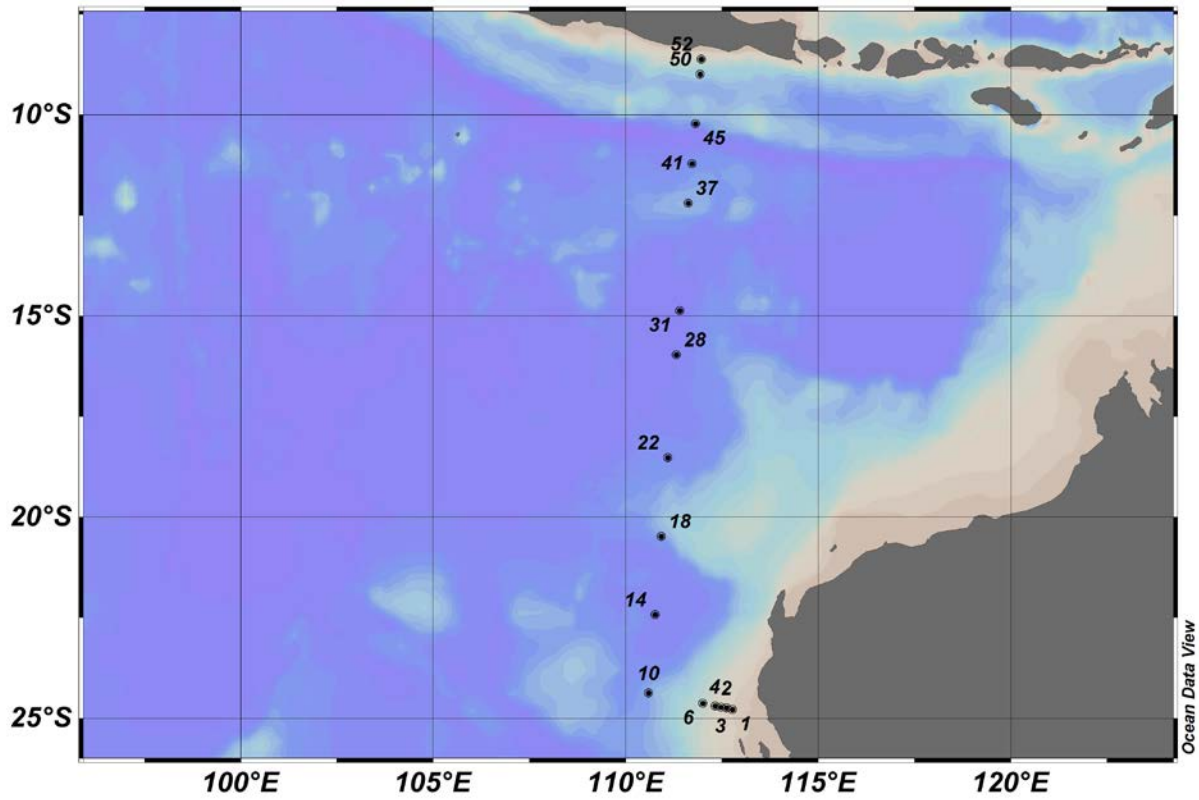

Fig. 3.11-1 Location of sampling stations for absorption coefficients of phytoplankton and CDOM along the I10 section in the Indian Ocean during MR15-05.

Table 3.11-1 List of sampling stations for absorption coefficients of phytoplankton (Ap) and CDOM during MR15-05.

Station	Date (UTC)	Time (UTC)	Latitude	Longitude	Sampling type	Cast No.	Sampling depth (db)	
							Particle absorbance	CDOM absorbance
1	12/28/2015	0:12	24.78 S	112.77 E	CTD + Bucket	1	0, 10, 50, 71	0, 10, 50, 71
2	12/28/2015	3:06	24.74 S	112.62 E	CTD + Bucket	1	none	93, 50, 10, 0
3	12/28/2015	5:38	24.73 S	112.47 E	CTD + Bucket	1	none	138, 100, 50, 10, 0
4	12/28/2015	8:08	24.70 S	112.31 E	CTD + Bucket	1	none	198, 100, 50, 10, 0
6	12/28/2015	14:05	24.63 S	112.00 E	CTD + Bucket	1	0, 10, 50, 100	698, 570, 370, 280, 200, 100, 50, 10, 0
10	12/29/2015	10:30	24.38 S	110.59 E	CTD + Bucket	3	0, 10, 50, 100	3210, 3000, 1000, 800, 600, 400, 300, 200, 100, 50, 10, 0
14	12/30/2015	12:55	22.42 S	110.76 E	CTD + Bucket	1	0, 10, 50, 100	5135, 3080, 1070, 830, 630, 430, 330, 200, 100, 50, 10, 0
18	12/31/2015	13:33	20.48 S	110.92 E	CTD + Bucket	1	0, 10, 50, 100	3704, 2930, 970, 770, 570, 370, 280, 200, 100, 50, 10, 0
22	01/01/2016	12:50	18.53 S	111.09 E	CTD + Bucket	2	0, 10, 50, 100	4797, 3000, 1000, 800, 600, 400, 300, 200, 100, 50, 10, 0
28	01/03/2016	3:36	15.97 S	111.30 E	CTD + Bucket	3	0, 10, 50, 100	5235, 5000, 3000, 1000, 800, 600, 400, 300, 200, 100, 50, 10, 0
31	01/04/2016	1:30	14.87 S	111.39 E	CTD + Bucket	1	none	5774, 5000, 3000, 1000, 800, 600, 400, 300, 200, 100, 50, 10, 0
37	01/05/2016	23:33	12.19 S	111.62 E	CTD + Bucket	4	0, 10, 50, 100	2800, 1000, 800, 600, 400, 300, 200, 100, 50, 10, 0
41	01/06/2016	18:03	11.21 S	111.72 E	CTD + Bucket	1	0, 10, 50, Chl_{max}(71), 100	4246, 3080, 1070, 830, 630, 430, 330, 200, 100, Chl_{max}(71), 50, 10, 0
45	01/07/2016	17:25	10.22 S	111.81 E	CTD + Bucket	1	0, 10, 50, Chl_{max}(65), 100	3648, 2930, 970, 770, 570, 370, 280, 200, 100, Chlmax(65), 50, 10, 0
50	01/08/2016	14:51	8.99 S	111.93 E	CTD + Bucket	1	0, 10, 50, Chl_{max}(63), 100	2005, 1070, 830, 630, 430, 330, 200, 100, Chl_{max}(63), 50, 10, 0
52	01/08/2016	21:57	8.62 S	111.96 E	CTD + Bucket	1	0, 10, 50, Chl_{max}(62), 100	549, 400, 300, 200, 100, Chl_{max}(62), 50, 10, 0

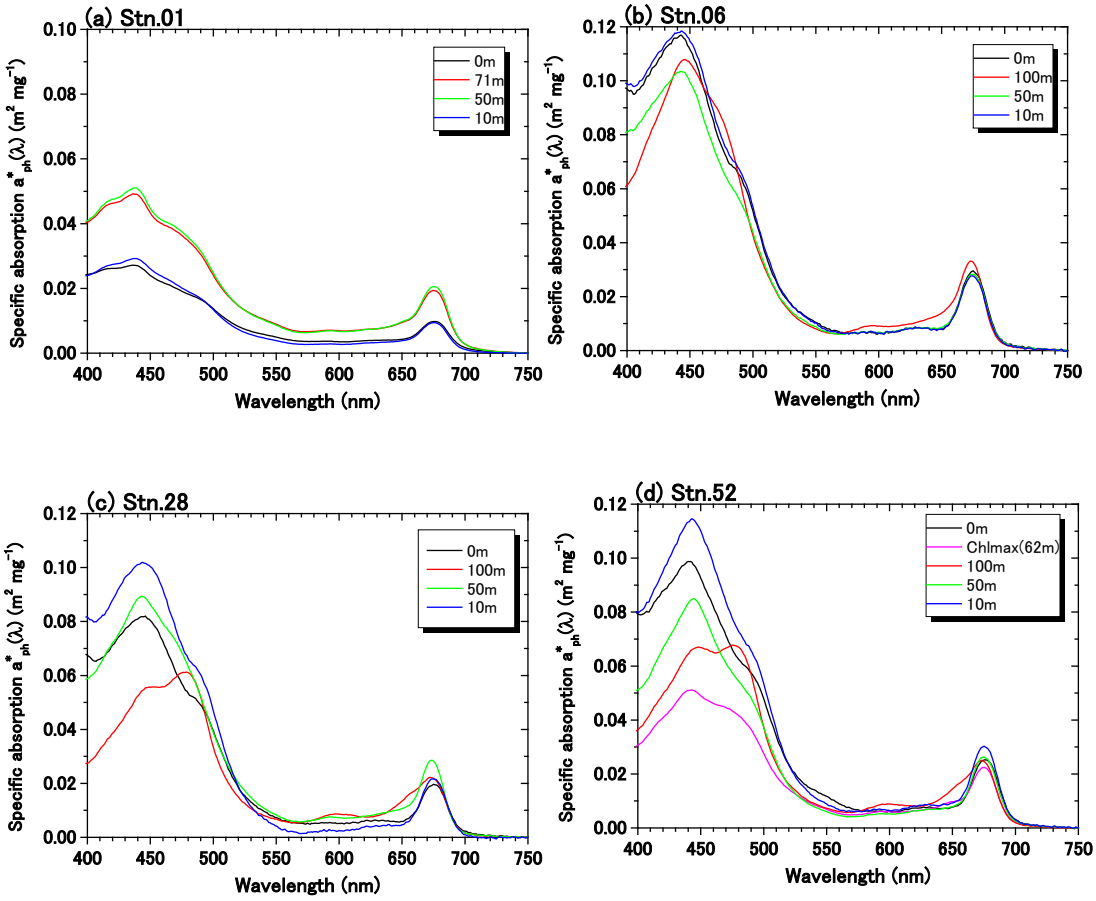

Fig.3.11-2 Examples of chlorophyll-specific phytoplankton absorption coefficient spectra ($a^*_{ph}(\lambda)$) at 400-750 nm, (a) Stn.01, (b) Stn.06, (c) Stn.28, (d) Stn.52. All spectra were normalized to 0.0 at 750nm.

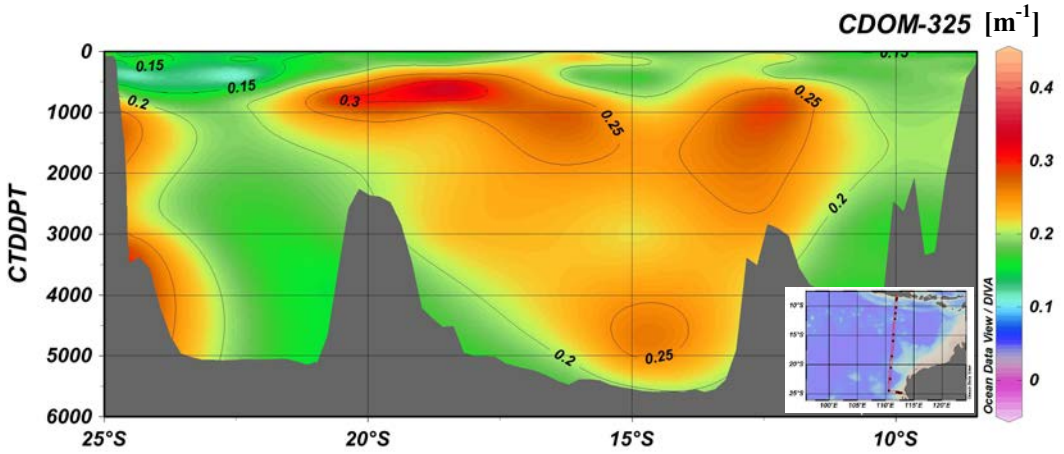

Fig.3.11-3 Contours showing distribution of CDOM (as absorption coefficient at 325 nm, unit = m^{-1}) along the I10 section during MR15-05.

3.12 Bio-sampling

3.12.1 Vertical profiles of microbial abundance, activity and diversity in the eastern Indian Ocean

(1) Personnel

Taichi Yokokawa (JAMSTEC)

Michinari Sunamura (University of Tokyo)

Takuro Nunoura (JAMSTEC)

Hirai Miho (JAMSTEC)

Chisato Yoshikawa (JAMSTEC)

Kanta Chida (Rakuno Gakuen University)

(2) Introduction

Prokaryotes (Bacteria and Archaea) play a major role in marine biogeochemical fluxes. Biogeochemical transformation rates and functional diversity of microbes are representative major topics in marine microbial ecology. However, the link between prokaryotes properties and biogeochemistry in the meso- and bathypelagic layers has not been explained systematically despite of the recent studies that highlight the role of microbes in the cycling of organic matter. (Herndl and Reinthaler 2013; Yokokawa et al. 2013). Moreover, microbial diversity and biogeography in bathypelagic and abyssal ocean and its relationship with upper layers and deep-water circulation have also not been well studied (Nagata et al. 2010).

The objectives of this study, which analyze the water columns from sea surface to just above the bottom of the eastern Indian Ocean, were 1) to determine the abundance of microbes; 2) to study the heterotrophic production and chemo-autotrophic production of prokaryotes; 3) to assess the community composition of prokaryotes; 4) to know microbial diversity through water columns along the latitudinal transect.

(3) Methods

Microbial abundance

Samples for microbial abundances (prokaryotes, eukaryotes and viruses) were collected in every routine cast and depth, and the three BIO casts. Samples were fixed with glutaraldehyde (final concentration 1%) or mixed with Glycerol-EDTA, and frozen at -80°C. The abundance of microbes and viruses will be measured by a flow cytometry in both University of Tokyo (Sunamura) and JAMSTEC (Nunoura) after nucleic acid staining with SYBR-Green I.

Prokaryotic activity measurements

^{3}H-leucine incorporation rate was determined as a proxy for heterotrophic or mixotrophic prokaryotic production. Triplicate subsamples (1.5 mL) dispensed into screw-capped centrifuge tubes amended with 10 nmol L^{-1} (final concentration) of [^{3}H]-leucine (NET1166, PerkinElmer) and incubated at

in situ temperature (± 2°C) in the dark. One trichloroacetic acid (TCA) killed blank was prepared for each sample. Incubation periods were 1 hour and 24 hours for the upper (0 – 250 m) and deeper (300 – bottom) water layers, respectively. After the incubation, proteins were TCA (final conc. 5%) extracted twice by centrifugation (15000 rpm, 10 min, Kubota 3615-sigma), followed by the extraction with ice-cold 80% ethanol.

The relative contribution of Archaea and Bacteria to total prokaryotic leucine incorporation was determined using antibiotics and an inhibitor; erythromycin (Sigma-Aldrich, final conc. 10 μg mL^{-1}) for bacteria, diphtheria toxin (Sigma-Aldrich, final conc. 10 μg mL^{-1}) and N1-Guanyl-1,7-Diaminoheptane (GC7, BIOSEARCH TECHNOLOGIES, final conc. 0.2 mM) for archaea, and (2-(4-carboxyphenyl)-4, 4,5,5-tetramethylimidazoline-1-oxyl-3-oxide) (carboxy- PTIO; Dojindo Molecular Technology, INC. final conc. 100 μM) for inhibiting ammonia-oxidizing archaea (AOA).

In the laboratory the samples will be radioassayed with a liquid scintillation counter using Ultima-GOLD (Packard) as scintillation cocktail. Quenching is corrected by external standard channel ratio. The disintegrations per minute (DPM) of the TCA-killed blank is subtracted from the average DPM of the samples, and the resulting DPM is converted into leucine incorporation rates.

DIC fixation was measured via the incorporation of 50 μCi of [^{14}C]-bicarbonate (NEC086H, PerkinElmer) in 20 ml seawater samples. Triplicate samples and formaldehyde-fixed blanks were incubated in the dark at in situ temperature (± 4°C) for 72 h. Incubations were terminated by adding formaldehyde (1% final concentration) to the samples.

The relative contribution of Archaea, Bacteria and AOA to total prokaryotic DIC fixation was determined using erythromycin (Sigma-Aldrich, final conc. 10 μg mL^{-1}), GC7 (BIOSEARCH TECHNOLOGIES, final conc. 0.2 mM) and PTIO (Dojindo Molecular Technology, INC. final conc. 100 μM) as bacterial, archaeal and AOA inhibitors of protein synthesis, respectively, and compared with the DIC fixation in the control sample.

In the laboratory, the samples will be filtered onto 0.2-μm polycarbonate filters. Subsequently, the filters are fumed with concentrated HCl for 12 h. The samples will be radioassayed with a liquid scintillation counter using Filter-count (PerkinElmer) as scintillation cocktail. Quenching is corrected by external standard channel ratio. The disintegrations per minute (DPM) of the formaldehyde-killed blank is subtracted from the average DPM of the samples, and the resulting DPM is converted into bicarbonate incorporation rates.

Samples for leucin incorporation activity measurements were taken at stations 1, 6, 10, 14, 18, 22, 26, 31, 37 in the routine casts, and those for inorganic carbon fixation rates assessed at stations 10, 22, 37 in the routine casts.

Microbial diversity

Microbial cells in water samples were filtrated on cellulose acetate filter (0.2μm) and stored at -80˚C. Environmental DNA or RNA will be extracted from the filtrated cells and used for 16S/18S rRNA

gene tag sequencing using MiSeq, quantitative PCR for genes for 16S rRNA, and/or metatranscriptomics. Moreover, selected water samples were mixed with glycerol-EDTA and stored at -80˚C for single cell genomic analyses. Samples for microbial diversity were taken at stations 1, 6, 10, 14, 18, 22, 26, 31, and 37 in the routine casts.

References

Herndl GJ, Reinthaler T (2013) Microbial control of the dark end of the biological pump. Nature geoscience, 6:718-724

Yokokawa T, Yang Y, Motegi C, Nagata T (2013) Large-scale geographical variation in prokaryotic abundance and production in meso- and bathypelagic zones of the central Pacific and Southern Ocean. Limnology and Oceanography, 58:61-73

Nagata T, Tamburini C, Aristegui J, Baltar F, Bochdansky AB, Fonda-Umani S, Fukuda H, Gogou A, Hansell DA, Hansman RL, Herndl GJ, Panagiotopulos C, Reinthaler T, Sohrin R, Verdugo P, Yamada N, Yamashita Y, Yokokawa T, Bartlett DH (2010) Emerging concepts on microbial processes in the bathypelagic ocean – ecology, biogeochemistry, and genomics. Deep-Sea Research II 57:1519-1536

3.12.2 Geochemistry and Microbiology: Nitrogen and carbon cycles in the eastern Indian Ocean

(1) Personnel

Akiko Makabe (JAMSTEC)

Chisato Yoshikawa (JAMSTEC)

Kanta Chida (Rakuno Gakuen University)

Keisuke Koba (Tokyo University of Agriculture and Technology)

Miho Hirai (JAMSTEC)

Osamu Yoshida (Rakuno Gakuen University)

Shotoku Kotajima (Tokyo University of Agriculture and Technology)

Taichi Yokokawa (JAMSTEC)

Takuro Nunoura (JAMSTEC)

(2) Introduction

Knowledge about oceanic nitrogen and carbon cycles has been dramatically changed in this decade. In nitrogen cycle, major ammonia oxidizers were believed to be a few lineages of Proteobacteria, but it has been revealed that archaeal ammonia oxidizers (AOA) shared more than 10% of microbial population in dark ocean, and nitrous oxide production is necessary for the growth of AOA. In addition, significant contribution of heterotrophic nitrogen fixation and anaerobic ammonia oxidizers are also been found in the oceanic nitrogen cycle. On the other hand, in carbon cycle, microbial life in dark ocean below mesopelagic water (corresponding to 200-1000 m depth range) is thought to be primarily supported by sinking organic carbons from surface waters. However, it has been recently revealed that the deep-sea biogeochemical cycles are more complex than previously expected, and the dark carbon fixation coupled with nitrification and sulfur- and hydrogen-oxidations is also recognized as another significant organic carbon source in dark ocean (Francis et al. 2007; Alonso-Sáez et al. 2010; Swan et al. 2011; Anantharaman et al. 2013; Herndl and Reinthalar 2013).

Nitrogen cycle

The marine nitrogen cycle in surface waters is known to control biological activity in the ocean, because inorganic forms of nitrogen such as nitrate are indispensable nutrients for phytoplankton. Following the primary production, organic nitrogen compounds are metabolized into ammonium and low molecular organic nitrogen compounds that are substrates for nitrification and/or nitrogen source of microbes. Among the components of marine nitrogen cycle, Nitrous Oxide (N_2O) is recognized as significant anthropogenic greenhouse gas and a stratospheric ozone destroyer. The estimation of global N_2O flux from ocean to the atmosphere is 3.8 $TgNyr^{-1}$ and the estimation varies greatly, from 1.8 to 5.8 $TgNyr^{-1}$ (IPCC, 2013). This is because previous models had estimated N_2O concentration from oxygen concentration indirectly. In fact, marine N_2O production processes are very complicated; hydroxylamine oxidation during nitrification, nitrite reduction during nitrifier denitrification and nitrite reduction during

denitrification produce N_2O and N_2O deduction during denitrification consumes N_2O (Dore et al. 1998; Knowles et al. 1981; Rysgaard et al. 1993; Svensson 1998; Ueda et al. 1993). In addition, currently, previously unknown systems in nitrification in AOA have been reported. One is the N_2O production with unknown pathway using NO as one of the substrate (Santoro et al. 2011; Stieglmeier et al. 2014), and the other is ammonia oxidation via urea degradation in AOA has also been reported (Alonso-Sáez et al. 2012). Therefore marine N_2O production processes are poorly understood quantitatively. N_2O isotopomers (oxygen isotope ratio ($\delta^{18}O$), difference in abundance of $^{14}N^{15}N^{16}O$ and $^{15}N^{14}N^{16}O$ (SP), and average nitrogen isotope ratio ($\delta^{15}N$)) are useful tracers to distinguish these processes and had revealed N_2O production processes in various ocean environments (e.g., Yoshida and Toyoda, 2000), but we need to improve the model with novel findings in the marine nitrogen cycle.

To reduce the uncertainties in global N_2O budget a marine N_2O model constrained by isotope dataset was developed and applied to the western North Pacific (Yoshikawa et al., *in press*). In this study we conducted water sampling for isotope analysis of N_2O and related substances (NO_3^-, phytoplankton and Chlorophyll-a) and some key reaction rates (nitrification rates) at three MBC shallow stations (above 500 m). By using the results of isotope analysis we will apply the model to the Indian Ocean and estimate the sea to air N_2O flux there. Moreover, we examine both inorganic and organic carbon uptake activity associated with AOA during and after the cruise, and identify genetic markers for each process of nitrogen cycle by molecular biology techniques.

Methane in ocean

The atmospheric concentrations of the greenhouse gases methane (CH_4) have increased since 1750 due to human activity. In 2011 the concentrations of CH_4 was 1803 ppb exceeded the pre-industrial levels by about 150% (IPCC 2013). In order to understand the current global CH_4 cycle, it is necessary to quantify its sources and sinks. At present, there remain large uncertainties in the estimated CH_4 fluxes from sources to sinks. The ocean's source strength for atmospheric CH_4 should be examined in more detail, even though it might be a relatively minor source, previously reported to be 0.005 to 3% of the total input to the atmosphere (Cicerone and Oremland 1988; Bange et al. 1994; Lelieveld et al. 1998).

To estimate an accurate amount of the CH_4 exchange from the ocean to the atmosphere, it is necessary to explore widely and vertically. Distribution of dissolved CH_4 in surface waters from diverse locations in the world ocean is often reported as a characteristic subsurface maximum representing a supersaturation of several folds (Yoshida et al. 2004; 2011). Although the origin of the subsurface CH_4 maximum is not clear, some suggestions include advection and/or diffusion from local anoxic environment nearby sources in shelf sediments, and in situ production by methanogenic bacteria, presumably in association with suspended particulate materials (Karl and Tilbrook 1994; Katz et al. 1999). These bacteria are thought to probable live in the anaerobic microenvironments supplied by organic particles or guts of zooplankton (Alldredge and Cohen 1987).

So, this study investigates in detail profile of CH_4 concentration in the water column in the

Eastern Indian Ocean to clarify CH_4 dynamics and estimate the flux of CH_4 to the atmosphere.

(3) Materials and methods

Seawater samples are taken by CTD-CAROUSEL system attached Niskin samplers of 12 L at 15 layers above 500 m and surface layer taken by plastic bucket at hydrographic stations as shown in Table 1.

Table 1. Parameters and hydrographic station names for this study.

Parameters	Hydrographic stations
1. $\delta^{15}N$ and $\delta^{18}O$ of NO_3^-	1, 6, 10, 14, 18, 22, 26, 31, 37
2. $\delta^{15}N$ of Chlorophyll *a*	10, 22, 37
3. $\delta^{15}N$ of Phytoplankton	10, 22, 37
4. $\delta^{15}N$, SP and $\delta^{18}O$ of dissolved N_2O	1, 6, 10, 14, 18, 22, 26, 31, 37
5. Nitrification rate	1, 6, 10, 18, 22, 26, 31, 37
6. Dissolved CH_4 and N_2O concentration	1, 4, 6, 8, 10, 14, 18, 22, 26, 28, 31, 35, 37
7. F430	10, 22, 37
8. $\delta^{13}C$ of CH_4	1, 6, 10, 14, 18, 22, 26, 31, 37

Isotopic analyses for N_2O, NO_3^-, chlorophyll a and phytoplankton, and concentration analyses for N_2O and CH_4

Sample for N_2O isotopomer analysis was transferred to two of 100 ml glass vials. After an approximately two-fold volume overflow, 200μL of saturated $HgCl_2$ solution were added. The vials were sealed with butyl rubbers and aluminum caps and stored in dark at 4°C until analysis. The $\delta^{15}N$, $\delta^{18}O$ and SP values and concentrations of N_2O in seawater will be determined by slightly modified version of GC-IRMS (PreCon/HP6890 GC/ MAT 252) at TIT described in detail in Yamagishi et al. (2007).

Sample for nitrate isotope analysis was collected into a 50 ml syringe equipped with a DISMIC® filter (pore size: 0.45 μm) and filtered immediately after sampling. These samples were removed nitrite with sulfamic acid using the method of Granger and Sigman (2009) and preserved at -23°C until chemical analysis. The $\delta^{15}N$ and $\delta^{18}O$ values of NO_3^- will be measured using the "bacterial" method of Sigman et al., (2001) in which N_2O converted from nitrate is analyzed using GasBench/ PreCon/IRMS.

Sample for chlorophyll isotope analysis was collected into a 20L light-blocking polypropylene tanks. The samples were filtered under reduced pressure and collected on two-three pre-combusted Whatman GF-75 filters. The filters were double up and wrapped in aluminum foil and stored at -23°C until analysis. Chlorophyll pigments will be extracted and split into each pigments by HPLS. The $\delta^{15}N$ values of Chlorophyll pigments will be measured by using EA-IRMS at JAMSTEC.

Sample for phytoplankton isotope analysis was collected into a 20L light-blocking polypropylene tanks. The samples were condensed using an ultrafiltration system and sorted for

phytoplankton samples using a cell sorter. The phytoplankton samples were filtered under reduced pressure and collected on pre-combusted Whatman GF-75 filters. The filters were stored at -23°C until analysis. The $\delta^{15}N$ values of phytoplankton will be measured by using EA-IRMS at JAMSTEC.

Sample for N_2O and CH_4 concentration analyses were carefully subsampled into 30 mL glass vials to avoid air contamination for analyses of N_2O and CH_4 concentration. The seawater samples were poisoned by 20 μL (30 mL vials) of mercuric chloride solution (Tilbrook and Karl 1995; Watanabe et al. 1995), and were closed with rubber-aluminum and plastic caps. These were stored in a dark and cool place until we got to land, where we conducted gas chromatographic analyses of N_2O and CH_4 concentration at the laboratory.

Nitrification activity measurements

Water samples for nitrification activity analysis were transferred into 100 mL glass vials without headspace. Combination of ^{15}N enriched substrates (ammonium, urea, and glutamine (amide group)) and inhibitors (carboxy-PTIO, allylthiourea, and GC7) were added to each vial. The final concentration of ^{15}N enriched substrates was 50 nM. The glass vials were incubated in dark for 12 hours or 3 days at in situ temperature. After incubation, the samples for nitrate analysis were filtered with a DISMIC® filter (pore size: 0.45 μm) and frozen until analysis. The samples for N_2O analysis were added by 0.2 mL of saturated $HgCl_2$ solution and stored at 4 ºC until analysis. The ^{15}N enrichment of nitrates will be measured by GC-IRMS after conversion to N_2O using the "bacterial" method of Sigman et al. (2001). The ^{15}N enrichment of N_2O will be measured by GC-IRMS described in detail in Yamagishi et al. (2007).

Nitrous oxide and methane concentration measurements

The measurement system consists of a purge and trap unit, a desiccant unit, rotary valves, gas chromatograph equipped with a electron capture detector for concentration of N_2O and a flame ionization detector for concentration of CH_4, and data acquisition units. The entire volume of seawater in each glass vial was processed all at once to avoid contamination and loss of N_2O and CH_4. Precision obtained from replicate determinations of N_2O and CH_4 concentration was estimated to be better than 5% for the usual concentration in seawater.

Isotopic analysis of methane

Water samples for $\delta^{13}C$-CH_4 analysis were transferred to 100 mL glass vials from the Niskin sampler without headspace. After the vials were sealed with butyl rubber and aluminum caps, 200 μL of saturated $HgCl_2$ solution was added. The water samples were stored until analysis on land. The $\delta^{13}C$ value of Methane will be measured using isotope ratio mass spectrometry using a method of Tsunogai et al. (1998 and 2000).

Biomarker of methanogens

Water samples for F430 analysis (5 or 10 L) were filtered (0.01 MPa) with a Whatman GF-75 filter (47 mm in diameter). The filter samples were wrapped with aluminum foil and stored at −20°C prior to analysis on land. Extraction and analysis of F430 will be conducted at JAMSTEC using a method of Kaneko et al. (2014).

Prokaryotic uptakes of organic and inorganic carbon measurements

See "Prokaryotic activity measurements" in the chapter "Vertical profiles of aquatic microbial abundance, activity and diversity in the eastern Indian Ocean".

Genetic markers of geochemical processes

Microbial cells in water samples were filtrated on cellulose acetate filter (0.2μm) and stored at -80˚C. Environmental DNA or RNA will be extracted from the filtrated cells and used for molecular analyses (e.g. clone analysis and quantitative PCR) to investigate the microbial components related to nitrification, nitrogen fixation and methanogenesis.

(4) Expected results

Nitrogen cycle and microbial carbon uptake associated with nitrogen cycle

In the surface layer, N_2O concentration of water affects the sea-air flux directly (Dore et al. 1998). However the pathway of N_2O production in surface layer is still unresolved. In the surface layer, N_2O is predominantly produced by nitrification, but also by nitrifer-denitrification and denitrification if oxygen concentration is low in the water mass or particles (Maribeb and Laura, 2004). The observed concentrations and isotopomer ratios of N_2O together with those values of substrates for N_2O (NO_3^-, phytoplankton and Chlorophyll-a) will reveal the pathway of N_2O production in the surface layer and will improve the marine N_2O isotopomer model. Moreover, the horizontal isotope dataset will help to apply the model to the Indian Ocean.

Methane

Subsurface maximum concentrations of CH_4 (>3 nmol kg^{-1}) were expected to be observed in the Indian Ocean. A commonly-encountered distribution in the upper ocean with a CH4 peak within the pycnocline (e.g., Ward et al. 1987; Owens et al. 1991; Watanabe et al. 1995; Yoshida et al. 2011). Karl and Tilbrook (1994) suggested the suboxic conditions would further aid the development of microenvironments within particles in which CH_4 could be produced. The organic particles are accumulated in the pycnocline, and CH_4 is produced in the micro reducing environment by methanogenic bacteria. Moreover, in situ microbial CH_4 production in the guts of zooplankton can be expected (e.g., Owens et al. 1991; de Angelis and Lee 1994; Oudot et al. 2002; Sasakawa et al. 2008). Watanabe et al.

(1995) pointed out that the diffusive flux of CH_4 from subsurface maxima to air-sea interface is sufficient to account for its emission flux to the atmosphere. In the mixed layer above its boundary, the CH_4 is formed and discharged to the atmosphere in part, in the below its boundary, CH_4 diffused to the bottom vertically. By using concentration and isotopic composition of CH_4 and hydrographic parameters for vertical water samples, it is possible to clarify its dynamics such as production and/or consumption in the water column.

A depth profile of F430 concentration in water column will provide information about quantitative distribution of methanogens. The $\delta^{13}C$ value of methane reflects carbon source and methaogenic pathway (Whiticar, 1999). If the profile correlate with other chemical profiles including concentrations of methane, chlorophyll and dissolved oxygen, it can be a strong evidence of that methanogens are source organisms for methane in the surface seawater. The $\delta^{13}C$ value of methane will support presence of methanogen and provide further constraints on methaongenic pathway, In addition with the vertical distribution, a lateral distribution (east-west) of F430 and other chemicals will provide insight into environmental factors controlling distribution of methanogens.

References

Alldredge AA, Cohen Y (1987) Can microscale chemical patches persist in the sea? Microelectrode study of marine snow, fecal pellets. Science, 235:689-691

Alonso-Sáez L, Galand PE, Casamayor EO, Pedrós-Alió C, Bertilsson S (2010) High bicarbonate assimilation in the dark by Arctic bacteria. ISME J, 174:1581–90

Anantharaman K, Breier JA, Sheik CS, Dick GJ (2013) Evidence for hydrogen oxidation and metabolic plasticity in widespread deep-sea sulfur-oxidizing bacteria. Proceedings of the National Academy of Sciences, 110:330–335

Bange, HW, Bartell UH, Rapsomanikis S, Andreae MO (1994) Methane in the Baltic and the North seas and a reassessment of the marine emissions of methane. Global Biogeochemical Cycles, 8:465–480

Cicerone RJ, Oremland RS (1988) Biogeochemical aspects of atmospheric methane, Global Biogeochemical Cycles, 2:299–327

Conrad R (2009) The global methane cycle: recent advances in understanding the microbial processes involved. Environmental Microbiology Report, 1:285-292

de Angelis MA, Lee C (1994) Methane production during zooplankton grazing on marine phytoplankton. Limnology and Oceanography, 39:1298-1308

Dore JE, Popp BN, Karl DM, Sansone FJ (1998) A large source of atmospheric nitrous oxide from subtropical North Pacific surface water. Nature, 396:63-66

Francis CA, Beman JM, Kuypers MM (2007) New processes and players in the nitrogen cycle: the microbial ecology of anaerobic and archaeal ammonia oxidation. ISME J 1: 19–27

German CR. et al. (2010) Diverse styles of submarine venting on the ultraslow spreading Mid-Cayman

Rise. Proceedings of the National Academy of Sciences, 107:14020–14025.

Granger J, Sigman DM (2009) Removal of nitrite with sulfamic acid for nitrate N and O isotope analysis with the denitrifier method. Rapid Communications in Mass Spectrometry, 23:3753-3762

Grossart HP, Frindte K, Dziallas C, Eckert W, Tang WK (2011) Microbial methane production in oxygenated water column of an oligotrophic lake. Proceedings of the National Academy of Sciences, 108:19657-19661

Herndl GJ, Reinthaler T (2013) Microbial control of the dark end of the biological pump. Nature Geoscience, 6:718–724

IPCC Working group I (2013): Climate change 2013: The physical science basis. IPCC The 5th Assessment report, http://www.ipcc.ch/report/ar5/wg1/.

Kaneko M, Takano Y, Chikaraishi Y, Ogawa ON, Asakawa S, Watanabe T, Shima S, Krüger M, Matsushita M, Kimura H, Ohkouchi N (2014). Quantitative Analysis of Coenzyme F430 in Environmental Samples: A New Diagnostic Tool for Methanogenesis and Anaerobic Methane Oxidation. Analytical Chemistry, 86:3633-3638

Karl DM, Tilbrook BD (1994) Production and transport of methane in oceanic particulate organic matter. Nature, 368:732–734

Karl DM, Beversdorf L, Björkman KM, Church MJ, Martinez A, DeLong EF (2008). Aerobic production of methane in the sea. Nature Geoscience, 1:473-478

Katz ME, Pak DK, Dickkens GR, Miller KG (1999) The source and fate of massive carbon input during the latest Paleocene thermal maximum. Scince, 286:1531–1533

Kawagucci S, Yoshida YT, Noguchi T, Honda MC, Uchida H, Ishibashi H, Nakagawa F, Tsunogai U, Okamura K, Takaki Y, Nunoura T, Miyazaki J, Lin W, Kitazato H, Takai K (2012) Disturbance of deep-sea environments induced by the M9.0 Tohoku Earthquake. Scientific Reports, 2:270.

Knapp AN, Sigman DM, Lipschultz F (2005) N isotopic composition of dissolved organic nitrogen and nitrate at the Bermuda Atlantic time-series study site. Global Biogeochemical Cycles, 19:GB1018

Knowles R, Lean DRS, Chan YK (1981) Nitrous oxide concentrations in lakes: variations with depth and time. Limnology and Oceanography, 26:855-866

Koba K, Inagaki K, Sasaki Y, Takebayashi Y, Yoh M (2010) Nitrogen isotopic analysis of dissolved inorganic and organic nitrogen in soil extracts. Earth, life, and isotopes, Kyoto University Press

Lelieveld J, Crutzen PJ, Dentener FJ (1998) Changing concentration, lifetime and climate forcing of atmospheric methane. Tellus Series B, 50:128–150

Maribeb CG, Laura F (2004) N_2O cycling at the core of the oxygen minimum zone off northern Chile. Marine Ecology Progress Series, 280:1-11

McIlvin MR, Altabet MA (2005) Chemical conversion of nitrate and nitrite to nitrous oxide for nitrogen and oxygen isotopic analysis in freshwater and seawater. Analytical Chemistry, 77:5589-5595

Revilla M, Alexander J, Glibert PM (2005) Urea analysis in coastal waters: comparison of enzymatic and direct methods. Limnology and Oceanography Methods, 3:290-299

Oudot C, Jean-Baptiste P, Fourre E, Mormiche Guevel C, Ternon JF-, Corre PL (2002) Transatlantic equatorial distribution of nitrous oxide and methane. Deep-Sea Research Part I, 49:1175–1193

Owens NJP, Law CS, Mantoura RFC, Burkill PH, Llewellyn CA(1991) Methane flux to the atmosphere from the Arabian Sea. Nature, 354:293–296

Rysgaard S, Risgaard-Petersen N, Nielsen LP, Revsbech NP (1993) Nitrification and denitrification in lake and estuarine sediments measured by the ^{15}N dilution technique and isotope pairing. Applied and Environmental Microbiology, 59:2093-2098

Sasakawa M, Tsunogai U, Kameyama S, Nakagawa F, Nojiri Y, Tsuda A (2008) Carbon isotopic characterization for the origin of excess methane in subsurface seawater. Journal of Geophysical Research, 113:C03012, doi: 10.1029/2007JC004217

Santoro AE, Buchwald C, McIlvin MR, Casciotti KL (2011) Isotopic signature of N_2O produced by marine ammonia-oxidizing Archaea. Science, 333:1282-1285

Scranton IM, Brewer GP (1977) Occurrence of Methane in near-Surface Waters of Western Subtropical North-Atlantic. Deep-Sea Research, 24:127-138

Sigman DM, Casciotti KL, Andreani M, Barford C, Galanter M, Boehlke JK (2001) A bacterial method for the nitrogen isotopic analysis of nitrate in seawater and freshwater. Analytical Chemistry, 73:4145-4153

Stieglmeier M, Mooshammer M, Kitzler B, Wanek W, Zechmeister-Boltenstern S, Richter A, Schleper C (2014) Aerobic nitrous oxide production through N-nitrosating hybrid formation in ammonia-oxidizing archaea. ISME J, 8:1135-1146

Swan BK, Martinez-Garcia M, Preston CM, Sczyrba A, Woyke T, Lamy, D, Reinthaler T, Poulton NJ, Masland ED, Gomez ML, Sieracki ME, DeLong EF, Herndl GJ, Stepanauskas R (2011) Potential for chemolithoautotrophy among ubiquitous bacteria lineages in the dark ocean. Science, 333:1296-1300

Svensson JM (1998) Emission of N_2O, nitrification and denitrification in a eutrophic lake sediment bioturbated by Chironomus plumosus. Aquatic Microbial Ecology, 14:289-299

Tilbrook BD, Karl DM (1995) Methane sources, distributions and sinks from California coastal waters to the oligotrophic North Pacific gyre. Marine Chemistry, 49:51–64

Tsunogai U, Ishibashi J, Wakita H, Gamo T (1998) Methane-rich plumes in the Suruga Trough (Japan) and their carbon isotopic characterization. Earth and Planetary Science Letters, 160:97-105

Tsunogai U, Yoshida N, Ishibashi J, Gamo T (2000) Carbon isotopic distribution of methane in deep-sea hydrothermal plume, Myojin Knoll Caldera, Izu-Bonin arc: Implications for microbial methane oxidation in the oceans and applications to heat flux estimation. Geochimca et Cosmochimca Acta, 64:2439-2452

Ueda S, Ogura N, Yoshinari T (1993) Accumulation of nitrous oxide in aerobic ground water. Water Research, 27:1787-1792

Ward BB, Kilpatrick KA, Novelli PC, Scranton MI (1987) Methane oxidation and methane fluxes in the

ocean surface layer and deep anoxic waters. Nature, 327:226–229

Watanabe S, Higashitani N, Tsurushima N, Tsunogai S (1995) Methane in the western North Pacific. Journal of Oceanography, 51:39–60

Whiticar MJ (1999) Carbon and hydrogen isotope systematics of bacterial formation and oxidation of methane. Chemical Geology, 161:291-314

Yamagishi H, Westley MB, Popp BN, Toyoda S, Yoshida N, Watanabe S, Koba K, Yamanaka Y (2007) Role of nitrification and denitrification on the nitrous oxide cycle in the eastern tropical North Pacific and Gulf of California. J. Geophys. Res. Biogeosciences, doi:10.1029/2006JG000227

Yoshida N, Toyoda S (2000) Constraining the atmospheric N_2O budget from intramolecular site preference in N_2O isotopomers. Nature, 405:330-334

Yoshida O, Inoue HY, Watanabe S, Noriki S, Wakatsuchi M (2004) Methane in the western part of the Sea of Okhotsk in 1998-2000. Journal of Geophysical Research, doi:10.1029/2003JC001910

Yoshida O, Inoue HY, Watanabe S, Suzuki K, Noriki S (2011) Dissolved methane distribution in the South Pacific and the Pacific Ocean in austral summer. Journal of Geophysical. Research, doi:10.1029/2009JC006089

Yoshikawa C, Abe H, Aita MN, Breider F, Kuzunuki K, Ogawa NO, Suga H, Ohkouchi N, Danielache SO, Wakita M, Honda MC, Toyoda S, Yoshida N (in prep.) Insights into the production processes of nitrous oxide in the western north Pacific by using a marine ecosystem isotopomer model.

3.13 Carbon isotopes

January 27, 2016

Yuichiro Kumamoto

Japan Agency for Marine-Earth Science and Technology (JAMSTEC)

(1) Personnel

Yuichiro Kumamoto

Japan Agency for Marine-Earth Science and Technology

(2) Objective

In order to investigate the water circulation and carbon cycle in the eastern Indian Ocean, seawaters for measurements of carbon-14 (radiocarbon) and carbon-13 (stable carbon) of total dissolved inorganic carbon (TDIC) were collected by the hydrocasts from surface to near bottom.

(3) Sample collection

The sampling stations and number of samples are summarized in Table 3.13.1. All samples for carbon isotope ratios (total 129 samples) were collected at 4 stations using 12-liter Niskin-X bottles. The seawater sample was siphoned into a 250 cm^3 glass bottle with enough seawater to fill the glass bottle 2 times. Immediately after sampling, 10 cm^3 of seawater was removed from the bottle and poisoned by 0.1 cm^3 □l of saturated $HgCl_2$ solution. Then the bottle was sealed by a glass stopper with Apiezon grease M and stored in a cool and dark space on board.

(4) Sample preparation and measurements

In our laboratory, dissolved inorganic carbon in the seawater samples will be stripped cryogenically and split into three aliquots: radiocarbon measurement (about 200 μmol), carbon-13 measurement (about 100 μmol), and archive (about 200 μmol). The extracted CO_2 gas for radiocarbon will be then converted to graphite catalytically on iron powder with pure hydrogen gas. The carbon-13 of the extracted CO_2 gas will be measured using Finnigan MAT253 mass spectrometer. The carbon-14 in the graphite sample will be measured by Accelerator Mass Spectrometry (AMS).

Table 3.13.1 Sampling stations and number of samples for carbon isotope ratios.

Station	Lat. (S)	Long. (E)	Sampling Date (UTC)	Number of samples	Number of replicate samples	Max. Pressure (dbar)
016	21-27.10	110-50.56	2015/12/31	33	2	5132
021	19-00.91	111-03.03	2016/01/01	27	2	3565
028	15-58.13	111-18.37	2016/01/02	33	2	5220
036	12-41.24	111-35.04	2016/01/05	28	2	3898
			Total	121	8	

3.14 Radioactive Cesium

January 27, 2016

Yuichiro Kumamoto

Japan Agency for Marine-Earth Science and Technology (JAMSTEC)

(1) Personnel

Yuichiro Kumamoto

Japan Agency for Marine-Earth Science and Technology

(2) Objective

In order to investigate water circulation and ventilation process in the eastern Indian Ocean, during MR15-05 cruise seawater samples were collected for measurements of radiocesium (Cs-134 and Cs-137), which were mainly released from the global fallout in the 1950s and 1960s and the Fukushima Daiichi nuclear power plant after its serious accident on the March 11 of 2011.

(3) Sample collection

The sampling stations and number of samples are summarized in Table 3.14.1. The total 126 of seawater samples for radioactive cesium were collected at 3 stations. The seawaters were sampled vertically using 12-liter Niskin-X bottles. Surface seawater were collected from pumping-up water from the bottom of the ship. The seawater sample for radiocesium was collected into a 20-L plastic container and after two time washing. Immediately after sampling, the seawater was acidified by adding of 40-cm^3 of concentrated nitric acid (85%, Wako Pure Chemical Industries, Ltd., Lot SAL6324) on board.

(4) Sample preparation and measurements

In our laboratory on shore, radiocesium in the seawater samples will be concentrated using ammonium phosphomolybdate (AMP) that forms insoluble compound with cesium. The radiocesium in AMP will be measured using Ge γ-ray spectrometer.

Table 3.14.1 Sampling stations and number of samples for radiocesium

Station	Lat. (S)	Long. (E)	Sampling Date (UTC)	No. of samples for radiocesium	Max. Pressure (dbar)
028	15-58.20	111-18.25	2016/01/03	42	802
033	14-08.52	111-27.52	2016/01/04	42	773
037	12-11.71	111-37.40	2016/01/05	42	803
			Total	126	

3.15 Stable Isotopes of Water

January 27, 2016

(1) Personnel

Hiroshi Uchida (JAMSTEC)

Katsuro Katsumata (JAMSTEC)

(2) Objectives

The objective of this study is to collect stable isotopes of water to use as a tracer of ocean circulation.

(3) Materials and methods

The hydrogen (H) and oxygen (O) isotopic ratio of seawater are defined as follows:

$\delta D\ [‰] = 1000\ \{(D/H)_{sample}/(D/H)_{VSMOW} - 1\}$

$\delta^{18}O\ [‰] = 1000\ \{(^{18}O/^{16}O)_{sample}/(^{18}O/^{16}O)_{VSMOW} - 1\}$

where D is deuterium and VSMOW is Vienna Standard Mean Ocean Water. The isotopic ratios of VSMOW water are defined as follows:

$(D/H)_{VSMOW} = 155.76 \pm 0.1$ ppm

$(^{18}O/^{16}O)_{VSMOW} = 2005.20 \pm 0.43$ ppm.

The isotopic ratios will be measured in a laboratory in the Japan Agency for Marine-Earth Science and Technology, Yokosuka, Japan, after the cruise with a Cavity Ring-Down Spectroscopy (CRDS, L112-i, Picarro Inc., Santa Clare, CA, USA).

The water samples were collected in 10-mL borosilicate glass bottles (Butyl rubber stopper with aluminum cap, Maruemu Co., Osaka, Japan). The collected samples were stored at room temperature. A total of 620 samples was collected including 37 pairs of replicate samples, except in the Exclusive Economic Zone (EEZ) of Indonesia.

3.16. Primary productivity

(1) Personnel

Kazuhiko Matsumoto (JAMSTEC) on board (Leg 1)

Yugo Kanaya (JAMSTEC) not on board

Fumikazu Taketani (JAMSTEC) not on board

Takuma Miyakawa (JAMSTEC) not on board

Hisahiro Takashima (JAMSTEC) not on board

Yuichi Komazaki (JAMSTEC) not on board

Hitoshi Matsui (JAMSTEC) not on board

(2) Objectives

The major objective is to investigate processes of biogeochemical cycles between the atmosphere and the ocean. We investigate the oceanic primary productivity to estimate the effect of atmospheric input of nutrients into the ocean. Primary productivity is estimated based on the incorporation of ^{13}C-labeled inorganic carbon into phytoplankton biomass via the photosynthesis. Particularly, to characterize the optimal productivity in response to light, we investigate the relationship between phytoplankton photosynthetic rate (P) and scalar irradiance (E) with the experiments of P vs. E curve.

(3) Methods and Instruments

i. Sampling

Seawater samples were collected using Teflon-coated and acid-cleaned Niskin bottles, except for the surface water, which was taken by a bucket. Samplings were conducted at three depths within the euphotic depth, and at five locations (Stations: 001, 012, 022, 030, 037). Seawater samples were transferred to acid-cleaned, transparent bottles (approx. 1 liter) before the incubation. When the sampling had been conducted during night, seawater samples were stored temporarily at a temperature of that depth in dark until the incubation experiments.

ii. Incubation

Just before the incubation, $NaH^{13}CO_3$ was added to each bottle at a final concentration of 0.2 mM, sufficient to enrich the bicarbonate concentration by about 10%. Incubators were filled with water, and water temperature was controlled appropriately by a circulating water cooler, respectively (Fig. 3.16). Each incubator was illuminated at one end by a 500W halogen lamp, and bottles were arranged linearly against the lamp and controlled light intensity by shielding with a neutral density filter on lamp side (Table 3.16). Incubations for the P vs. E curve experiment were conducted around noon for 3-h.

In addition, another incubation experiments were conducted to the surface sample for 24-h from the early morning to estimate the incorporation of carbon and nitrate in a day with adding $NaH^{13}CO_3$ and $K^{15}NO_3$ in the on-deck bath with running surface seawater.

iii. Measurement

After the incubation, water samples were immediately filtered through a pre-combusted GF/F filter, then the filters were kept in a deep-freezer (-80 ºC). Inorganic carbon in the filter will be removed by fuming HCl before the analysis, and the ^{15}N and ^{13}C content of the particulate fraction will be measured with an automatic nitrogen and carbon analyzer mass spectrometer (Sercon, Ltd.) at the laboratory based on the method of Hama et al. (1983).

The analytical function and parameter values used to describe the relationship between the photosynthetic rate (P) and scalar irradiance (E) are best determined using a least-squares procedure from the following equation (Platt et al., 1980).

$$P = P_{max}(1-e^{-\alpha E/Pmax})e^{-b\alpha E/Pmax}$$

where, P_{max} is the light-saturated photosynthetic rate, α is the initial slope of the P vs. E curve, b is a dimensionless photoinhibition parameter.

Measurements with a high-performance liquid chromatography (Agilent Technologies Inc.) and a flow cytometer (Sony Biotechnology Inc.) are scheduled to estimate phytoplankton composition and abundance of the samples conducted the P vs. E curve experiments.

(4) Preliminary results

N/A (Data analysis is to be conducted.)

(5) Data archives

These data obtained in this cruise will be submitted to the Data Management Group of JAMSTEC, and will be opened to the public via "Data Research System for Whole Cruise Information in JAMSTEC (DARWIN)" in JAMSTEC web site.

http://www.godac.jamstec.go.jp/darwin/e

(6) References

Platt T, Gallegos CL, Harrison WG (1980) Photoinhibition of photosynthesis in natural assemblages of marine phytoplankton. Journal of Marine Research 38: 687-701.

Hama T, Miyazaki T, Ogawa Y, Iwakuma T, Takahashi M, Otsuki A, Ichimura S (1983) Measurement of photosynthetic production of a marine phytoplankton population using a stable ^{13}C isotope. Marine Biology 73: 31-36.

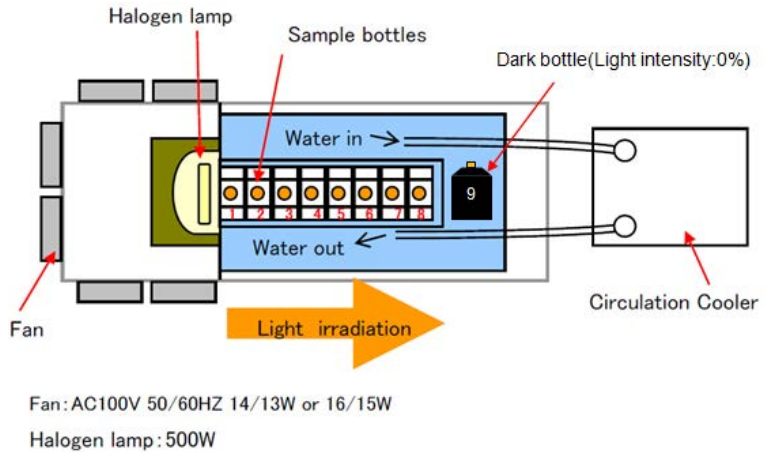

Fig. 3.16 Look down view of incubator for the P vs. E curve experiment

Table 3.16 Light intensity of each bottle in the incubators

	A	B	C
Bottle No.	Light intensity (μmol quanta m^{-2} sec^{-1})		
1	2400	1600	2000
2	1500	1000	1350
3	820	530	720
4	440	280	360
5	210	150	190
6	105	80	96
7	54	40	47
8	25.5	20	23
9	0	0	0

3.17 Lowered Acoustic Doppler Current Profiler

(1) Personnel

Shinya Kouketsu (JAMSTEC) (principal investigator)
Hiroshi Uchida (JAMSTEC)
Katsurou Katsumata (JAMSTEC)

(2) Overview of the equipment

An acoustic Doppler current profiler (ADCP) was integrated with the CTD/RMS package. The lowered ADCP (LADCP), Workhorse Monitor WHM300 (Teledyne RD Instruments, San Diego, California, USA), which has 4 downward facing transducers with 20-degree beam angles, rated to 6000 m. The LADCP makes direct current measurements at the depth of the CTD, thus providing a full profile of velocity. The LADCP was powered during the CTD casts by a 48 volts battery pack. The LADCP unit was set for recording internally prior to each cast. After each cast the internally stored observed data was uploaded to the computer on-board. By combining the measured velocity of the sea water and bottom with respect to the instrument, and shipboard navigation data during the CTD cast, the absolute velocity profile can be obtained (e.g. Visbeck, 2002).

The instrument used in this cruise was as follows.

Teledyne RD Instruments, WHM300
S/N 20754(CPU firmware ver. 50.40)

(3) Data collection

In this cruise, data were collected with the following configuration.

Bin size: 4.0 m
Number of bins: 25
Pings per ensemble: 1
Ping interval: 1.0 sec

Reference

Visbeck, M. (2002): Deep velocity profiling using Lowered Acoustic Doppler Current Profilers: Bottom track and inverse solutions. *J. Atmos. Oceanic Technol.*, **19**, 794-807.

3.18 XCTD

February 1, 2016

(1) Personnel

Hiroshi Uchida (JAMSTEC)

Katsuro Katsumata (JAMSTEC)

Fadli Syamsudin (BPPT)

Wataru Tokunaga (GODI)

Yutaro Murakami (GODI)

Tetsuya Kai (GODI)

Ryo Kimura (MIRAI crew)

(2) Objectives

XCTD (eXpendable Conductivity, Temperature and Depth profiler) measurements were carried out to examine a hydrographic structure along south coast of Java Island and to evaluate the fall rate equation and the thermal bias by comparing with CTD (Conductivity, Temperature and Depth profiler) measurements.

(3) Instrument and Method

The XCTD used was XCTD-2 (Tsurumi-Seiki Co., Ltd., Yokohama, Kanagawa, Japan), except for XCTD-1 (Tsurumi-Seiki Co., Ltd.) at station I10_0, with an MK-150N deck unit (Tsurumi-Seiki Co., Ltd.). The manufacturer's specifications are listed in Table 3.18.1. In this cruise, the XCTD probes were deployed by using 8-loading automatic launcher (Tsurumi-Seiki Co., Ltd.). For comparison with CTD, XCTD was deployed at about 10 minutes after the beginning of the down cast of the CTD (I10_44, 45, 46, 48, 49 and 50). For correction of the sound velocity profile used in the bathymetry observation, XCTD-1 was deployed near station I10_1.

The fall-rate equation provided by the manufacturer was initially used to infer depth Z (m), $Z = at - bt^2$, where t is the elapsed time in seconds from probe entry into the water, and a (terminal velocity) and b (acceleration) are the empirical coefficients (Table 3.18.2).

(4) Data Processing and Quality Control

The XCTD data were processed and quality controlled based on a method by Uchida et al. (2011). Differences between XCTD and CTD depths were shown in Fig. 3.18.1. The terminal velocity error was estimated for the XCTD-2 (Table 3.18.2). The XCTD-2 data were corrected for the depth error by using the estimated terminal velocities. Differences of temperature on pressure surfaces were examined by using side-by-side XCTD and CTD data (Fig. 3.18.3). Average thermal bias below 900 dbar was –0.003 °C. The XCTD data were corrected for the thermal bias. Differences of salinity on reference

temperature surfaces were examined by using CTD data (Fig. 3.18.4). The XCTD data were corrected for the estimated salinity bias.

(5) Results

Temperature-salinity plot using the quality controlled XCTD data is shown in Fig. 3.18.3. Potential temperature cross section is shown in Fig. 3.18.4.

(6) References

Kizu, S., H. Onishi, T. Suga, K. Hanawa, T. Watanabe, and H. Iwamiya (2008): Evaluation of the fall rates of the present and developmental XCTDs. *Deep-Sea Res I*, **55**, 571–586.

Uchida, H., K. Shimada, and T. Kawano (2011): A method for data processing to obtain high-quality XCTD data. *J. Atmos. Oceanic Technol.*, **28**, 816–826.

Uchida, H., A. Murata, and T. Doi (eds.) (2014): WHP P10 Revisit in 2011 Data Book, 179 pp., JAMSTEC.

Uchida, H., K. Katsumata, and T. Doi (eds.) (2015): WHP P14S/S04I Revisit in 2012/2013 Data Book, 187 pp., JAMSTEC.

Uchida, H and T. Doi (eds.) (2016): WHP P01 Revisit in 2014 Data Book (in prep.)

Table 3.18.1. Manufacturer's specifications of XCTD-2.

Parameter	Range	Accuracy
Conductivity	0 ~ 60 mS cm^{-1}	±0.03 mS cm^{-1}
Temperature	–2 ~ 35 °C	±0.02 °C
Depth	0 ~ 1850 m	5 m or 2%, whichever is greater *

* Depth error is shown in Kizu et al (2008).

Table 3.18.2. Manufacturer's coefficients for the fall-rate equation.

Model	*a* (terminal velocity, m/s)	*b* (acceleration, m/s^2)	*e* (terminal velocity error, m/s)
XCTD-4	3.43898	0.00031	–0.0198

Table 3.18.3. Thermal biases of the XCTD temperature data.

Cruise	Average thermal bias (°C)	Depth range	Source
MR09-01	0.016	>= 1100 dbar	Uchida et al. (2011)
KH-02-3	0.019	>= 1100 dbar	Uchida et al. (2011)
MR11-08	0.014	>= 1100 dbar	Uchida et al. (2014)
MR12-05	0.009	>= 400 dbar	Uchida et al. (2015)
MR14-04	0.011	>= 900 dbar	Uchida et al. (2016)
MR15-05	–0.003	>= 900 dbar	This report
Mean	0.011 ± 0.008		

Table 3.18.4. Salinity biases of the XCTD data.

XCTD station	Salinity bias	Reference temperature (°C)	Reference salinity	Reference CTD stations
44	–0.008	3.0	34.7209	44,45,46,48,49,50
45	–0.003	3.0	34.7209	44,45,46,48,49,50
46	–0.022	3.0	34.7209	44,45,46,48,49,50
48	–0.016	3.0	34.7209	44,45,46,48,49,50
49	–0.015	3.0	34.7209	44,45,46,48,49,50
50	–0.010	3.0	34.7209	44,45,46,48,49,50
901	–0.035	6.0	34.6558	51
902	–0.034	4.2	34.6532	44,45,46,48,49,50
903	–0.023	4.2	34.6532	44,45,46,48,49,50
904	–0.040	3.0	34.7209	44,45,46,48,49,50
905	–0.034	3.0	34.7209	44,45,46,48,49,50
906	–0.035	3.0	34.7209	44,45,46,48,49,50
907	–0.033	3.0	34.7209	44,45,46,48,49,50
908	–0.030	3.0	34.7209	44,45,46,48,49,50
909	–0.042	3.0	34.7209	44,45,46,48,49,50
910	–0.022	3.0	34.7209	44,45,46,48,49,50
911	–0.022	3.0	34.7209	44,45,46,48,49,50
912	–0.037	3.0	34.7209	44,45,46,48,49,50
913	–0.035	4.2	34.6532	44,45,46,48,49,50

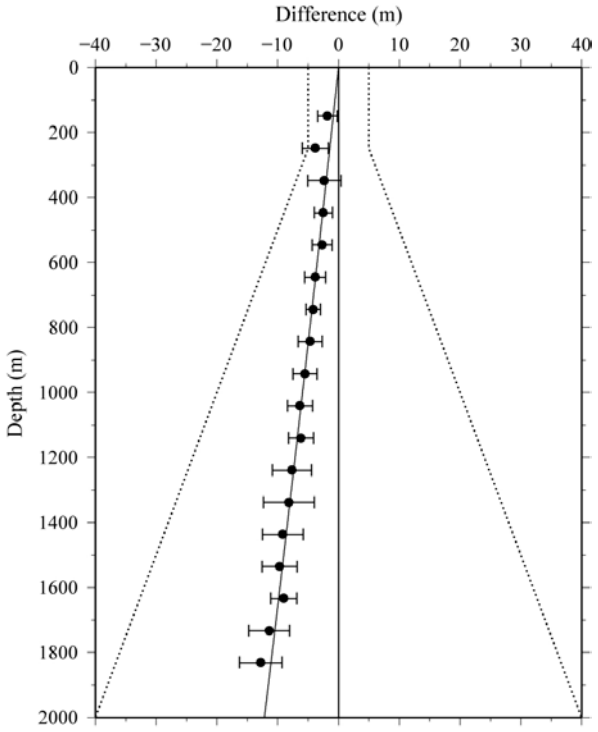

Figure 3.18.1. Differences between XCTD and CTD depths for XCTD-2. Differences were estimated with the same method as Uchida et al. (2011). Standard deviation of the estimates (horizontal bars) and the manufacturer's specification for XCTD depth error (dotted lines) are shown. The regression for the data (solid line) is also shown.

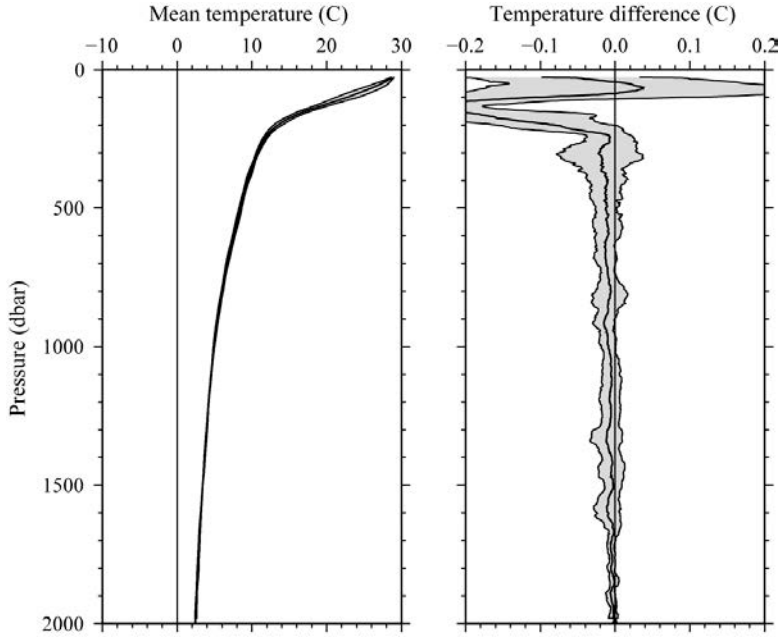

Figure 3.18.2. Comparison between XCTD and CTD temperature profiles. (a) Mean temperature of CTD profiles with standard deviation (shade) and (b) mean temperature difference with standard deviation

(shade) between the XCTD and CTD. Mean profiles were low-pass filtered by a running mean with a window of 51 dbar.

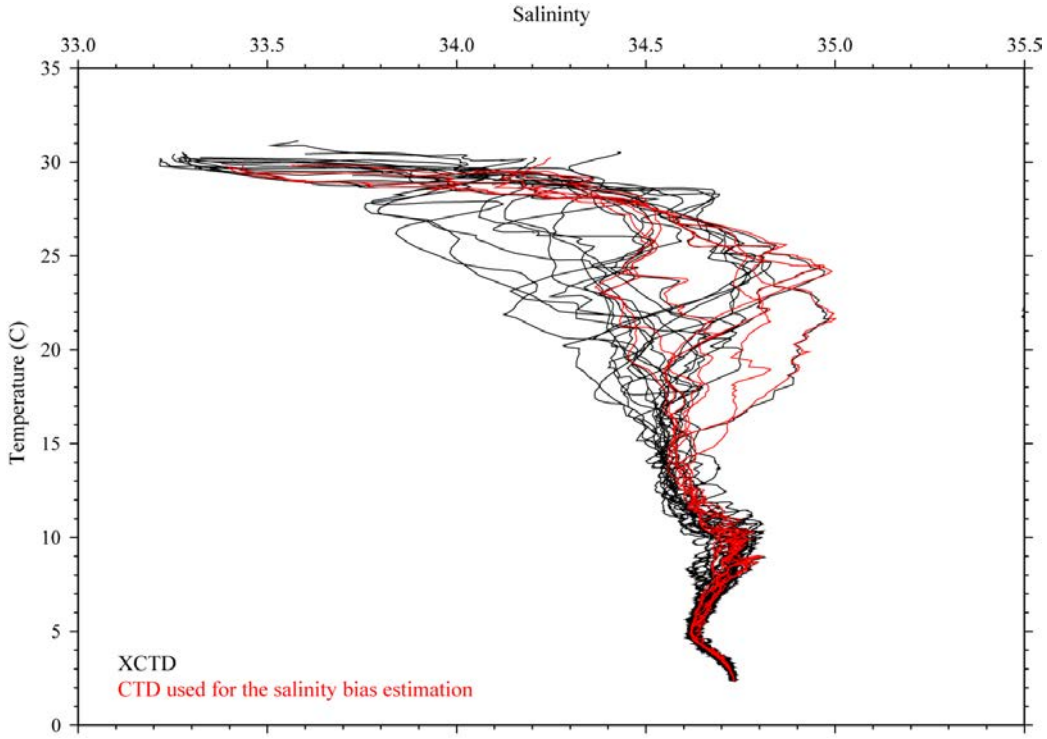

Figure 3.18.3. Comparison of temperature-salinity profiles of CTD data (red lines) used for the XCTD salinity bias estimation and salinity bias-corrected XCTD data (black lines).

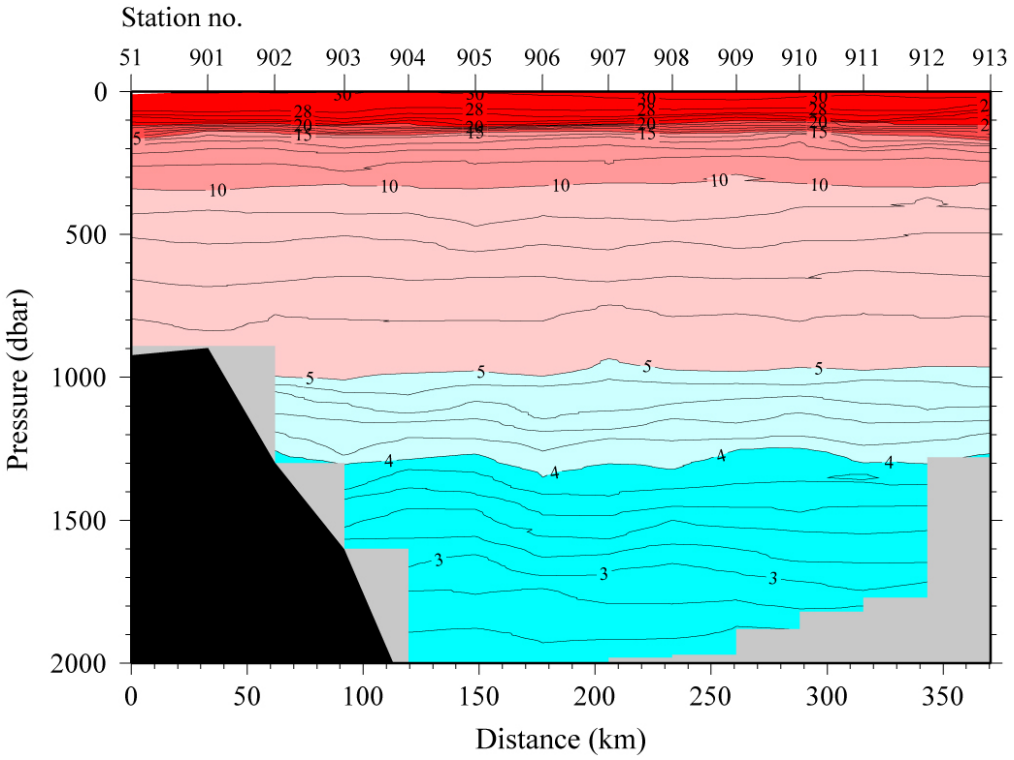

Figure 3.18.4. Potential temperature (˚C) section along south coast of Java Island.

3.19 Micro Rider

- **(1) Personnel**

  Shinya Kouketsu (JAMSTEC)

  Hiroshi Uchida (JAMSTEC)

  Katsurou Katsumata (JAMSTEC)

  Ichiro Yasuda (AORI)

- **(2) Objective**

  Microstructure observations to evaluate vertical mixing.

- **(3) Instruments and method**

  Micro structure observations were carried out by micro-Rider 6000 (MR6000; Rockland Scientific International Inc.), which is mounted CTD rosette and is powered from SBE 9plus. We mounted two FP07 thermistors to obtain the high-frequency changes in temperature. We sometimes replaced the probes during this cruise, as the probes didn't work well. The high-frequency pressure and acceleration profiles are also obtained by the sensors in MR6000. The low-frequency profiles of temperature are archived in the MR6000 from the cables connected with SBE-3 sensor on the CTD system. We download the profile data from the MR6000 a cast. During this cruise, as we attached a bottom contact detector in some casts (Stations 001, 002, and 013), the string and weight with the detector may affect the microstructure measurements. After the cruise, we plan to examine the methods of the correction and measurement quality evaluation with the comparison among the micro temperature with CTD rosette, those with free fall instruments, and free fall micro shear structure observations.

- **(4) Micro-Temperature measurement history**
  - Station 001-030: T1111 and T1112
  - Station 031-052: T1114 and T1115

4. Floats, Drifters, and Moorings

4.1 Argo floats

(1) Personnel

Katsuro Katsumata	***(JAMSTEC)***
Ann Thresher	***(CSIRO) not onboard***
Mizue Hirano	***(JAMSTEC) not onboard***
Shungo Oshitani	***(MWJ) Technical Staff***
Shinsuke Toyoda	***(MWJ) Technical Staff***

(2) Objectives

Now Argo floats are one of the core components of the Global Ocean Observing System http://www.ioc-goos.org/). The data from these floats are indispensable for both operational and scientific purposes. We contribute to the maintenance of this system by deploying new floats.

(3) Deployments

The floats usually drift at a depth of 1000 dbar (called the parking depth), diving to a depth of 2000 dbar and rising up to the sea surface by decreasing and increasing their volume and thus changing the buoyancy in ten-day cycles. During the ascent, they measure temperature, salinity, and pressure. They stay at the sea surface, transmitting the CTD data to the land and then return to the parking depth by decreasing volume. These floats measure temperature, salinity, and pressure. Detail of deployments is shown in Table 4.1.1.

Table 4.1.1 Argo floats

Time	Location	CTD station, if avalable	Water Depth (m)	Serial Number (Hull)	WMO ID
24 Dec 2015, 00:34	8-14.84S, 105-31.45E	-	3410	7435	5905006
24 Dec 2015, 07:36	9-29.74S, 106-2.96E	-	6258	7426	5905007
24 Dec 2015, 15:33	10-45.06S, 106-35.02E	-	5855	6542	5905008
25 Dec 2015, 04:38	12-30.15S, 107-20.25E	Station 900	4668	7041	5905009
25 Dec 2015, 14:13	14-15.04S, 108-5.04E	-	5331	7042	5905010
31 Dec 2015, 15:18	20-28.37S, 110-55.37E	Station 18	3673	7040	5905011
1 Jan 2016, 14:57	18-31.68S, 110-5.57E	Station 22	4737	7039	5905012
2 Jan 2016, 21:36	16-19.92S, 111-16.59E	Station 27	5186	7430	5905013
4 Jan 2016, 04:04	14-52.02S, 111-23.75E	Station 31	5682	7431	5905014
4 Jan 2016, 19:25	14-8.15S, 111-35.04E	Station 33	5650	7429	5905015
5 Jan 2016, 14:13	12-41.08S, 111-27.15E	Station 36	3868	7428	5905016
7 Jan 2016, 01:56	10-57.86S, 111-44.82E	Station 42	4606	7432	5905017
7 Jan 2016, 23:40	10-2.72S, 111-49.84E	Station 46	2122	7427	5905018

8 Jan 2016, 12:00	9-14.05S, 111-54.13E	Station 49	3045	7434	5905019
10 Jan 2016, 00:55	9-9.68S, 113-49.97E	-	2232	7425	5905020
10 Jan 2016, 21:55	9-9.91S, 115-14.77E	-	3095	7433	5905021
Leg 2					
19 Jan 2016, 23:03	21-59.84N, 134-59.91E	-	5462	OIN 11JAP-ARI-01	5901937

Sixteen floats (Teledyne Webb Research) deployed during Leg 1 were purchased by Marine and Atmospheric Research CSIRO, transported by air from Australia to Japan, and loaded to *R/V Mirai* at Hachinohe on 6 Nov 2015. Before loading, all floats went through pre-deployment tests. These floats were deployed from the stern of the vessel using the harness-and-cardboard deployment system. After deployment, water pressure triggers internal electrical switch of the floats. The trigger of the deployment system for two floats (S/N 7040 and 7429) failed so that these floats were deployed using traditional snap-ring shackle. At CTD stations, floats were deployed just after the CTD/sampler system is recovered on deck.

The float deployed during Leg 2 (Arvor –I, nke Instrumentation) was purchased by JAMSTEC. The float was activated using magnetic switch and deployed from the stern using snap-ring shackle.

(4) Data archive

The real-time data are provided to meteorological organizations, research institutes, and universities via Global Data Assembly Center (GDAC: http://www.usgodae.org/argo/argo.html, http://www.coriolis.eu.org/) and Global Telecommunication System (GTS), and utilized for analysis and forecasts of sea conditions.

III. Notice on Using

This cruise report is a preliminary documentation as of the end of the cruise.

This report may not be corrected even if changes on contents (i.e. taxonomic classifications) may be found after its publication. This report may also be changed without notice. Data on the cruise report may be raw or unprocessed. If you are going to use or refer to the data written on this report, please ask the Chief Scientist for latest information.

Users of data or results on this cruise report are requested to submit their results to the Data Management Group of JAMSTEC.